FORMULATION AND DEVELOPMENT OF UV ACTIVATED POLYMER MICROBUBBLES AS ULTRASOUND CONTRAST AGENTS FOR IMAGING AND DRUG DELIVERY

by

Muskan Pawar

APPROVED BY SUPERVISORY COMMITTEE:

_____
Dr. Shashank Sirsi, Chair

_____
Dr. Taylor Ware

_____
Dr. Danieli Rodrigues

Dedicated to my brother, my parents, and my dear friends.

FORMULATION AND DEVELOPMENT OF UV ACTIVATED POLYMER MICROBUBBLES AS ULTRASOUND CONTRAST AGENTS FOR IMAGING AND DRUG DELIVERY

by

MUSKAN PAWAR

THESIS

Presented to the Faculty of

The University of Texas at Dallas

in Partial Fulfillment

of the Requirements

for the Degree of

MASTER OF SCIENCE IN

BIOMEDICAL ENGINEERING

THE UNIVERSITY OF TEXAS AT DALLAS

May 2020

ACKNOWLEDGMENTS

This thesis work was accomplished well within the timeline, and I want to acknowledge certain outstanding people without whom the thesis could not have been completed.

I express my sincere gratitude and best regards to my mentor and research advisor, Dr. Shashank R. Sirsi, for giving me the opportunity to work in Sirsi lab. I want to thank him for believing in me, giving me an independent project, and guiding me at every step.

I would like to thank my committee members, Dr. Taylor H. Ware, for giving me an in-depth knowledge of polymer concepts and Dr. Danieli C. Rodrigues for teaching me the concepts of biomaterials and for agreeing to be my committee members.

I want to acknowledge Dr. Taylor H. Ware, primarily for providing me access to Ware Lab resources and Dr. Xili Lu, for providing me synthesized polymer Azobenzene. I would like to extend my gratitude to all the members of Sirsi lab. A special thanks to Arvin Honari for being a good mentor and always motivating me to work independently, Aditi Bellary and Sugandha Chaudhary, for always being constant supports and guides. I would like to thank Hamza Lalami for assisting me towards the completion of this project, especially in quantitative analysis of microbubbles, and Darrah Merillat, for statistical analysis.

Words are inadequate to express my great feelings for my parents for their unconditional love. I would like to especially thank my brother Mohit Pawar for believing in me and encouraging me to pursue my research. Finally, I would like to thank my roommates and friends for the constant support and being a part of my research journey.

April 2020

FORMULATION AND DEVELOPMENT OF UV ACTIVATED POLYMER MICROBUBBLES AS ULTRASOUND CONTRAST AGENTS FOR IMAGING AND DRUG DELIVERY

Muskan Pawar, MS
The University of Texas at Dallas, 2020

Supervising Professor: Dr.Shashank Sirsi

Microbubbles, as contrast agents and drug carriers, have been widely used for theranostic applications with ultrasound technology over the past three decades. Research in microbubbles has undergone numerous improvements from a compositional perspective as researchers aim for enhanced targeted drug delivery. Microbubbles shells, which typically encapsulate a gaseous core, are conventionally classified into three type's proteins, lipids, and polymers. Polylactic Acid (PLA) polymers are FDA approved and have proven to be one of the best biomaterials for fabricating drug delivery vehicles owing to its stability when introduced in vivo. When PLA is used to fabricate microbubbles, drugs of interest can be encapsulated into the polymer shells and can be released at the site with the application of ultrasound to achieve targeted drug delivery. But two limitations encountered with this microbubbles are a lack of controlled drug release upon triggering and elasticity of polymer shell in an ultrasound field.

This research focuses on the development of novel Ultraviolet (UV) sensitive shape changeable polymer microbubbles to improve polymer shell properties. Fabrication of these microbubbles was done by modifying a double emulsification method. A UV sensitive shape changeable polymer, Azobenzene, has been used along with PLA to address the elasticity issue. This blend of two polymers present in the microbubble shell has resulted in structural changes like pores, cracks, and golf-ball like appearances, in response to UV light. These structural changes are indicative of a change in flexibility of otherwise stiff PLA microbubble shell.

Scanning Electron Microscopy images show a clear structural difference in UV exposed microbubbles. UV-Vis Spectroscopy results show the optical properties of these microbubbles and confirm the activation of UV sensitive polymer present on the microbubble shell. The reported differences confirm the change in structure and lay the foundation for future work where acoustic properties of this novel polymer microbubbles tested for elasticity followed by testing of drug encapsulation and drug release profile for controlled delivery and cell toxicity testing for biocompatibility of the azobenzene.

TABLE OF CONTENTS

LIST OF FIGURES

LIST OF TABLES

CHAPTER 1

INTRODUCTION AND MOTIVATION

Introduction

A significant advancement in the medical community in the last two decades has been the push towards personalized therapies using bio-imaging as feedback. Personalized therapies involve a multi-faceted approach to individualizing patient care that not only improves our ability to diagnose and treat disease but also offers the potential to detect disease at an earlier stage before the angiogenic switch (Frangioni, 2008), a stage wherein treatment would be more effective. Currently, the primary imaging modalities used for theranostic purposes are X-ray, CT, optics, nuclear medicine (PET and SPECT), Ultrasound, and MRI. (Wu & Shu, 2018) Modalities that use X-Ray and nuclear medicine expose the body to potentially harmful ionizing radiation and injected radioisotopes. Optical imaging has limited depth penetration. MRI lacks portability and has an extended processing time. Hence this leaves Ultrasound as the first choice for theranostic as it is less expensive and more portable. Ultrasound waves are harmless and propagate through the exterior of the body and body fluids until they hit tissue or bone surface. Despite the advantages, ultrasound waves fail to distinguish between a healthy and diseased tissue since the intensity of reflection of sound waves of their interface is the same, resulting in reduced contrast images. This limitation makes detection difficult which led to the development of ultrasound contrast agents.

1.1 Ultrasound Contrast Agents ("Microbubbles")

Microbubbles are compressible; they oscillate in an acoustic field producing acoustic responses that can be uniquely distinguished from surrounding tissue, resulting in a substantial enhancement in imaging signal-to-noise ratio. The structure of microbubbles also allows drugs or genes to be loaded and used in therapy. Ultrasound can trigger the release of this drug upon the targeted site. (de Jong et al., 1992) Microbubble behavior depends on acoustic frequency and pressure, bubble size, and physical properties of the shell and core. At low ultrasound acoustic pressures, most microbubbles oscillate stably. At high acoustic pressures, substantial cycles of expansion and contraction can result in instability that results in disruption of the shell with the gaseous core diffusing in the vicinity. Microbubble destruction then results in the release of the encapsulated drug, making it a capable drug carrier. (Chomas et al., 2001)(de Jong et al., 2000)

1.2 History of Ultrasound Contrast Agents

The first use of contrast agents had taken place in echocardiography to diagnose atrial septal defects. The study is known as "bubble study" as it involved the intravenous injection of agitated saline mixed with air. This agitation causes the formation of gas-filled mini bubbles that served to improve the echocardiographic resolution and providing real-time assessment of intracardiac blood leakage due to the septal defects. These bubbles were first-generation microbubbles that provided opacification when imaged using ultrasound. Bubbles produced were too large to cross pulmonary capillaries, and

therefore in the absence of the right to left shunt, these remains confined to the right side of the heart, which is known as a negative contrast echocardiogram. (Romero et al., 2009) In contrast, the appearance of these bubbles in the left atrium and left ventricle or aorta referred to as positive contrast echocardiogram. The result indicates that these bubbles worked as contrast agents. However, these microbubbles are non-encapsulated nitrogen and oxygen and hence disappear in a few seconds after intravenous administration as the solubility of air in the blood is high, and the lungs filter microbubbles, especially those with higher diameters. (Stewart, 2003)(DIJKMANS et al., 2004). This limitation drove research towards improving the stability of these bubbles to increase the life of microbubbles in vivo, which formed second-generation microbubbles. Two ways achieved improved stability: incorporation of inert and safe high molecular gases which are less diffusible than nitrogen and oxygen and the encapsulation material that is with proteins, polymers, lipids, which reduces surface tension and control size distribution. The development of more stable contrast agents has significantly increased its utility in imaging and drug therapy applications. The FDA approved imaging technique was performed to image microbubbles from left ventricular opacification or for perfusion imaging. (DIJKMANS et al., 2004) (Szabo, 2004)

1.3 Biomedical Applications using Microbubbles

Tumor imaging is one application that is enhanced using microbubble contrast agents, with the advancement in ultrasound imaging techniques. Ultrasound has been able to mark its place in cancer treatment and diagnosis as one of the most important theranostic modality for imaging as well as achieving targeted drug delivery to the tumor site. With targeted drug delivery, the aim is to deliver more drugs to the target site and avoid its influence on healthy tissue and, in turn, unwanted toxicity. (Shashank R. Sirsi & Borden, 2014) There are two forms of contrast-enhanced ultrasounds untargeted and targeted. Untargeted ultrasound contrast agents are FDA approved and are used in clinical trials, whereas targeted ultrasounds are still under pre-clinical trials.

For ultrasound-triggered drug delivery, the main requirements that are necessary to achieve are (1) stable encapsulation of the drug compound before application of ultrasound, (2) release of the drug by ultrasound stimulation and (3) the ability to image the carrier and monitor the delivery of the drug cargo.(Shashank R. Sirsi & Borden, 2014)Physical effects of ultrasound wave propagation in vivo include pressure variation of sound waves, acoustic fluid streaming, cavitation of compressible entities, and local hyperthermia observed in an ultrasound field. These phenomena exploited to initiate drug delivery and trigger release on demand. (Shashank R. Sirsi & Borden, 2014)

A milestone achieved in cancer treatment with personalized therapies is Image-guided drug delivery, which includes the development of drug carriers, contrast imaging agents, and focused drug delivery systems. With cancer being a constantly researched area, there is a pressing need for improved imaging and therapeutic systems.(Bertier et al.,

2016) Over the past two decades, ample research has done to improve theranostic techniques, one being the use of microbubbles. With a size approximating that of red blood cells (less than 10 μm diameter), microbubbles can easily circulate within the body (Fu et al., 2019). The general composition of a microbubble is a gas core stabilized by a shell comprised of proteins, lipids or polymers. Each type of shell has its unique advantages and tailored to perform specialized functions. (S. R. Sirsi & Borden, 2009)Microbubbles as contrast agents can respond well to the ultrasound as they can strongly scatter because of the large difference in acoustic impedance between the suspending medium (blood) and the microbubbles.(Shashank R. Sirsi & Borden, 2014) The interaction of microbubbles with ultrasound results in oscillation in terms of expansion and contraction owing to their compressible nature and then later can lead to their disruption depending upon the intensity of the ultrasound field. (Wilson & Burns, 2010) (Qin et al.,2009) In response to compression and rarefaction of the ultrasound waves, these volumetric oscillations occur, which can be identified by clinical ultrasound scanners. (Qin et al.,2009)

While there is extensive use of microbubbles in pre-clinical studies and clinical trials are still in the early stages of development for both diagnostic and treatment purposes, the greatest challenge that still needs to be addressed to develop effective agents for dual imaging and drug therapy approaches in personalized therapy regiments.

It is important to note that currently, there is no FDA-approved microbubble formulation designed for drug delivery or theranostic applications. Methods of simultaneously imaging and delivering high payloads of drug on-demand using contrast agents heavily

explored.(Shashank R. Sirsi & Borden, 2014) Rationally designing microbubbles for on-demand drug delivery requires careful consideration. Based on microbubble thickness, microbubbles classified into two types: soft-shelled and hard-shelled microbubbles. The former comprises of a thin surfactant shell material, proteins, phospholipids, whereas the latter comprises of cross-linked or entangled polymeric chains that form thicker and less compliant microbubble shell. (Lentacker et al., 2009) Both types of microbubbles have their advantages and disadvantages. Soft-shelled microbubbles have thinner shells, hence making them more echogenic. The shells are flexible, which are held together by hydrophobic interactions. The disadvantage is that they have limited drug loading capacity. Polymer microbubbles have a thicker shell which is responsible for providing high shelf stability and higher drug payload in comparison to lipids and proteins microbubbles.(Bloch et al., 2004) Polymer microbubbles exhibit stability, elasticity, good drug-carrying capability, all contribute towards potential targeted drug delivery vehicles. (Cui et al., 2005). Their stability in an ultrasound field is due to good mechanical strength imparted by how much it can be expanded and compressed. This research thus focuses on the development of novel polymer microbubble by adjusting the chemical composition of the polymeric shell material.

1.4 PLA/PLGA Microbubbles

Degradable Polymer bubbles have previously developed using Poly-lactic Acid (PLA) and poly (L-lactide-co-glycolide) (PLGA) polymers (Wheatley et al., 2006)(Narayan & Wheatley, 1999). PLA polymers are biocompatible as well as biodegradable, and conventionally used for making polymer microbubbles. (Cui et al., 2005)PLA holds the

potential for better stability and control over the encapsulation properties of ultrasound contrast microbubbles. Also, PLA microbubbles have a prolonged degrading rate, thus having a higher shelf life, which does not favor clearance from the body. PLGA (poly(L-lactide-co-glycolide) has excellent biocompatibility and degrades more quickly in vivo into lactic and glycolic acid, which further degrades into carbon dioxide and water via the tricarboxylic acid cycle. Hence PLGA is proven to be one of the best synthetic biodegradable polymers in drug delivery systems, tissue engineering, and other biomedical applications. PLGA has long-shelf-life and can be stored for years. PLA and PLGA are particularly advantageous for drug delivery applications because the shell materials can incorporate a high amount of drug content. However, the limitation of PLA and PLGA microbubbles is that they are less echogenic than lipid microbubbles due to increased shell thickness. The thickness of the PLGA shell is 200 nm, compared to lipid bubbles, which have ~3 nm thin, flexible shells; thus, the polymer bubbles resist expansion and contraction. Methods of controlling the shell properties would be highly desirable to utilize their functionality in imaging and drug delivery applications. It can be done by providing external stimuli like pH, temperature, light, electric field, magnetic field, and ultrasound. There are many stimuli-responsive drug delivery systems that have been previously studied and have various advantages as well as limitations. The paper introduces a light-responsive material to control the shell properties. On-demand drug delivery systems with light stimuli allow a high degree of temporal and spatial control. Ideal light-responsive delivery systems provide control over drug release, utilize nonionizing radiation, are composed of biocompatible materials, and can be easily

tailored for desired clinical application. Many light-based strategies have been used to design novel delivery systems and they can be classified into three broadly defined categories, (1) photochemically triggered, where the absorbed light energy is sufficient to break covalent bonds directly or by a photochemical reaction, (2) photoisomerization, where the excess energy causes structural changes and (3) photothermal, where the absorbed photon energy is dissipated via vibrational motion.

1.5 Azobenzene

It is proposed in this study that UV sensitive biomaterial into the shell can control the shell properties with the application of UV light. It is believed that modulating the shell's structural properties can enhance echogenicity and enable the controlled release of drug at target sites. Azobenzene is a versatile and polymorphic molecule that has been extensively and successfully used for photoswitching applications. Azobenzene was first reported in 1834. (Rustler et al., 2019) In 1937 Hartley published a study that explains conformational changes to Azobenzene polymer on the exposure of light. (Hartley, 1937)Azobenzene exists in two forms, cis isomers and trans isomers and acts as a molecular switch, interconverting between both photochemically and thermally. Chemically, Azobenzene is organic in nature that has two aromatic rings linked by an azo group (N=N). Isomerization of N=N double bonds occurs in the presence of a light source, imparting the photochromatic properties. (Linsley & Wu, 2017) The main advantage of introducing azobenzene is its structure can be controlled by turning on and turning off light as an external stimulus. Previous studies have been done with azobenzene to functionalize liposomes and micelles with different phospholipids that resulted in the

triggered release of drugs with UV light irradiation, and it was proven that it was biocompatible.(Merino & Ribagorda, 2012)Mesoporous silica nanoparticles are popular candidates for on-demand drug-delivery systems that also work via photoisomerization. These nanoparticles were desired for drug delivery, owing to their biocompatibility, high pore volume, tunable pore size, and versatile chemistry for surface functionalization.

On the basis of the successful use of azobenzene in the above applications, it was decided to incorporate azobenzene with PLA in microbubble shells to fine-tune the shell properties. PLA/Azobenzene microbubbles on the application of UV light exhibited photoisomerization of azobenzene in the polymeric shell, and this is corroborated by the change in shell porosity.(Merino & Ribagorda, 2012)

1.6 Synthesis Techniques for Formulation of Microbubbles

There are many synthesis techniques used for the fabrication of lipid, protein, and polymers microbubbles. Synthesis of microbubbles usually done using sonication, mechanical agitation, and flow-focusing devices such as T-junction and microfluidic devices, amalgamation, freeze-drying, and saline shaking. (Upadhyay & Dalvi, 2019)In Sonication, cavitation occurs during the propagation of high-intensity ultrasonic waves. The technique uses ultrasonic waves that cause compression and rarefaction of the liquid resulting in the formation of small microbubbles in the solution. This technique produces a high concentration of microbubbles at a high production rate; however, this technique produces polydisperse microbubbles. The polydisperse microbubbles can be produced by size isolation techniques such as centrifugation and floating. The isolation techniques generally affect the stability of the microbubbles because of the extended exposure to an

aqueous medium in which the microbubbles can dissolve. Microfluidics with flow-focusing synthesis technique used to produce a highly narrow size range microbubbles. In this technique, the monodisperse microbubbles produced with control over flow of shell material and the gas core in the microfluidic device. This technique is complicated in the sense of producing narrow sized microbubbles with a reduced production rate. Methods such as amalgamation and saline shaking are used to prepare polydisperse microbubbles suspension. In amalgamation, the solution is shaken vigorously where the shell material used is a lipid and mixed along with gas in a capsule tube. The lipid solution heated above the glass transition temperature of the lipid and the headspace above the solution replaced with the gas that needs to be encapsulated in microbubbles followed by the agitation of the tube over time to produce microbubbles. Microbubbles produced using this technique can be used for sound mediated gene transfer and ultrasound imaging. This technique also produces polydispersed microbubbles. (Upadhyay & Dalvi, 2019)

Double emulsification and Freeze-drying constitute a technique used to formulate polymer-coated microbubbles. In this synthesis technique, the emulsification of an aqueous solution in an oil phase (W/O) is done, followed by the secondary emulsion of continuous aqueous phase (W/O/W). The emulsion formed is converted to microbubbles by freeze-drying. This technique gives the advantage that it enables the encapsulation of both hydrophilic and hydrophobic drugs. Microbubbles produced are highly stable because of the polymer entanglement

In this study, a blend of Azobenzene and PLA was used to make microbubbles using a double emulsification method. The results of this formulation of two polymer mixed

microbubbles were characterized in this research. For the development of these microbubbles, the tasks were divided into sub-parts, including optimizing the formulation of polymer microbubbles, characterizing size and porosity, and determining the effects of UV exposure:

1. Formulation of Microbubbles: There are various methods used for the formulation of microbubbles, which are: single emulsion, double emulsion-solvent evaporation, spray drying, and coacervation. The method used in this study for the formulation of polymer microbubble was double emulsion. The technique can be used to encapsulate both hydrophobic drugs (in the oil phase) and hydrophilic drugs (in the water phase). (Cavalieri et al., 2005)
2. Physical Characteristics: After the development of polymer microbubbles, characteristics analysis was performed. Particle size, the concentration of microbubbles, shape, and size were evaluated.
3. UV activation of the polymer in microbubble shell: The presence of a UV sensitive material that was incorporated in the microbubble shell was tested by analyzing the optical properties of Azobenzene-PLA microbubble followed by evaluation of structural difference before and after UV exposure.

1.7 Hypothesis and Specific Aims

The main objective of the thesis was to formulate Azobenzene-PLA bubbles, characterize their properties, and utilize UV-shape changing polymers to control the shell properties of polymer microbubble. The hypothesis and specific aims of the project are explained below:

Hypothesis: Incorporating Azobenzene, a UV-sensitive shape changeable polymer in microbubble shells, can alter the size and shell porosity.

Specific Aim 1: Formulation of polymer microbubbles by incorporating Azobenzene, a UV sensitive shape changeable polymer with PLA, by optimizing the double emulsion fabrication process. Physical characterization of the Azobenzene/PLA microbubbles was studied to identify size distribution by Multisizing and by microscopy techniques.

Specific Aim 2: To demonstrate and define the effects of Azobenzene inside the polymer microbubble shell and show the activation with UV exposure by UV-vis Spectroscopy and Scanning Electron Microscopy.

CHAPTER 2

FORMULATION OF POLYMER MICROBUBBLES

Introduction

As shown in Figure 2.1, Polymer microbubbles comprised of gas cores stabilized by the polymeric shell. The stable shell reduces the rate at which the gaseous core diffuses into the surrounding media. (Klibanov, 2006) The polymeric shell acts as a barrier of 100-200 nm thickness between the encapsulated gas core and the surrounding aqueous medium. (S. R. Sirsi & Borden, 2009) Polymer due to its entanglement forms a thick or bulky shell that resists compression and expansion of the microbubble. Polymeric shell leads to a loss of echogenicity of microbubble, which, in turn, is essential for ultrasound-guided drug delivery. Many material choices in the past investigated for the formulation of microbubble, including polysaccharides (such as starch, alginate, and agarose), proteins (such as gelatin and albumin), fats and fatty acids (such as palmitic and stearic acid), lipids and polymers. Each material has its own benefits with regard to the microbubble end use and application. Previously established polymer microbubbles like PLA; PLGA(50:50) poly(D,L-lactide-co-glycolide) are being used as diagnostic contrast agents as PLGA is FDA approved and is proven to be biodegradable and biocompatible (Makadia & Siegel, 2011)(El-Sherif & Wheatley, 2003)

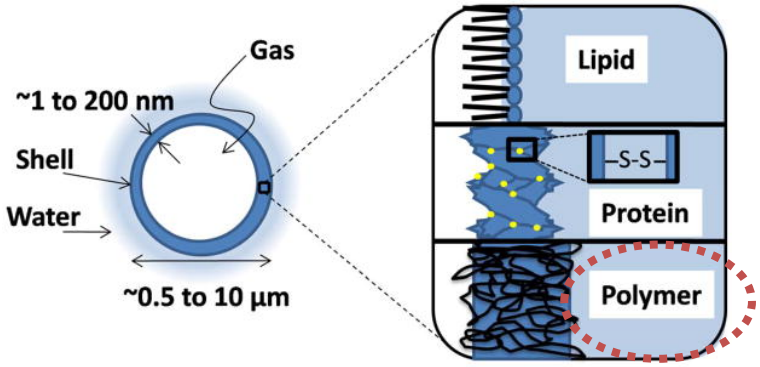

Figure 2.1. Schematic structure of Microbubble composition (S. R. Sirsi & Borden, 2009)

PLGA is a copolymer of polylactic acid (PLA) and polyglycolic acid, which exhibits excellent biocompatibility and other properties suitable for continuous drug release, widely used in biomedical applications. (Cui et al., 2005) PLGA shells are more rigid than those of surfactants and lipids and can achieve better active targeting to specific tissues and cells.

PLA microbubbles have the advantage of having a thicker shell that allows better drug loading, have a high shelf life and thus last longer. But it has various disadvantages like reduced release profile, a slow degrading compound which takes 6-12 months to degrade. Hence, to address these problems, a drug carrier is prepared, which can achieve the timed release of drugs in a controlled fashion. For this purpose, a UV sensitive shape changeable polymer introduced that has the potential to be altered on the application of UV light and also result in changing the rigidity of the microbubble to improve the shell's ability to contract and expand.

This chapter explains the methods and materials required for the development of novel UV-sensitive shape changeable polymer microbubble. After successfully developing

these microbubbles, microbubbles characterized using Multisizer, Microscopy, and Scanning Electron Microscopy.

2.1 Experimental Materials and Methods

The formulation of polymer microbubbles can be done by using various techniques such as single/double emulsion, which is also known as solvent evaporation, coacervation, and spray drying. (El-Sherif & Wheatley, 2003) Single emulsion technique is a sophisticated technique and is used to encapsulate hydrophobic drugs. It is either W/O emulsification where the oil phase is in a continuous aqueous phase or an O/O emulsification where removal of oil from the finished product is required. In double emulsification, the emulsification of an aqueous solution in an oil phase (W/O) followed by the secondary emulsion of continuous aqueous phase (W/O/W). This technique used to encapsulate both hydrophilic and hydrophobic drugs. Coacervation is a sophisticated technique that is based on a colloid phenomenon. The colloid solubility in a solvent solution is reduced by various changes (for example, pH or temperature). A large part of the colloid is separated out into a new phase. The productive colloid phase coalesces into the coacervate layer, which produces the shell of the microcapsule. Spray drying is widely used for the fabrication of microparticles. Spray drying can be applied to heat resistant, heat-sensitive, water-soluble and water-insoluble drugs. All these techniques used for the fabrication of microcapsules produce different properties of microcapsules such as size, surface chemistry, and texture, morphology, and composition. These methods also result in chemical and physical changes to the microcapsule system. (El-Sherif & Wheatley, 2003)

The methods followed for the formulation of polymer microbubble are from a thesis of Drexel University by Dalia El-Sherif “Development of Novel Contrast Agents for use as Ultrasound Targeted Drug Delivery Vehicle.”

Pre-Fabrication:

1. ***Poly (vinyl alcohol) PVA****:* PVA is a biocompatible water-soluble synthetic polymer with a melting point being at 200ºC. It exhibits excellent emulsifying properties and hence can act as a surfactant. The chemical formula for PVA is $[CH_2\text{-}CHOH\text{-}]_n$ and the chemical structure is shown in Figure 2.2.

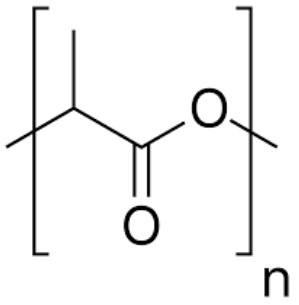

Figure 2.2. Chemical structure of Poly (vinyl alcohol)

5w/v% PVA solution was prepared at least 24 hours prior to microcapsule fabrication. The stock solution of PVA was prepared, which was sufficient for 10 batches. Making a large volume (500 ml) of PVA was a time-consuming process. The preparation of 5w/v% PVA solution was explained in Figure 2.8, 25 g of PVA powder (white in color) was weighed out and dissolved in 500 ml of deionized water in a beaker. Before dissolving, the deionized water was heated up to reach the temperature of (40-45ºC). Stir bar plate was used, the highest vortex was created, and a small amount (1/5) of PVA was dissolved at a time until a complete 25 g was fully dissolved. It should be

noted that 25 g of PVA should not be mixed all at once as it results in settling down and adhering to the stir bar, which can be difficult to dissolve. It took approximately 3 hours to mix thoroughly. Once this process was over, warm PVA was filtered through a bottle top filter three times into a glass bottle. The filtration process took 1 hour approximately. During the filtration process, the filter would get blocked several times because of the chunks of undissolved PVA, so it was recommended the filter be changed during the first filtration itself (sometimes in the second filtration as well). After the filtration was done, the PVA solution was stored in a bottle at 4 ºC. PVA's temperature is vital as it has shown to have an effect on microcapsule fabrication.

2. ***Ammonium Carbonate Solution****:* Ammonium carbonate is a salt that degrades to gaseous ammonia and carbon dioxide on heating and hence is termed as a leaving agent. The melting point of ammonium carbonate is 58 ºC. The chemical formula for Ammonium Carbonate is $(NH4)_2CO_3$, and the chemical structure is shown in Figure 2.3.

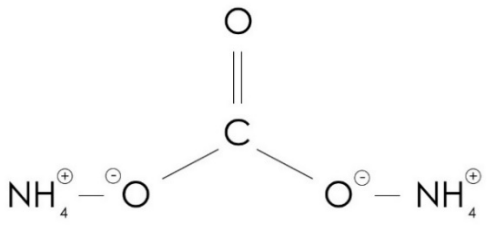

Figure 2.3. Chemical structure of Ammonium Carbonate

Ammonium carbonate is hydrophilic in nature and can be encapsulated in the water phase. As explained in Figure 2.9, 4 w/v% ammonium carbonate was required and prepared 30 minutes before the emulsion. The time taken to prepare ammonium carbonate can impact the acoustic properties of the microbubbles. A total of 10 ml of the solution was prepared by dissolving 400mg in 10 ml of deionized water. Though 1ml of ammonium carbonate dissolved in deionized water was required more considerable amount was prepared to avoid the error caused due to small quantities.

3. ***Azobenzene:*** Azobenzene is a UV sensitive shape changeable polymer. Azobenzene is made of organic molecules with photochromatic properties formed with two aromatic rings linked by azo group (N=N) that undergoes isomerization in the presence of light source. (Merino & Ribagorda, 2012) (Zollinger & Nwslen, n.d.) Azobenzene has a melting point of 69ºC, and the chemical structure is shown in Figure 2.4.

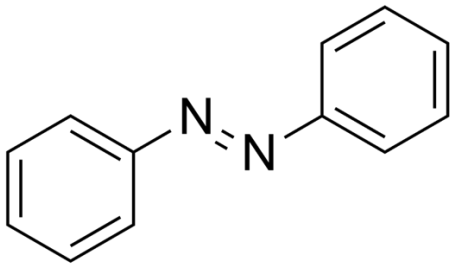

Figure 2.4. Chemical Structure of Azobenzene

Azobenzene Synthesis:

Materials: LC monomer RM82 was purchased from Wilshire Technologies, Inc. Azobenzene monomer was purchased from SYNTHON Chemicals GmbH & Co. KG.

Thiol chain extender 2,2 ′-(ethylenedioxy) diethanethiol (EDDT), base-catalyst triethylamine (TEA), and the radical inhibitor butylated hydroxytoluene (BHT) were purchased from Sigma Aldrich.

Synthesis of Azobenzene-containing Polymer: As shown in Figure 2.5, 10% Azobenzene Polymer was synthesized via a thiol-acrylate Michael addition. Typically, a stoichiometric amount of RM82 (353.0 mg, 0.9 eq), azobenzene monomer (35.4 mg, 0.1 eq), EDDT (99.7 µl, 1.05 eq), TEA (6.9 µl, 1 wt%) and BHT (10 mg, 2 wt%) were heated to 100 °C and then mixed uniformly in a 7 ml vial. The molar ratio of acrylate over thiol was 1:1.05. The resulting mixtures were kept at 65 °C for 12 hours to yield a yellow solid.

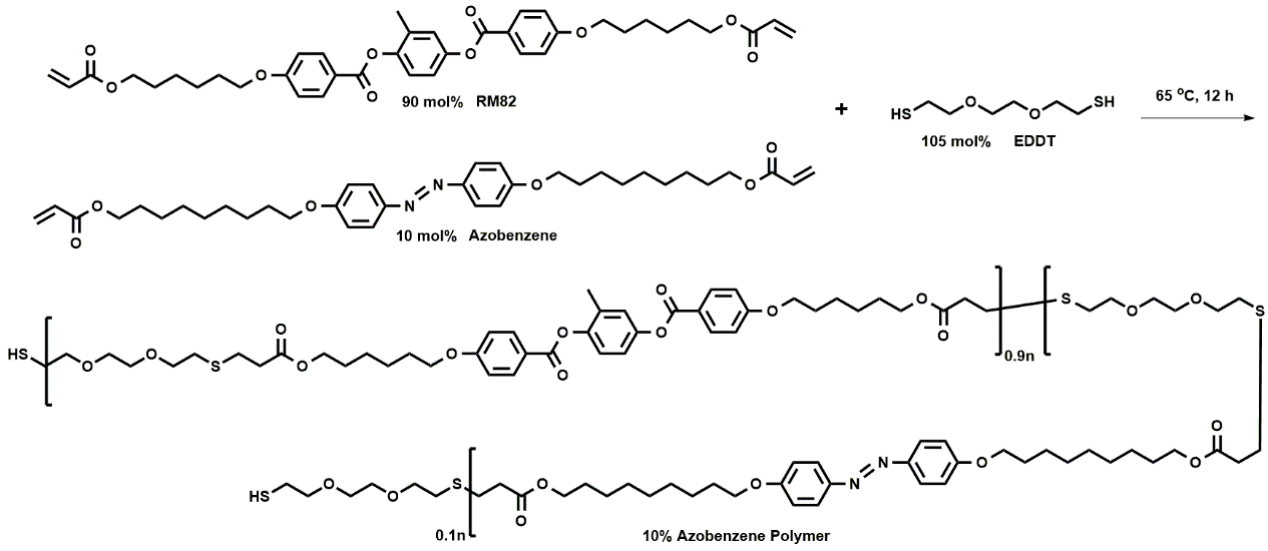

Figure 2.5. Synthesis of 10% Azobenzene Polymer

As shown in Figure 2.6, The samples of 100% azobenzene polymer were prepared through similar procedures. Typically, a stoichiometric amount of azobenzene monomer

(308.1 mg, 1 eq), EDDT (107.1 µl, 1.05 eq), TEA (6.9 µl, 1 wt %) and BHT (10 mg, 2 wt %) were heated to 100 °C and then mixed uniformly in a 7 ml vial. The molar ratio of acrylate over thiol was 1:1.05. The resulting mixtures were kept at 65 °C for 12 h to yield a yellow solid.

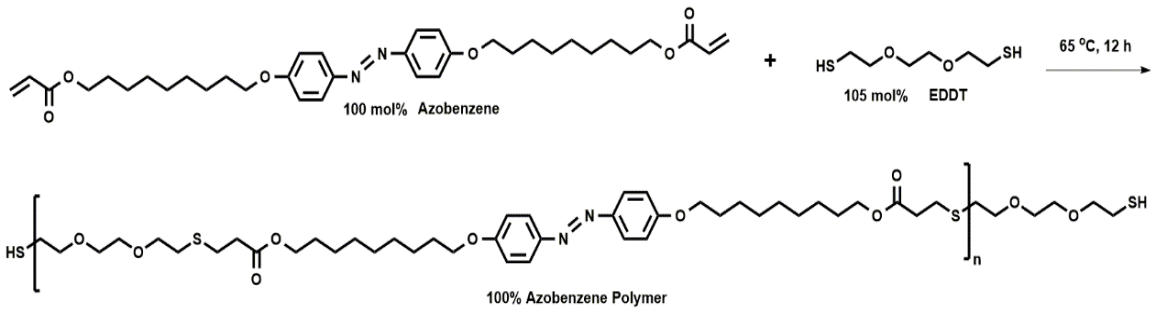

Figure 2.6. Synthesis of 10% Azobenzene Polymer

***Azobenzene Blend ratios*:** There were two types of Azobenzene composition used with polymer PLA in the preparation of polymer microbubbles explained in Figure 2.10. One was 100% Azo in Azobenzene, which was abbreviated as Ab1, and the second was 10% Azo and 90% RM82, which was abbreviated as Ab2. The synthesis for both polymers was explained above in Figure 2.5 and Figure 2.6.

Azobenzene blend ratios with PLA: In this research, there were many ratios of Azobenzene (Ab1 and Ab2) used to see the effect of different percentages of Azo. Different ratios were 10%Ab2:90% PLA (which had 1%Azo); 20%Ab2:80%PLA (which had 2% Azo); 30%Ab2:70%PLA (which had 3% Azo); 50%Ab2:50%PLA (which had 5% Azo) and 10% Ab1 with 90% PLA (which had 10% Azo).

Double Emulsification process for fabrication of microbubble:

The double emulsion process for generating PLA and PLGA microbubbles was developed in the lab of Dr. Margaret Wheatley (El-Sherif & Wheatley, 2003) and was used as the basis for creating Azo-PLA bubbles(Figure 2.7). Double emulsions, also known as “emulsions of emulsions,” is a complex system that contains two immiscible liquids. Water-in-Oil-in-Water emulsion is a two-step process in which the inner aqueous phase is dispersed in the oil phase, which contains a lipophilic emulsifier in the first step, which is followed by dispersion of the primary emulsion into an outer aqueous phase containing hydrophilic emulsifier. The double emulsion has an advantage of encapsulating both hydrophilic and hydrophobic drug (Iqbal et al., 2015)

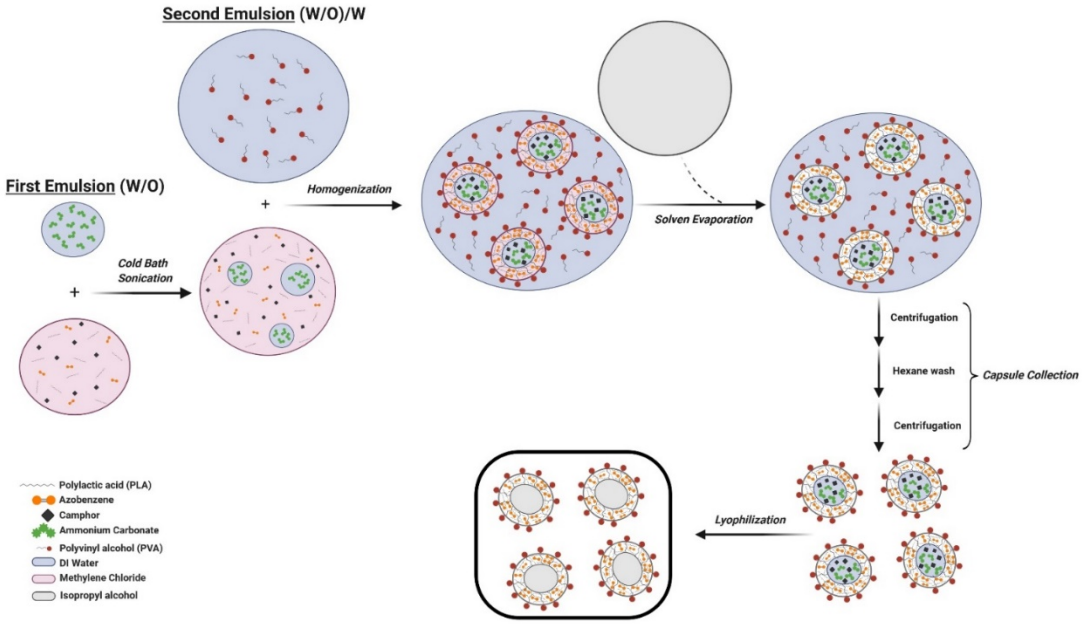

Figure 2.7. Schematic representation of the fabrication process of polymer microbubble by double emulsion

Day 1: First emulsion, Second emulsion, Solvent evaporation

The mixture of Poly (lactic acid) and Azobenzene ultrasound contrast agents fabricated using a double emulsion technique. 500 mg of PLA dissolved in 10 ml of methylene chloride, and 500 mg of Azobenzene dissolved in 10 ml of methylene chloride. Different ratios of PLA and Azobenzene dissolved in methylene chloride was taken to make different blend ratios. In this research, different blend ratios have been formulated. Polymers were dissolved entirely with different blend ratios, 50 mg of camphor added to a total of 10 ml. After the polymers and camphor wholly dissolved,1 ml of ammonium carbonate solution (4% w/v) added to the polymer solution, and then immediately sonicated in ice for 30 seconds (10 pulses of 3 seconds each separated by 1 second) with 30% amplitude and 110W power applied. The solution turned from transparent to opaque, which indicates the mixing of the two phases (water and oil). The resulting water in oil emulsion was immediately added to 50 ml of a cold 5% w/v PVA solution to avoid phase separation of two phases and homogenized for 10 minutes at 9500 rpm with saw tooth homogenizer probe. The homogenization process was responsible for breaking the water and oil emulsion into small particles. The bright foam observed on the top of the solution after this step. Immediately the following homogenization 100 ml of 2% v/v isopropanol alcohol added to the emulsion, and then stirred overnight to allow the volatile methylene chloride to evaporate. The complete setup was kept under the hood on a stir/bar plate on room temperature covered with aluminum foil. The holes were made to let methylene chloride evaporate. The evaporation of methylene chloride resulted in the hardening of the capsules. The complete procedure for Day 1 represented in Figure 2.11.

Day 2-Day 5: Capsule Collection and Lyophilization

Microcapsules then collected by centrifugation. The overnight stirred solution was divided into 3 to 4 50 ml centrifuge tubes and centrifuged at 5000xg for 5 minutes at 15 ºC. The supernatant removed from the tubes, and each of them settled down. The pellet was collected in one tube from all 3 to 4 tubes and washed one more time with deionized water to prevent the loss of capsules. The capsule collection was a critical step as the yield of capsules was dependent on this step. The collected capsules were washed three times with 10 ml hexane and added to the centrifuge tube, and the pellets were broken up and manually stirred with a metal spatula. The hexane was removed with a glass pipette between each wash very carefully. After the first wash, the pellets were hard, and after the second and third wash, it became soft and comfortable to stir. After allowing any residual hexane for almost 1 hour to evaporate, the particles washed in deionized water, and the capsules were collected using centrifugation at 5000xg at 15ºC for 5 minutes. After collecting capsules, they resuspended in 2-3 ml of deionized water, and the snap freeze was done using liquid nitrogen for almost 1 minute and lyophilized for 70 hours. The capsules were frozen in a freeze dryer to dry the capsules and sublime the encapsulated water thoroughly. Freeze drying time was dependent on the total amount of water volume in the centrifuge tube. The capsules were lyophilized for 70-72 hours. The lyophilization was followed by pre-freezing for 30 minutes, then freezing for 11 hours, with variable drying time and then final drying time of 24 hours. The dried microcapsules weighed into a 20 ml glass vial, the vial screw cap tightened, wrapped in parafilm, and the vial stored in the refrigerator.

Water and ammonium carbonate from the core of the particles and the camphor from the polymer shell were allowed to sublimate during lyophilization to create a polymer shell encapsulating a void that was filled with air when the microbubbles returned to the atmospheric pressure. The expected yield of the polymer microbubble observed to be 75-85%, and results were tabulated in Table 2.1. Contrast agents in the form of a dry powder were refrigerated and stored until ready to use. The complete procedure from Day 2-5 represented in Figure 2.12.

Complete Fabrication Process

Pre-fabrication:

1. PVA solution:

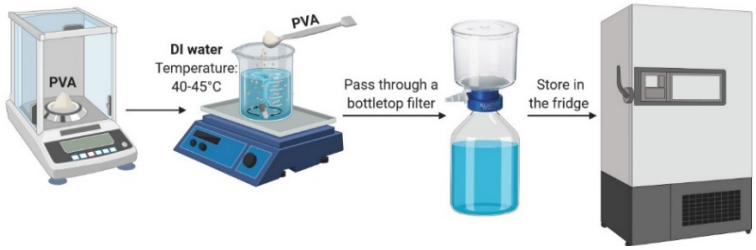

Figure 2.8. Steps involved in making PVA solution

2. Ammonium Carbonate:

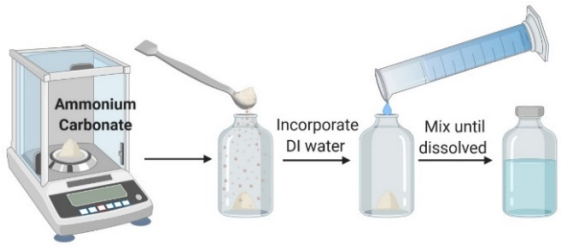

Figure 2.9. Steps involved in making Ammonium Carbonate Solution

3. Azobenzene:

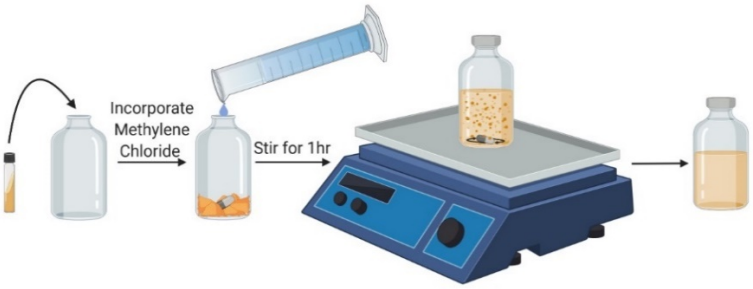

Figure 2.10. Steps involved in making of Azobenzene polymer solution in methylene chloride

Day 1: First emulsion, Second emulsion, Solvent evaporation

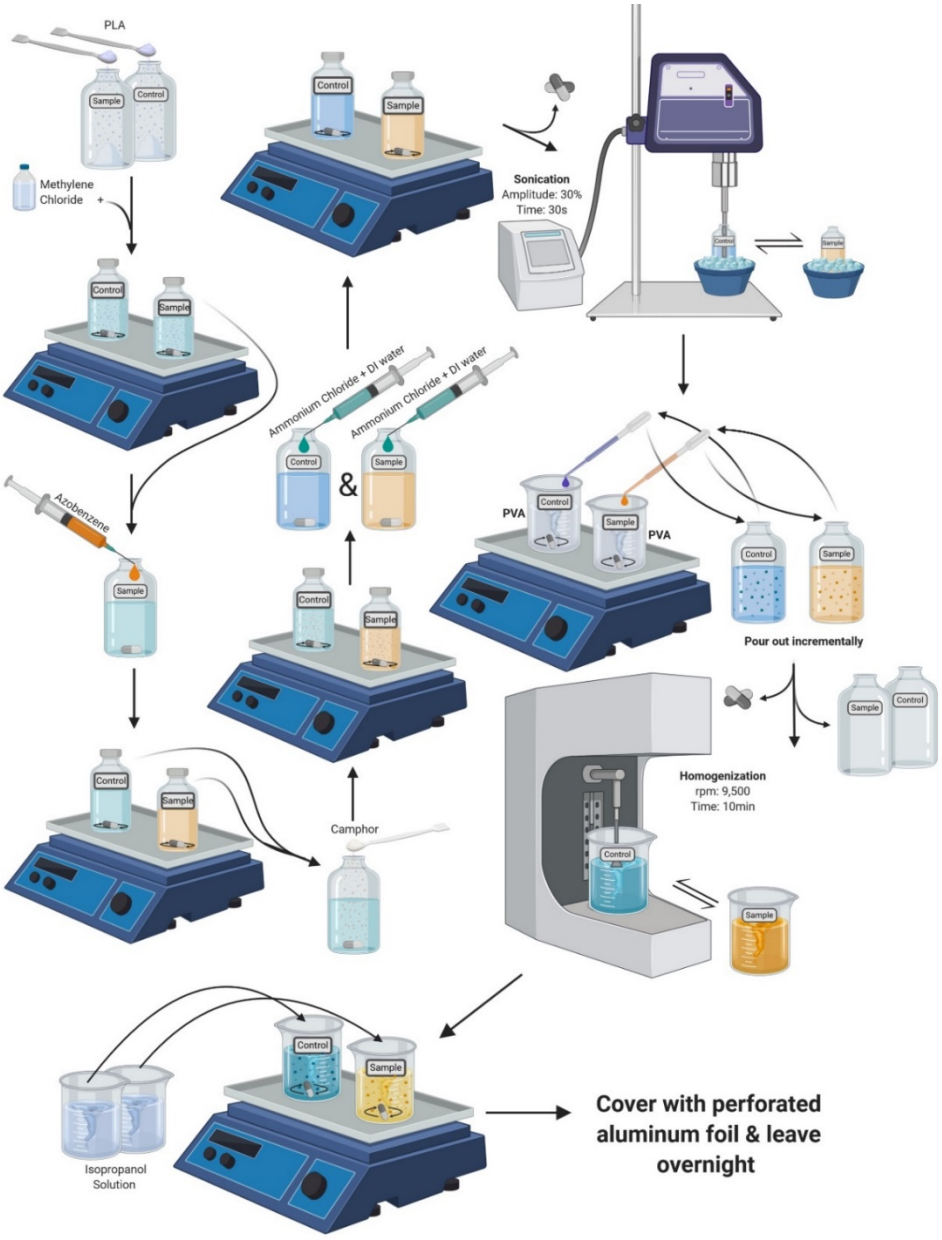

Figure 2.11. Fabrication process representing first emulsion, second emulsion, and solvent evaporation

Day 2-Day 5: Capsule Collection and Lyophilization

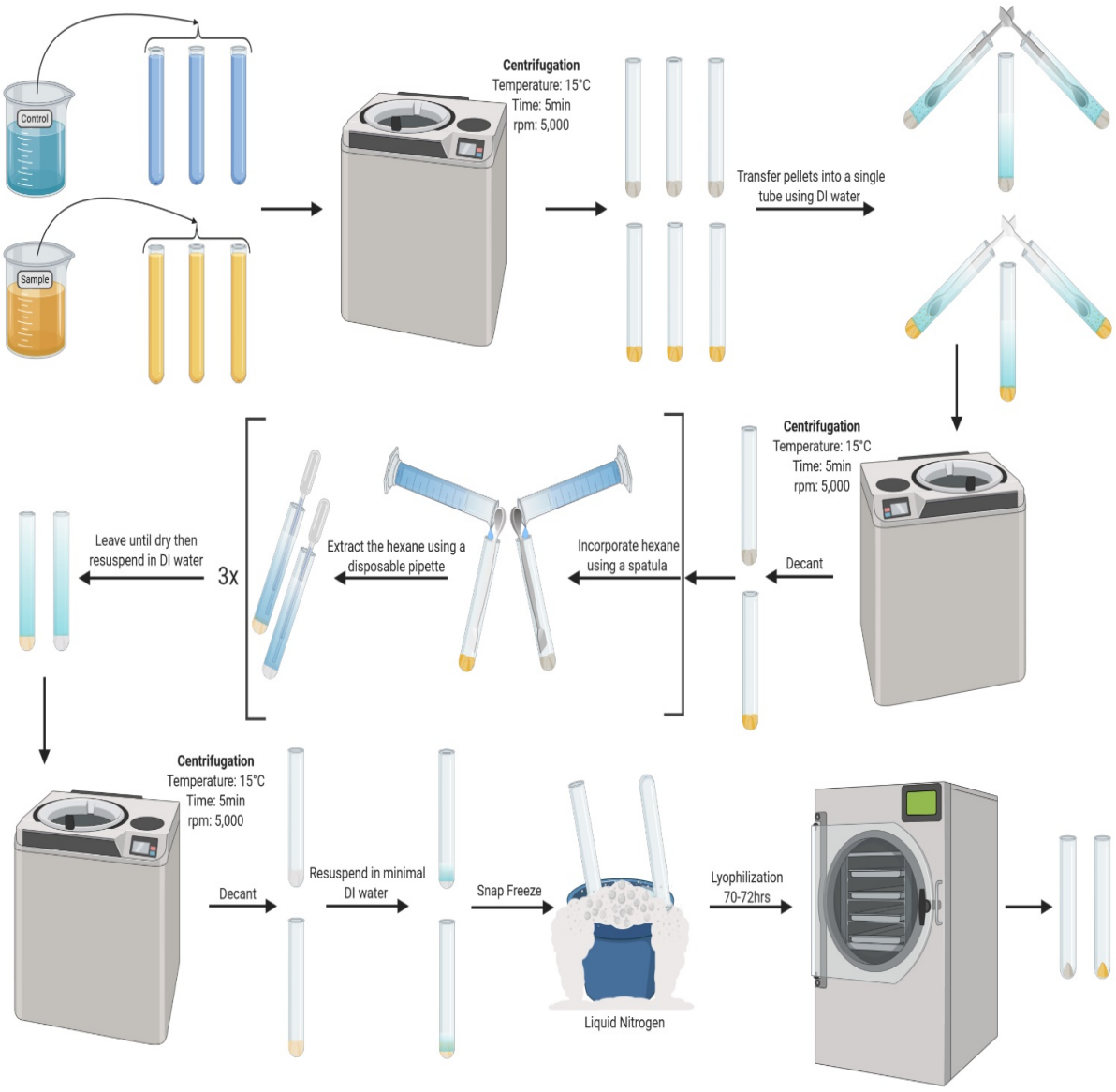

Figure 2.12. Fabrication process representing capsule collection and lyophilization

2.2 Polymer Yield after Formulation:

Table 2.1. Average Polymer yield percentage after lyophilization

Type of Polymer Microbubble	Yield of Polymer
100% PLA	81%
10%Ab2:90%PLA	80%
20%Ab2:80%PLA	84%
30%Ab2:70%PLA	82%
50%Ab2:50%PLA	80%
10%Ab1:90%PLA	72%

2.3 Characterization of Polymer Microbubbles

Polymer microbubbles characterized to see the formulation of microbubbles, its surface, and morphology. Various characterization techniques used in this study were Multisizing, Microscopy, and Fluorescent Microscopy. All the techniques are briefly explained with the results as follows:

2.3.1 Size Distribution Measurement: Multisizing: The basis of particle analyzer is the Coulter Principle, also known as the Electrical sensing zone, to detect particles regardless of the particle's nature, color, and shape. Multisizer Coulter Counter is a highly versatile particle counting and characterization system. The system calculates an average concentration of microbubbles per ml per decade, particle average mean and average median diameter in micrometers, and standard deviation.

Sample Preparation: It is sensitive equipment, so sample preparation is an important step. The dry powder after the freeze-drying process washed using centrifugation to collect the microbubbles. Microbubbles were collected using centrifugation at 300xg for three times. Different speeds have been compared (300,600,900 xg), and after observation, we can say that at 300 xg, we got the optimum range of 3-5 μm sized microbubbles. Microbubble sample was too concentrated, so 10 fold dilution in 1 X PBS was done, followed by sample characterization in filtered acetone.

2.3.2 Microscopy

Sample Preparation: After getting the concentration from the multisizing, it was required to dilute the sample to make microscopic slides. The sample diluted with the desired concentration of 5.40E+07 microbubble/ml.

2.4 Multisizing and Microscopy Results

The results for the multisizer and microscopy images were shown from Figure 2.13 to Figure 2.24 for the different blend ratios and the results for multisizer where average concentrations of microbubbles and average mean and median diameter were tabulated in Table 2.2.

- **100%PLA**

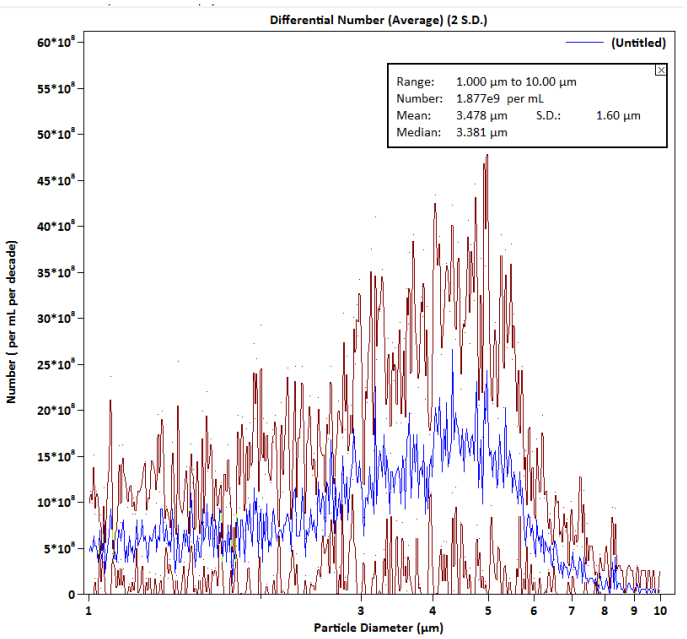

Figure 2.13. 100% PLA Average Multisizer representation

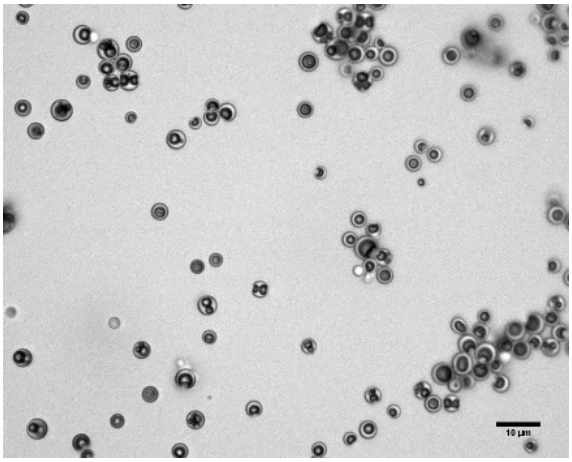

Figure 2.14. 100% PLA Microscopy Image

- **10%Ab2:90%PLA**

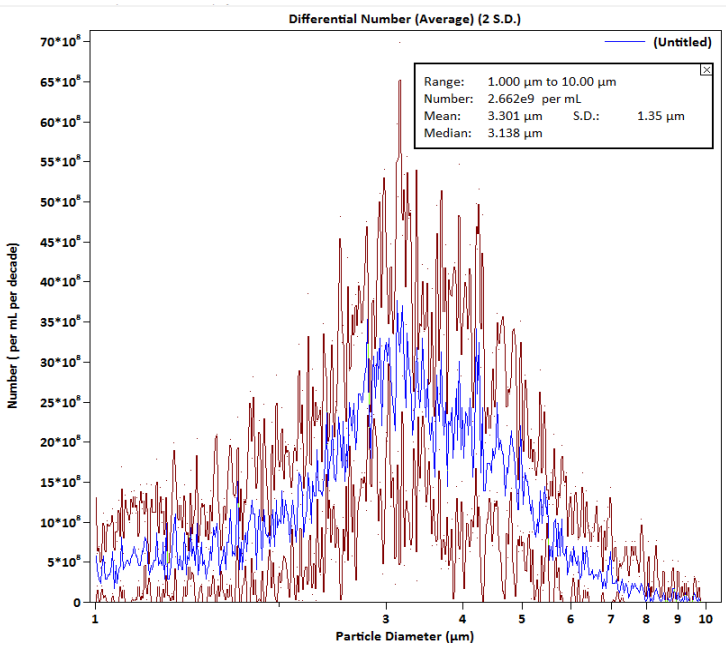

Figure 2.15. 10%Ab2:90%PLA Average Multisizer representation

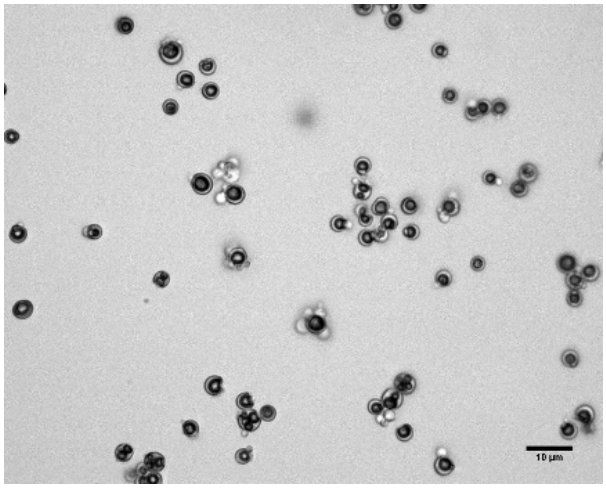

Figure 2.16. 10%Ab2:90%PLA Microscopy Image

- **20%Ab2:80%PLA**

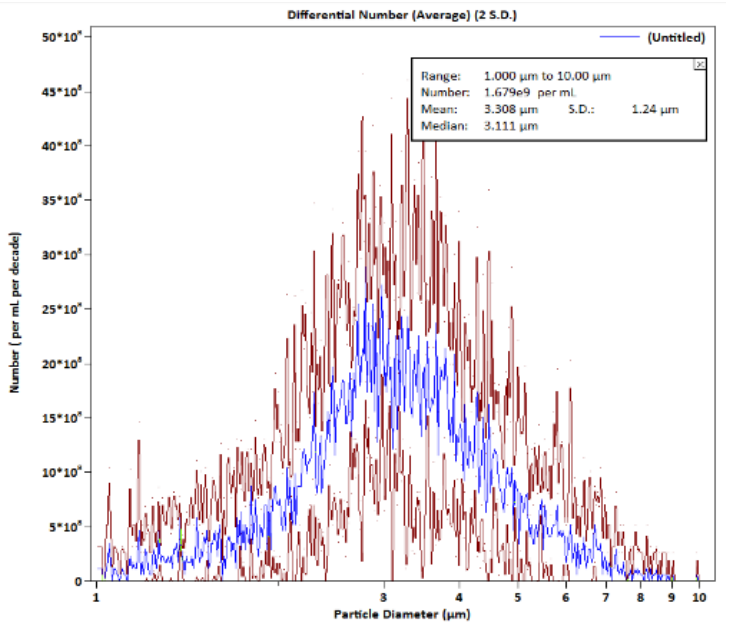

Figure 2.17. 20%Ab2:80%PLA Average Multisizer representation

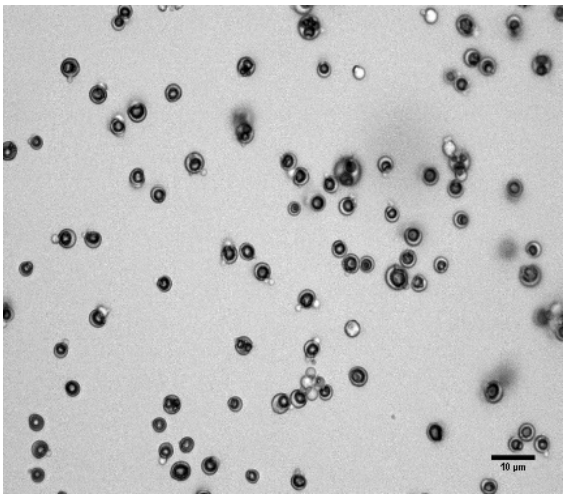

Figure 2.18. 20%Ab2:80%PLA Microscopy Image

- **30%Ab2:70%PLA**

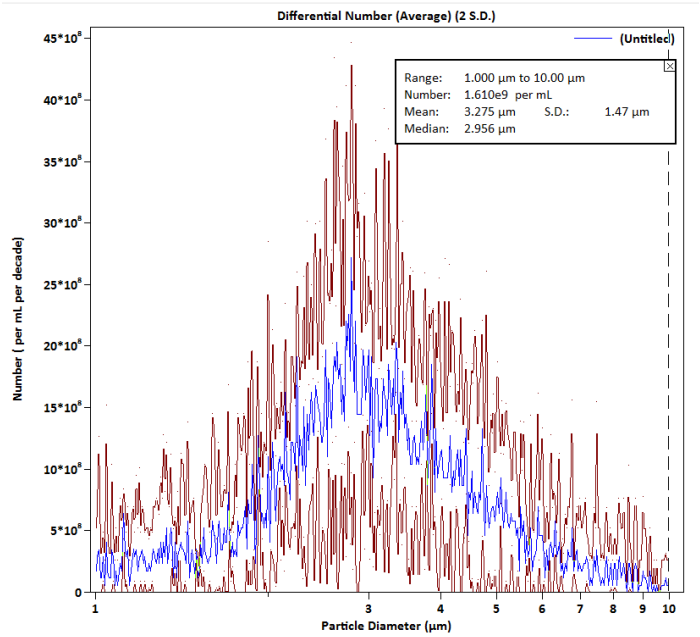

Figure 2.19. 30%Ab2:70%PLA Average Multisizer representation

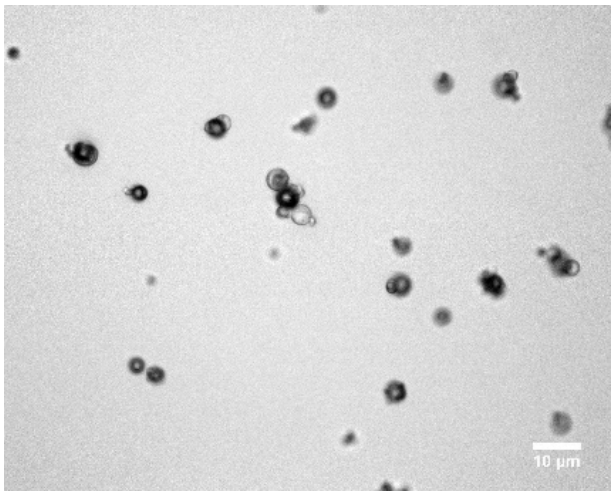

Figure 2.20. 30%Ab2:70%PLA Microscopy Image

- **50%Ab2:50%PLA**

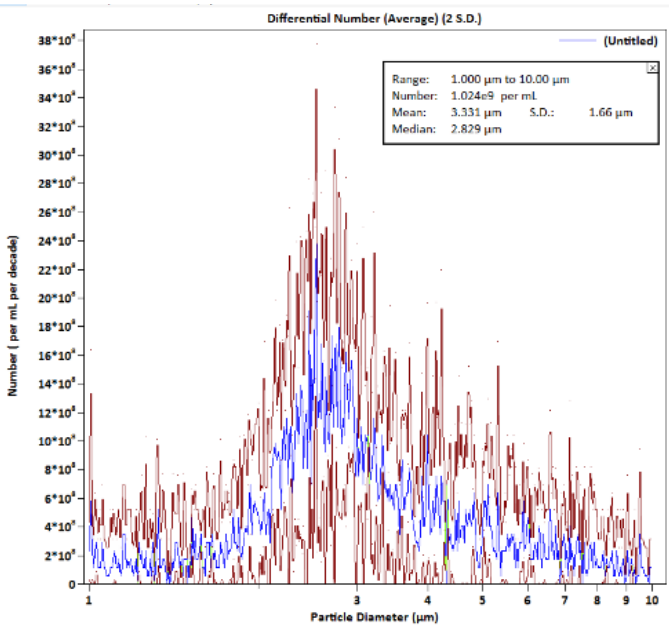

Figure 2.21. 50%Ab2:50%PLA Average Multisizer representation

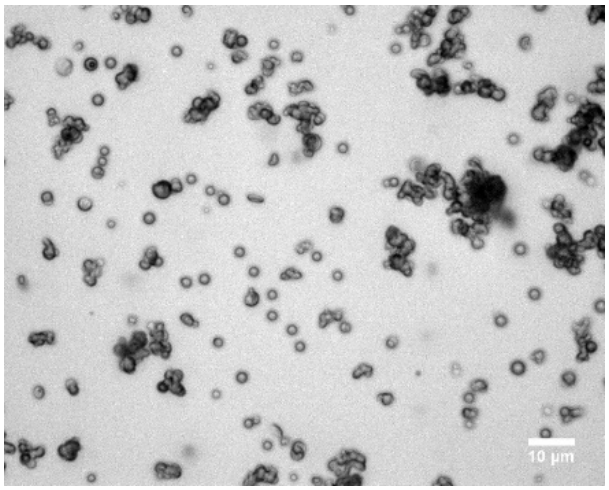

Figure 2.22. 50%Ab2:50%PLA Microscopy Image

- **10%Ab1:90%PLA**

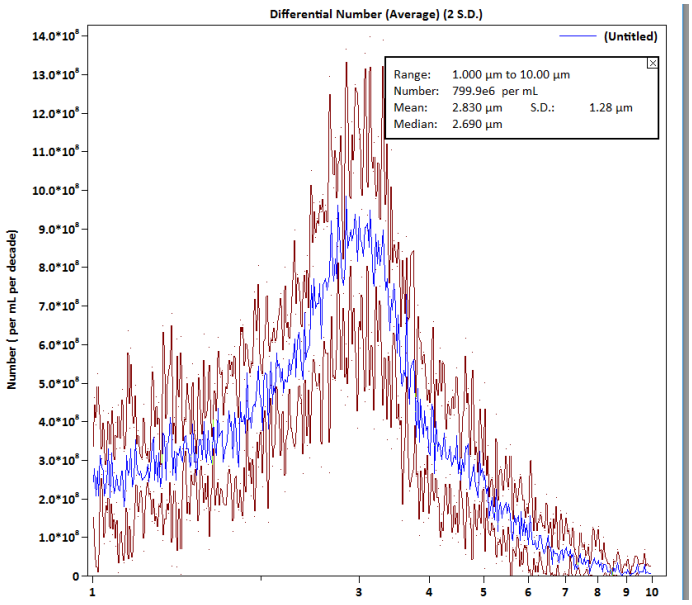

Figure 2.23. 10%Ab1:90%PLA Average Multisizer representation

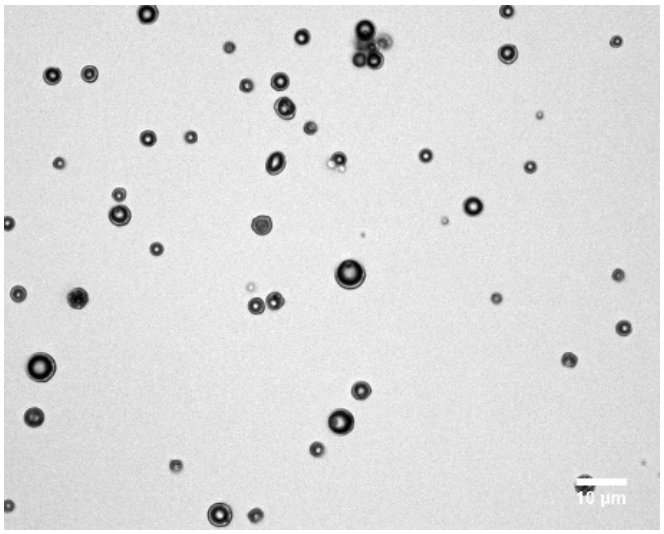

Figure 2.24. 10%Ab1:90%PLA Microscopy Image

Table 2.2. Average concentration, the average mean and median diameter, and standard deviation.

Type of Polymer Microbubbles	Average Concentration (microbubbles/ml)	Average Mean Diameter	Average Median Diameter	Standard Deviation
100% PLA	1.877E+09	3.45μm	3.33μm	1.59μm
10%Ab2:90%PLA	2.66E+09	3.29μm	3.12μm	1.34μm
20%Ab2:80%PLA	1.67E+09	3.30μm	3.12μm	1.23μm
30%Ab2:70%PLA	1.61E+09	3.27μm	2.95μm	1.47μm
50%Ab2:50%PLA	1.02E+09	3.33μm	2.82μm	1.66μm
10%Ab1:90%PLA	7.99E+08	2.83μm	2.69μm	1.28μm

2.5 Fluorescent Microscopy:

Nile Red, a fluorescent dye, was incorporated inside the microbubbles shell to see the internal structure as it can stain polymer chains. During the double emulsion process, Nile red added in the first emulsion with the polymer. Images are shown in Figure 2.19, and Figure 2.20 shows the bright field and fluorescent microscopy images for different locations for 10%Ab2:90%PLA polymer microbubbles blend ratio.

Results:

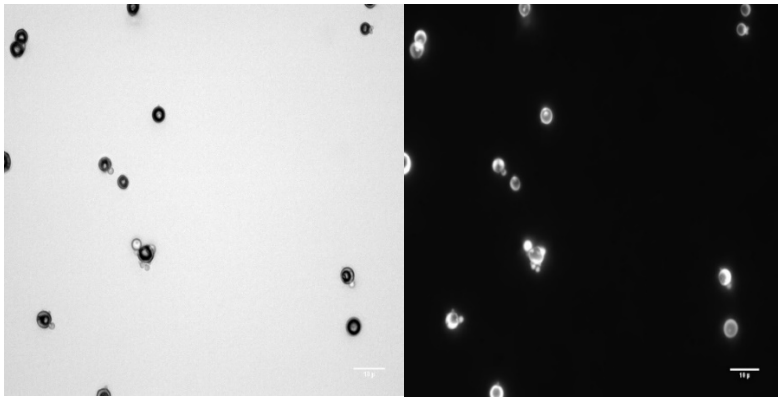

Figure 2.19. Bright Field Microscopy Image
(Left) and Fluorescent Microscopy Image (Right) Location 1

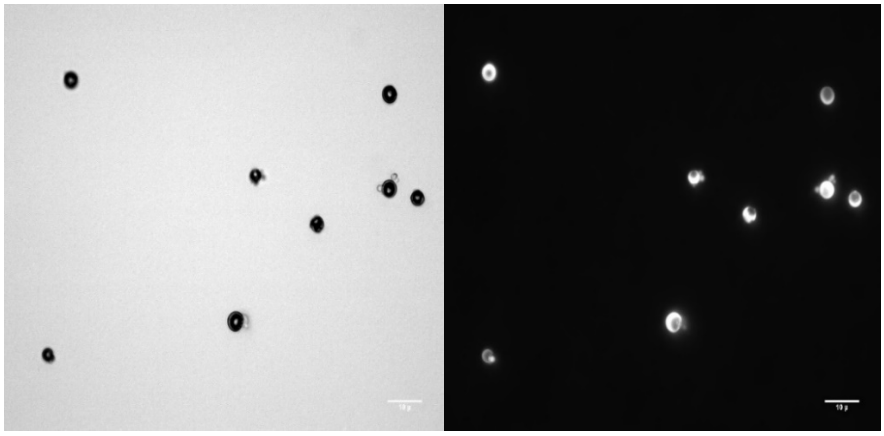

Figure 2.20 Bright Field Microscopy Image
(Left) and Fluorescent Microscopy Image (Right) Location 2

CHAPTER 3

DETERMINING THE PRESENCE OF AZOBENZENE INSIDE THE POLYMER MICROBUBBLE SHELL AND ITS ACTIVATION WITH UV LIGHT

Introduction

After the formulation of polymer microbubbles, the next task was to determine the presence of Azobenzene incorporation inside the shell. Azobenzene is a UV sensitive polymer and gets activated when exposed to UV light. As explained in the synthesis and activation of Azobenzene, Azobenzene isomer goes from trans isomer (Z form) state to cis isomer (E form) state with the light intensity of 6.2mW /cm2 for 15 minutes. This process is known as photoisomerization or trans-cis isomerization. The trans-azobenzene easily isomerizes to the cis isomer by irradiation of the trans isomer with a wavelength between 320–350 nm, and the trans isomer is recovered when the cis isomer irradiated with light of 400–450 nm, or heated. As shown in Figure 3.1, the conversion from trans-cis is a reversible process. The trans to cis photochemical conversion takes place within picoseconds, while from cis to trans, the thermal relaxation takes milliseconds to days. This photoisomerization result changes in the physical properties of the molecule, such as a change in molecular geometry. The structure of trans isomer is almost flat whereas cis isomer present angular geometry.(Merino & Ribagorda, 2012)Photo isomerization also results in a change in the dipole moment and absorption spectrum.

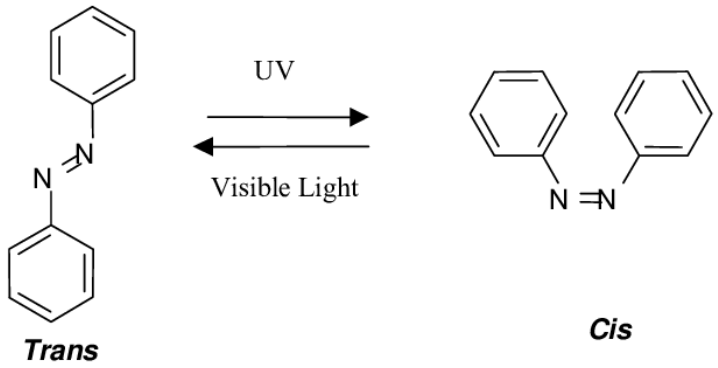

Figure 3.1. Photo-isomerization process of Azobenzene (Merino & Ribagorda, 2012)

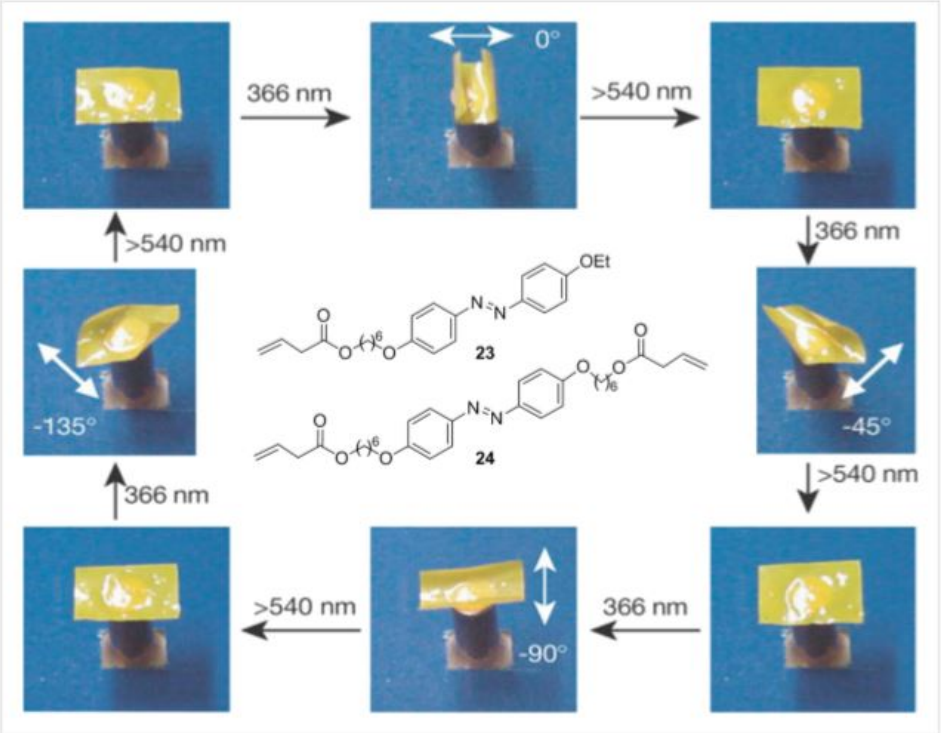

Figure 3.2. Effect of irradiation with linearly polarized light on azo-liquid crystal elastomer showing collapse and expansion of LCE films. (Yu et al., 2003)

Figure 3.2 explains the molecular motion of photoisomerization. The irradiation of azo polymers containing light-sensitive molecules leads to photo-contraction of the polymer resulting in the conversion of radiant energy to mechanical energy. (Yu et al., 2003)

3.1 UV/ visible Spectrum of Azobenzene:

Azobenzene isomers have specific absorbance in the UV/ visible spectrum. In Figure 3.3, for unsubstituted azobenzene, the trans isomer has a strong absorption peak at 320 nm for the π → π* transition and weak absorption at 440 nm for the n → π* transition. The cis-azobenzene has a stronger n → π* peak at 440 nm and has shorter wavelength peaks at 250 nm and280 nm. (Bunnett, 1962)(Merino & Ribagorda, 2012)

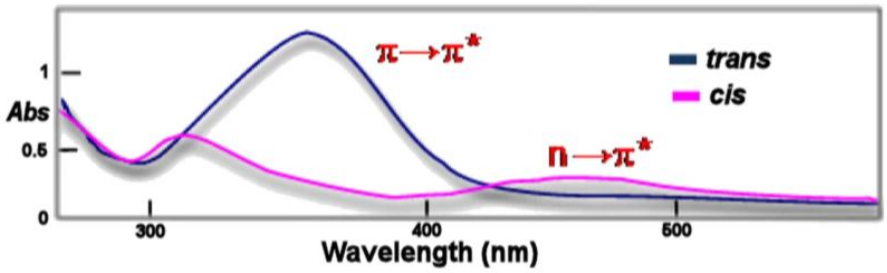

Figure 3.3. Representation of the Azobenzene UV spectrum.(Merino & Ribagorda, 2012)

3.2 Methods for determining the presence of Azobenzene inside the polymer microbubble shell and its activation with UV exposure:

3.2.1. UV-Vis Spectroscopy of microbubbles broken open by sonication: UV-Vis spectroscopy was one of the essential characterization techniques used to study the optical properties. UV-vis measures the absorption of light across the desired optical range when light strikes on microbubble core or anywhere where you have Azobenzene. Wavelength and absorbed light plotted on the graph giving information about light absorption by Azobenzene. Figure 3.4 explains the schematic representation of the UV-

Vis Spectroscopy setup. The sample dispensed into a cuvette and placed in the path between the optical light source and a detector.

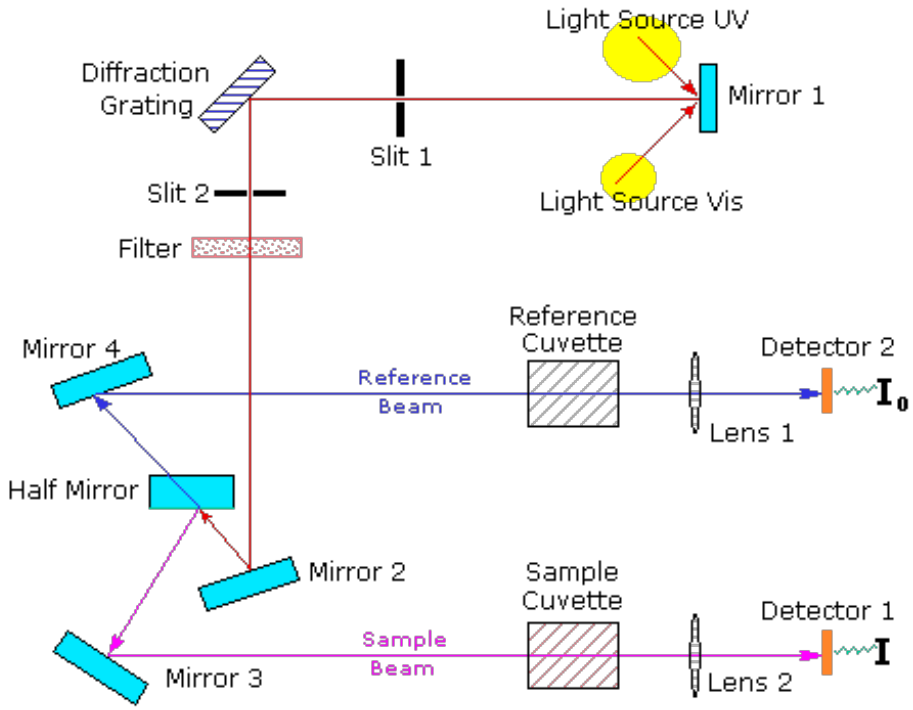

Figure 3.4. Schematic representation of UV-vis Spectroscopy setup (UV-Visible Spectroscopy)

Sample Preparation: Azobenzene incorporated in the shell of the microbubbles. Hence it was required to break the microbubbles. Microbubbles have broken down using bath sonication for 30 minutes at room temperature. Two samples prepared, one in which the microbubbles collected using centrifugation in a syringe tube and the other which had polymer powder obtained from lyophilization, is weighed out. Both types of samples, solution, and powder were dissolved in 1 x PBS and bath sonicated for 30 minutes. UV-vis spectroscopy performed on both the samples before and after UV exposure. The

samples then exposed to UV light for 15 minutes. Homogenous exposure to the UV light ensured by lightly shaking the vial to mix the sample after every 5 minutes of exposure.

3.3 Results

UV-Vis Spectroscopy performed on the sample contained in Quartz cuvette and placed between the source and the detector.

UV/Vis Spectroscopy on Unwashed sample

In this analysis, the term 'unwashed sample' used when formulated polymer powder was directly weighed out (20 mg) and diluted with 3 ml 1xPBS.The prepared solution was bath sonicated for 30 minutes at room temperature. After the microbubbles were wholly broken, the UV/ Vis Spectroscopy done before exposing it to UV light. Then the sample was exposed to UV light with an intensity of 6.2mW/cm2 for a total of 15 minutes, and the results were plotted as shown in Figure 3.5

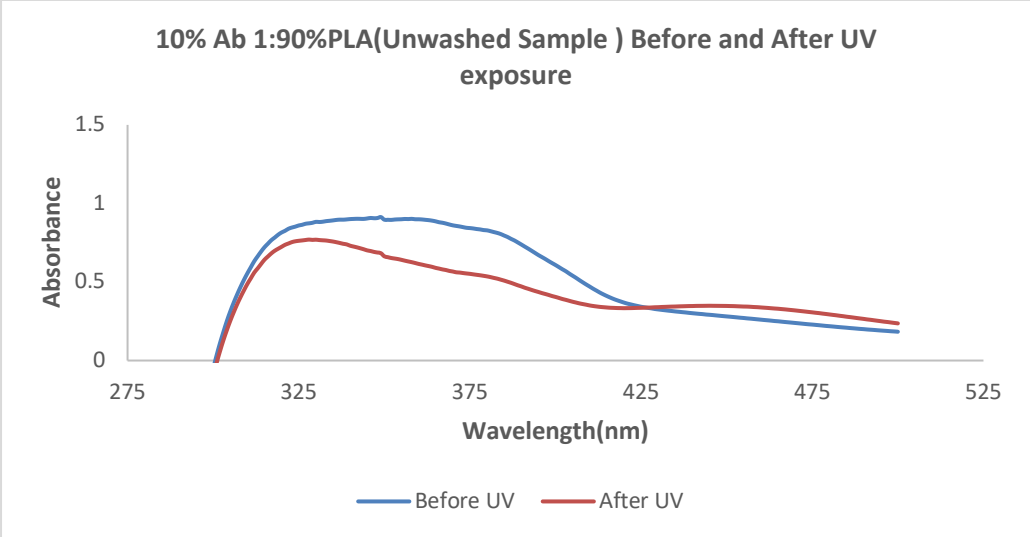

Figure 3.5. Absorption spectra of 10% Ab 1:90%PLA (Unwashed Sample) before and after UV exposure [UV exposure time: 15 minute; Light Intensity: 6.2mW /cm2]

UV/Vis Spectroscopy on Washed sample

In this analysis, the term 'washed sample' used when the polymer powder centrifuged three times to collect the microbubbles. The microbubbles were light and rose on the top of the centrifuge tube, and the supernatant discarded. The collected microbubbles then diluted in 3 ml of a total of 1xPBS with the desired concentration of 5.4E+07 microbubble/ml. The prepared solution was bath sonicated for 30 minutes at room temperature. After the bubbles have wholly broken, the UV/ Vis Spectroscopy performed before exposing it to UV light. Then the sample was exposed to UV light with an intensity of 6.2mW/cm2 for a total of 15 minutes, and the results were plotted as shown in Figure 3.6 and Figure 3.7 for 100% PLA and 20%Ab2:80%PLA before and after UV exposure.

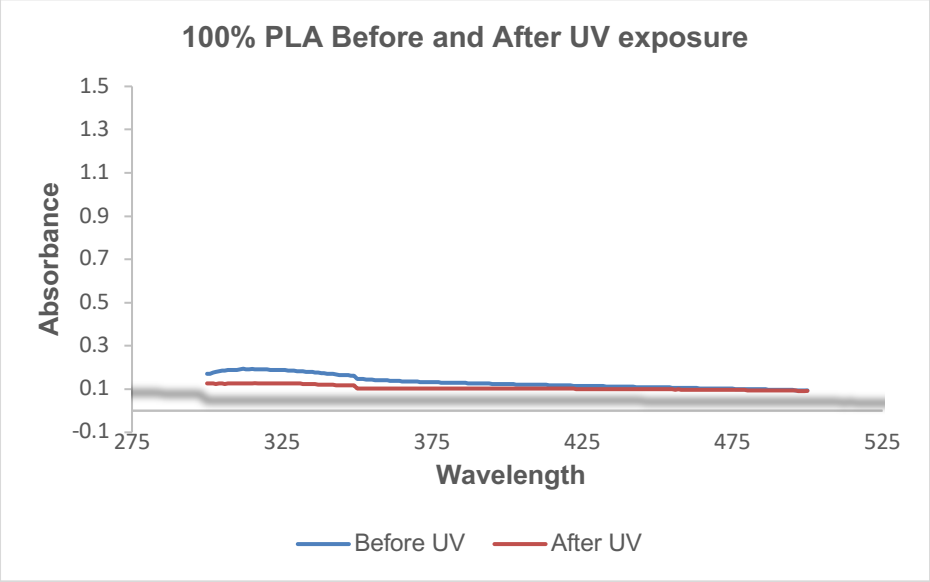

Figure 3.6. Absorption spectra of 100% PLA (washed sample) before and after UV exposure [UV exposure time: 15 minute; Light Intensity: 6.2mW /cm2]

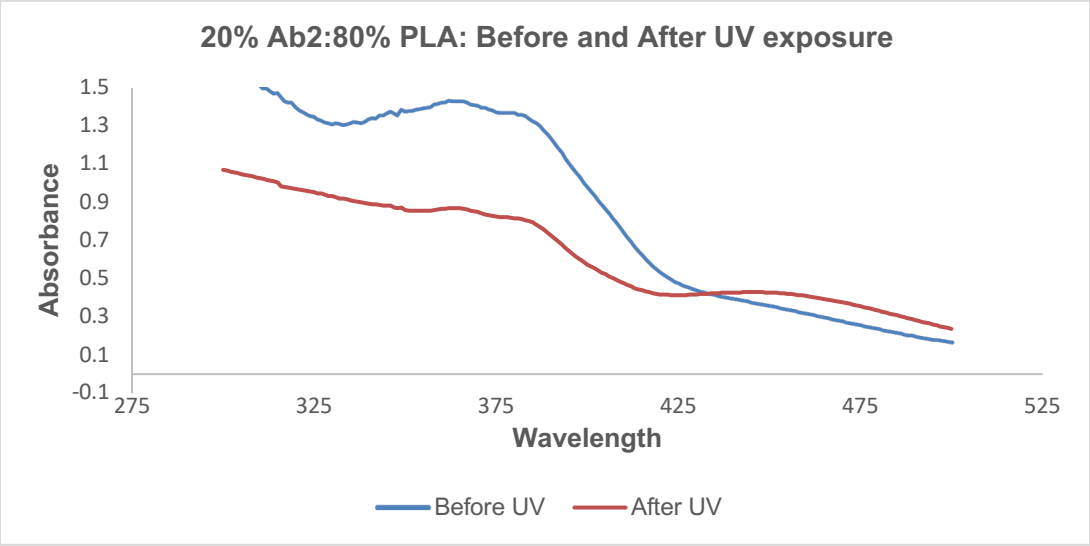

Figure 3.7. Absorption spectra of 20% Ab2: 80%PLA (washed sample) before and after UV exposure [UV exposure time: 15 minute; Light Intensity: 6.2mW /cm2]

3.4 Conclusion:

From the results above, we can conclude that Azobenzene present inside the microbubbles have activated after exposing it to UV light. In Figure 3.6., 100% PLA polymer microbubbles show no peaks for the wavelength and absorbance for both before and after UV exposure. But, with 20% Ab2:80%PLA polymer microbubbles, in Figure 3.7., an absolute absorption peak was observed at 375 nm before UV exposure and a more definite absorption peak at 450 nm after UV exposure. As a positive control, the optical analysis performed on the unwashed sample of 10%Ab1:90% PLA observes a strong absorbance peak at 325 nm before UV exposure and 425-450 nm after UV exposure. Hence, these results imply that azobenzene was present inside the microbubbles and have activated upon exposure to UV light.

3.5 Scanning Electron Microscopy Analysis of fabricated microbubbles

SEM data examine the surface and cross-sectional morphology of microbubbles. The structural differences observed after UV exposure. The structural difference was in the form of pores, cracks, golf ball-like structures denoted as G-structures.

Sample Preparation: SEM slides prepared for both before and after the UV exposed sample. Microbubbles collected after centrifugation diluted in a total of 300 µl of the 1x PBS solution. Microbubble dilution was to achieve the desired concentration of 5.4E+07 microbubbles/ml. The same sample then exposed to UV light for 15 minutes. Make sure the sample was dried entirely. An ultra-thin coating of gold-palladium (Au/PD) was sputter-coated onto a non-conducting microbubble sample. The conducting layer of metal on the microbubble sample created to improve the secondary electron signal required for topographic examination in the SEM and to reduce thermal damage.

3.6 Results:

The analysis divided into three steps: Firstly, the structural differences observed before and after UV exposure. Visual analysis was done on 10 µm and 2 µm SEM area locations manually. In visual, quantitative analysis, the total number of pores, cracks, g-structures calculated, as shown in Figure 3.8. Melting observed after exposing it to UV light. The results were as follows:

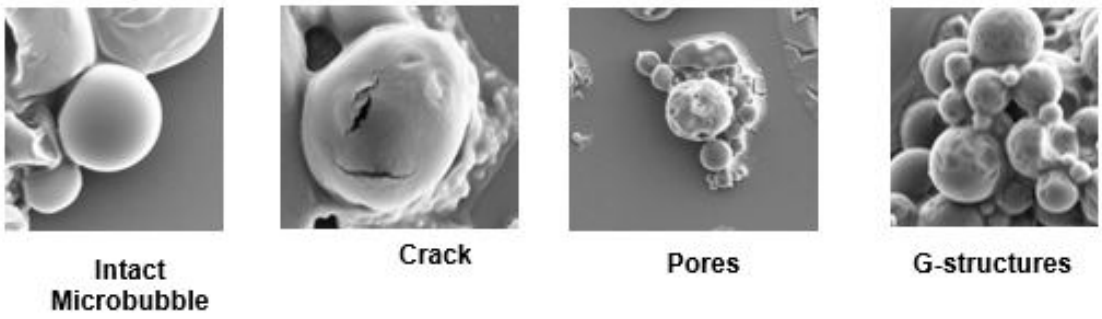

Figure 3.8. SEM images representing structural differences

Results:

In this section from Figure 3.9-Figure3.18, SEM images were represented for different blend ratios for different locations before and after UV exposure.

SEM images for before and after UV exposure

- **100%PLA**

Before UV exposure

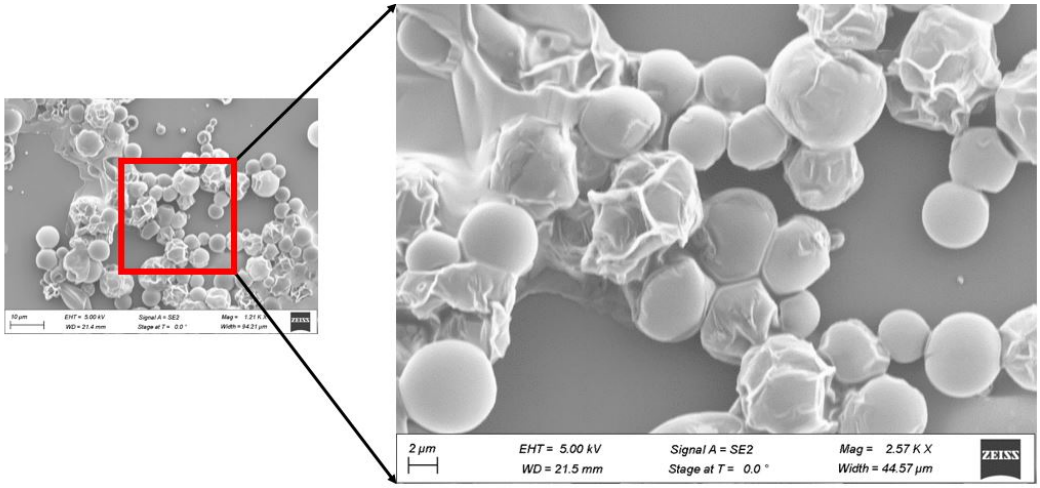

Figure 3.9. 100% PLA SEM images before UV exposure

After UV exposure

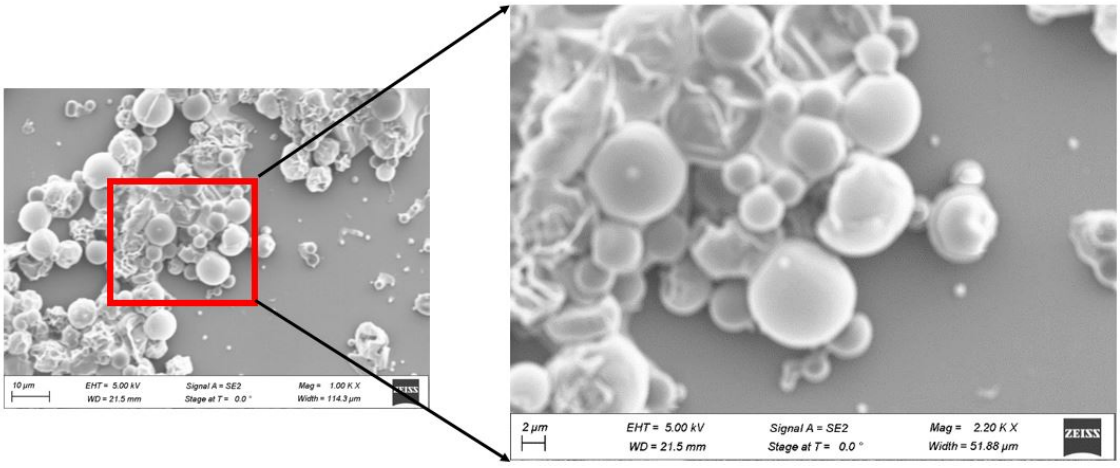

Figure 3.10. 100% PLA SEM images after UV exposure

SEM images for before and after UV exposure

- **10% Ab2: 90% PLA**

Before UV exposure

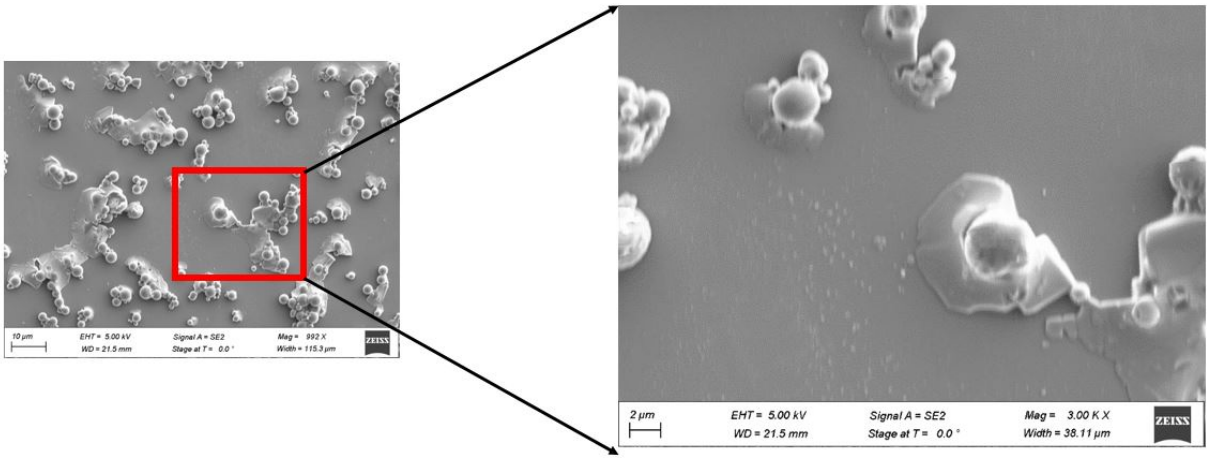

Figure 3.11. 10% Ab2:90% PLA SEM images before UV exposure

After UV exposure

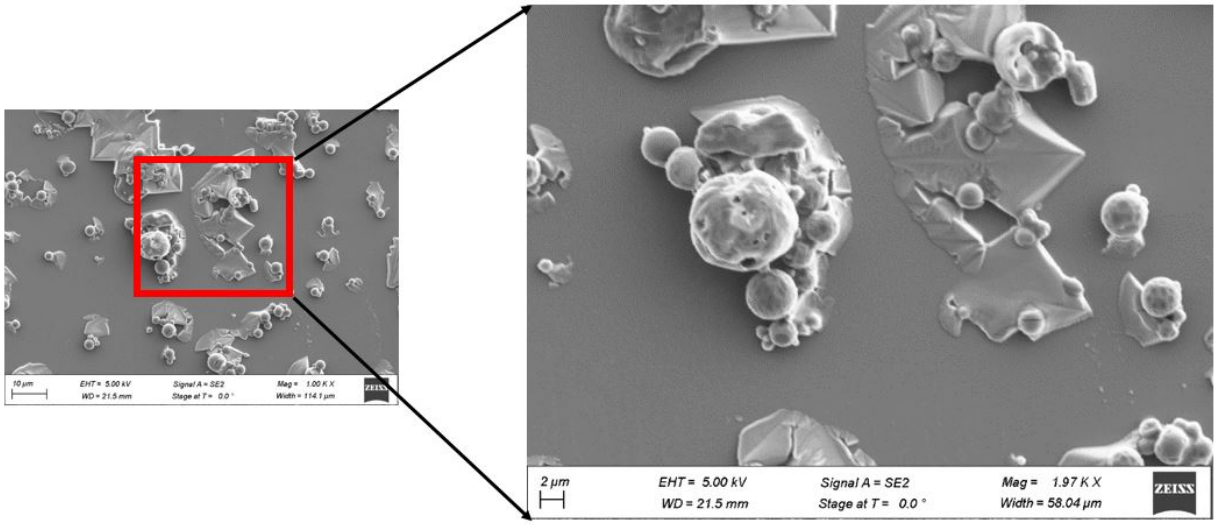

Figure 3.12. 10% Ab2:90% PLA SEM images after UV exposure

SEM images for before and after UV exposure

- **30% Ab2: 70% PLA**

Before UV exposure

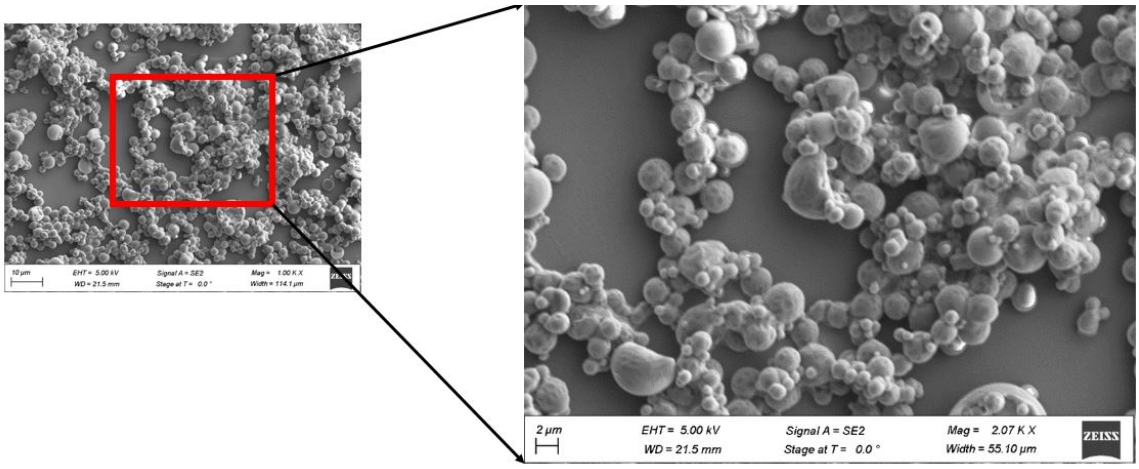

Figure 3.13. 30% Ab2:70% PLA SEM images before UV exposure

After UV exposure

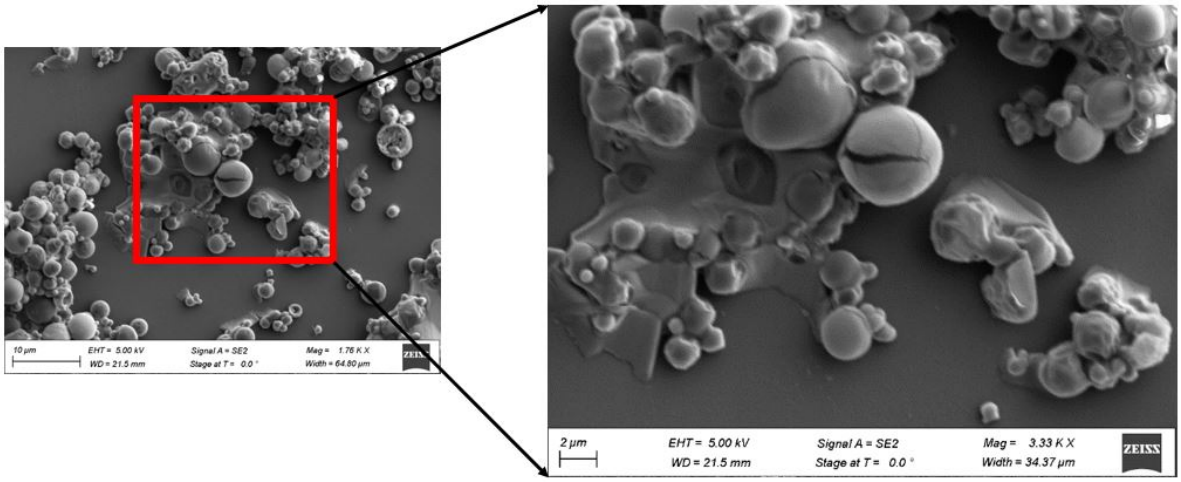

Figure 3.14. 30% Ab2:70% PLA SEM images after UV exposure

SEM images for before and after UV exposure

- **50% Ab2: 50% PLA**

Before UV exposure

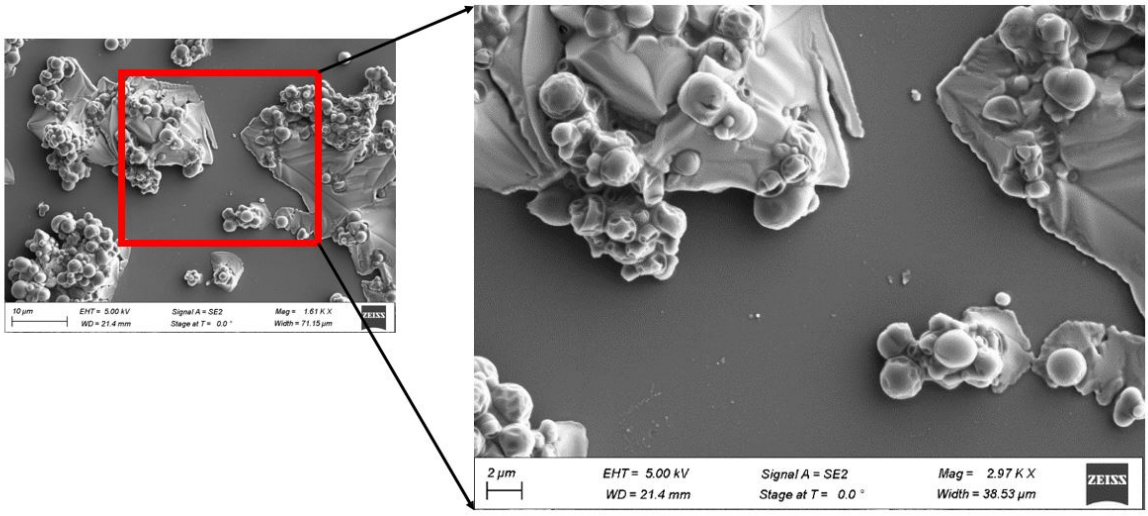

Figure 3.15. 50% Ab2:50% PLA SEM images before UV exposure

After UV exposure

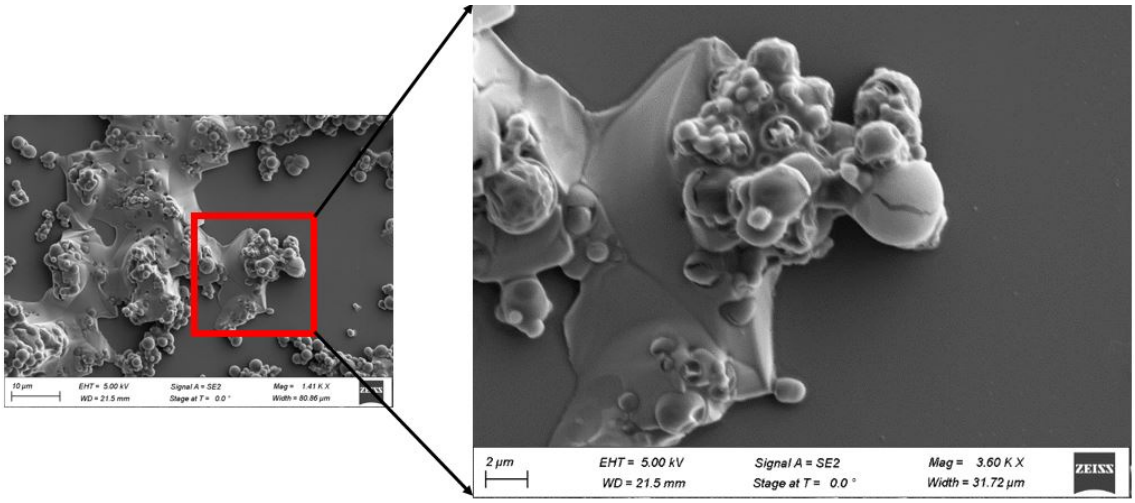

Figure 3.16. 50% Ab2:50% PLA SEM images after UV exposure

SEM images for before and after UV exposure

- **10%Ab1: 90% PLA**

Before UV exposure

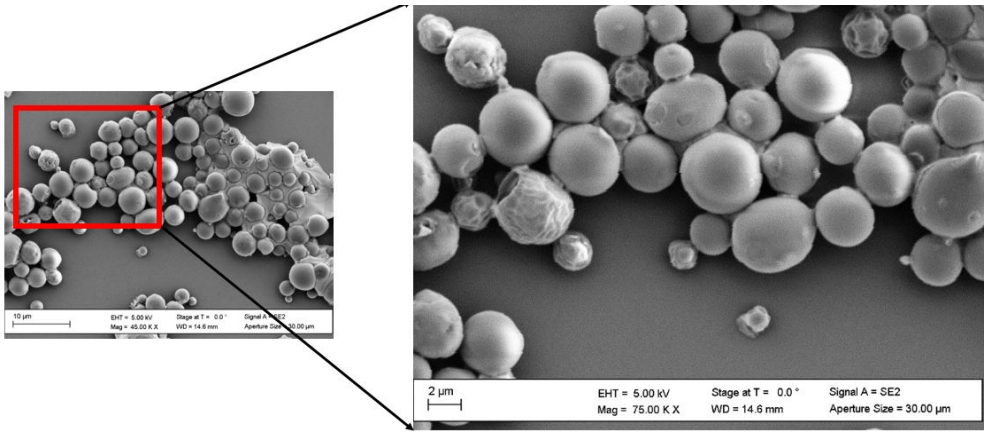

Figure 3.17. 10% Ab1:90% PLA SEM images before UV exposure

After UV exposure

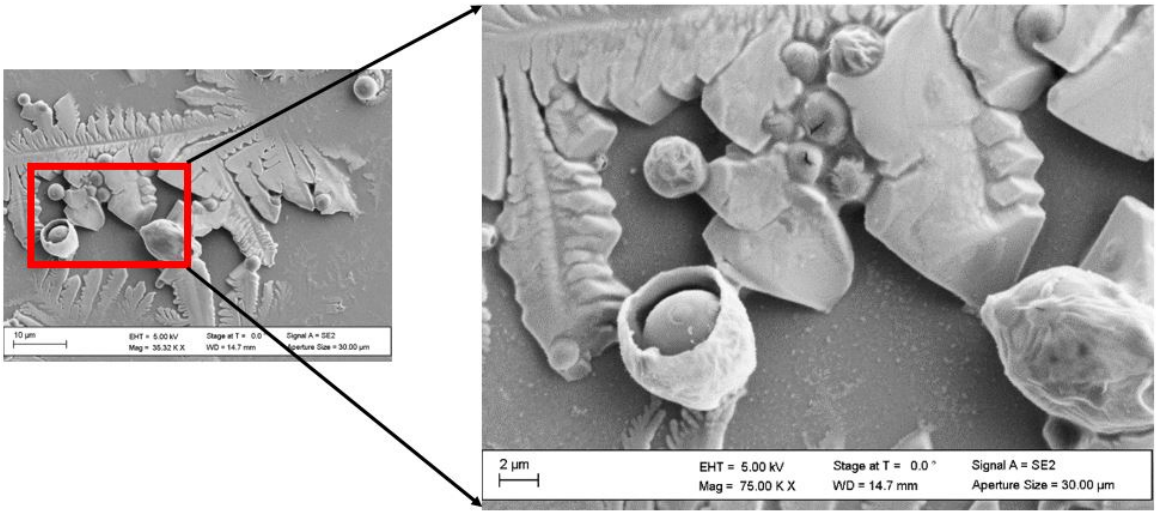

Figure 3.18. 10% Ab1:90% PLA SEM images after UV exposure

Quantitative Analyses of Pores, Cracks, and G-Structure

1. 100% PLA Before and After Exposure:

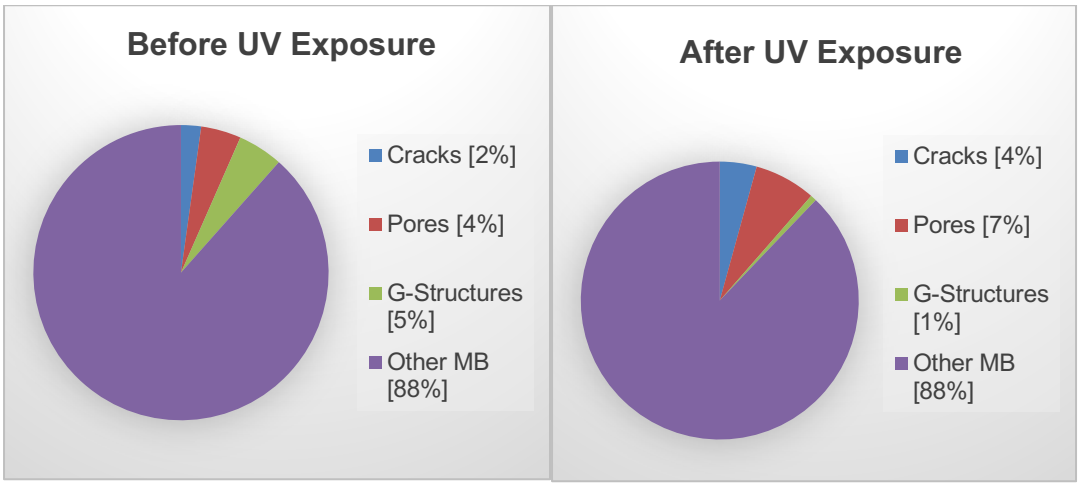

Figure 3.19. Structural difference comparison of 100% PLA before and after UV exposure

Table 3.1. 100% PLA Average number of total microbubbles; cracks; pores; G-structures

100% PLA Before UV exposure					
	Magnification (K X)	Total number of microbubbles	Cracks	Pores	G-Structures
Average:	40	61	1	3	3
100% PLA After UV exposure					
	Magnification (K X)	Total number of microbubbles	Cracks	Pores	G-Structures
Average:	41.11	70	3	5	1

2. 10% Ab 2: 90% PLA Before and After Exposure:

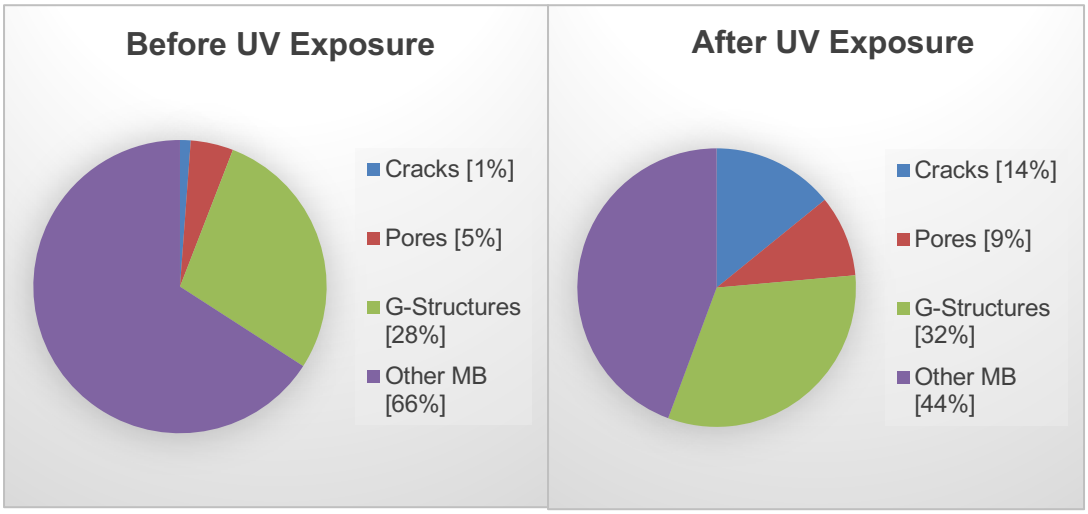

Figure 3.20. Structural difference comparison of 10% Ab2:90% PLA before and after UV exposure

Table 3.2. 10%Ab2:90% PLA Average number of total microbubbles; cracks; pores; G-structures

10%Ab2:90%PLA Before UV exposure					
	Magnification (K X)	Total number of microbubbles	Cracks	Pores	G-Structures
Average:	2.69	28	1	1	8
10%Ab2:90%PLA After UV exposure					
	Magnification (K X)	Total number of microbubbles	Cracks	Pores	G-Structures
Average:	2.27	35	5	3	11

3. 30% Ab2:70% PLA Before and After Exposure:

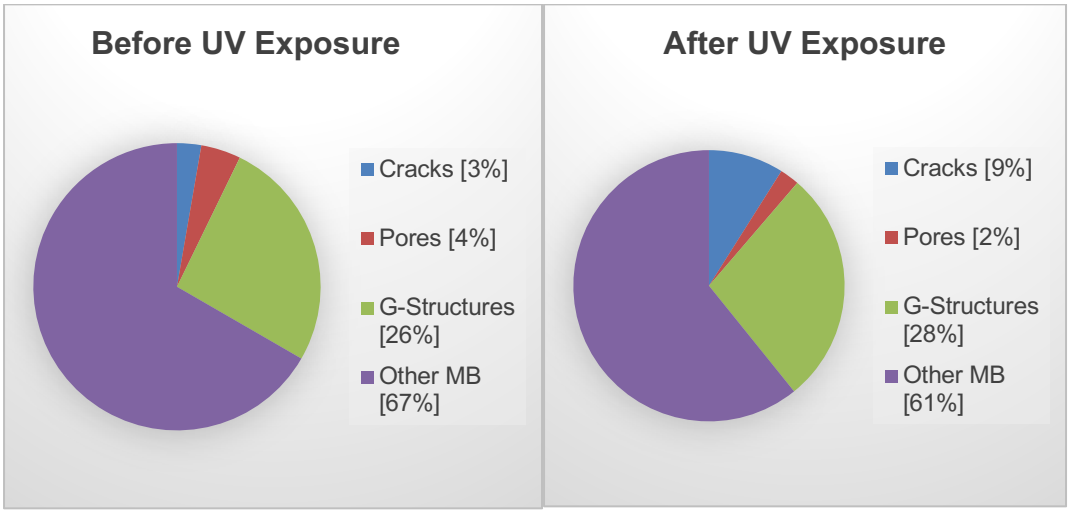

Figure 3.21. Structural difference comparison of 30% Ab2:70% PLA before and after UV exposure

Table 3.3. 30%Ab2:70% PLA Average number of total microbubbles; cracks; pores; G-structures

30%Ab2:70%PLA Before UV exposure					
	Magnification (K X)	Total number of microbubbles	Cracks	Pores	G-Structures
Average:	2.15	208	6	9	54
30%Ab2:70%PLA After UV exposure					
	Magnification (K X)	Total number of microbubbles	Cracks	Pores	G-Structures
Average:	2.72	100	9	2	28

4. 50% Ab2:50% PLA Before and After Exposure:

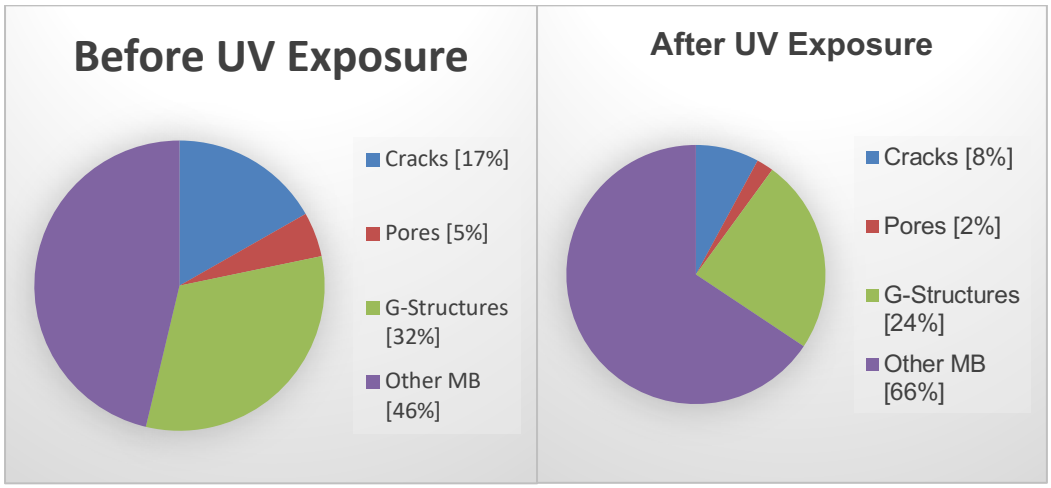

Figure 3.22. Structural difference comparison of 50% Ab2:50% PLA before and after UV exposure

Table 3.4. 50%Ab2:50% PLA Average number of total microbubbles; cracks; pores; G-structures

50%Ab2:50%PLA Before UV exposure					
	Magnification (K X)	Total number of microbubbles	Cracks	Pores	G-Structures
Average:	2.54	107	18	5	34
50%Ab2:50%PLA After UV exposure					
	Magnification (K X)	Total number of microbubbles	Cracks	Pores	G-Structures
Average:	2.70	110	9	2	27

5. 10% Ab 1: 90% PLA Before and After Exposure:

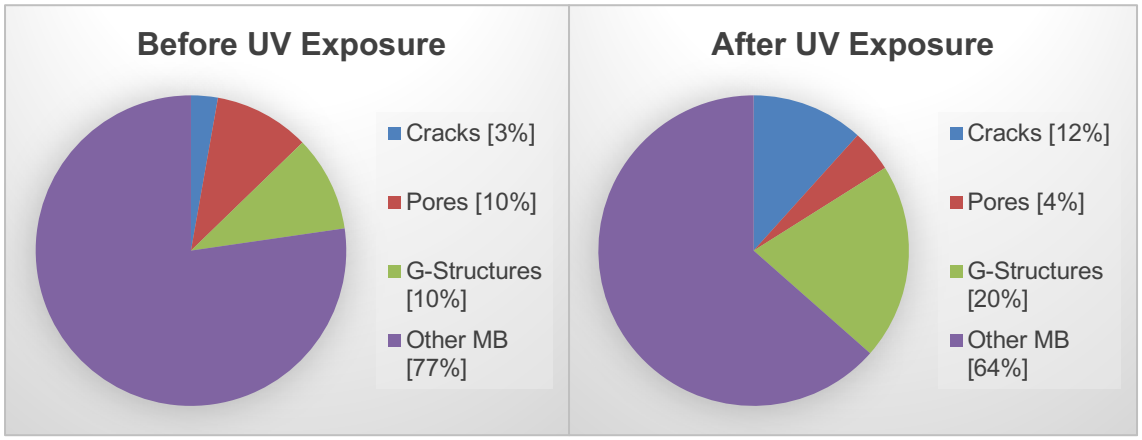

Figure 3.23. Structural difference comparison of 10% Ab1:90% PLA before and after UV exposure

Table 3.5. 10%Ab1:90% PLA Average number of total microbubbles; cracks; pores; G-structures

10%Ab1:90%PLA Before UV exposure					
Location	Magnification (K X)	Total number of microbubbles	Cracks	Pores	G-Structures
Average:	45.76	84	2	8	8
10%Ab1:90%PLA After UV exposure					
Location	Magnification (K X)	Total number of microbubbles	Cracks	Pores	G-Structures
Average:	38.91	34	4	2	7

Comparison of Pores, Cracks, and G-structures:

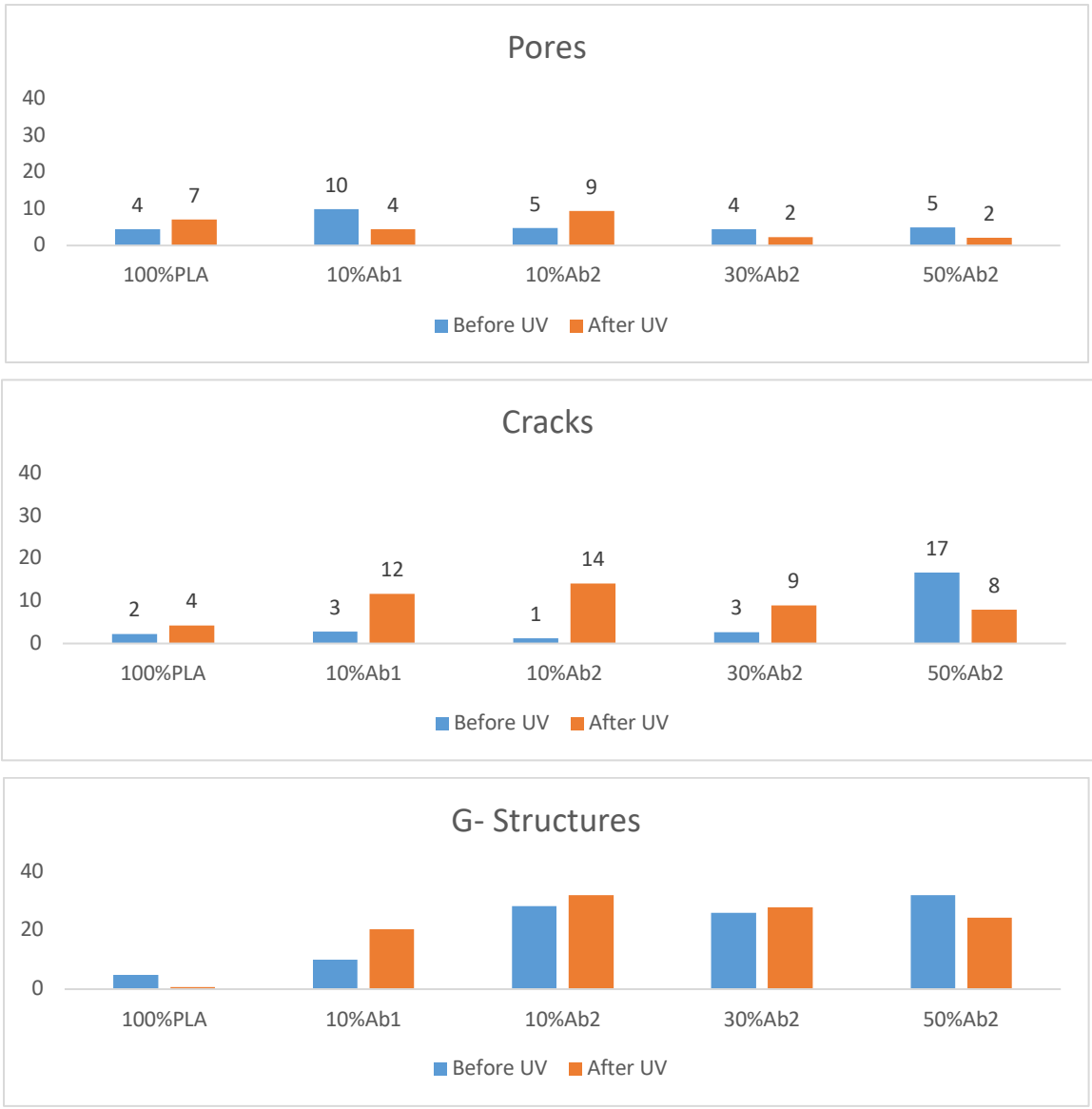

Figure 3.24. Summary of before and after UV exposure on different blend ratios of Azobenzene/PLA microbubbles. (A)Pores (B)Cracks (C)G-structures

3.7 Melting Observation Before and After UV exposure

100% PLA microbubbles

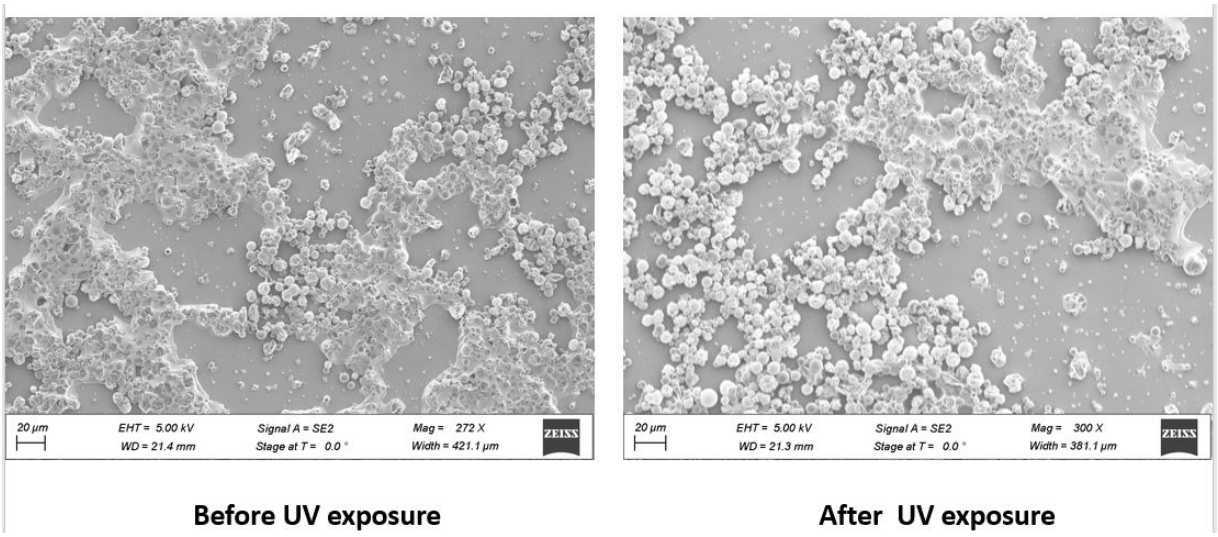

Figure 3.25. 100% PLA SEM images showing melting before and after UV exposure

10%Ab2:90% PLA microbubbles

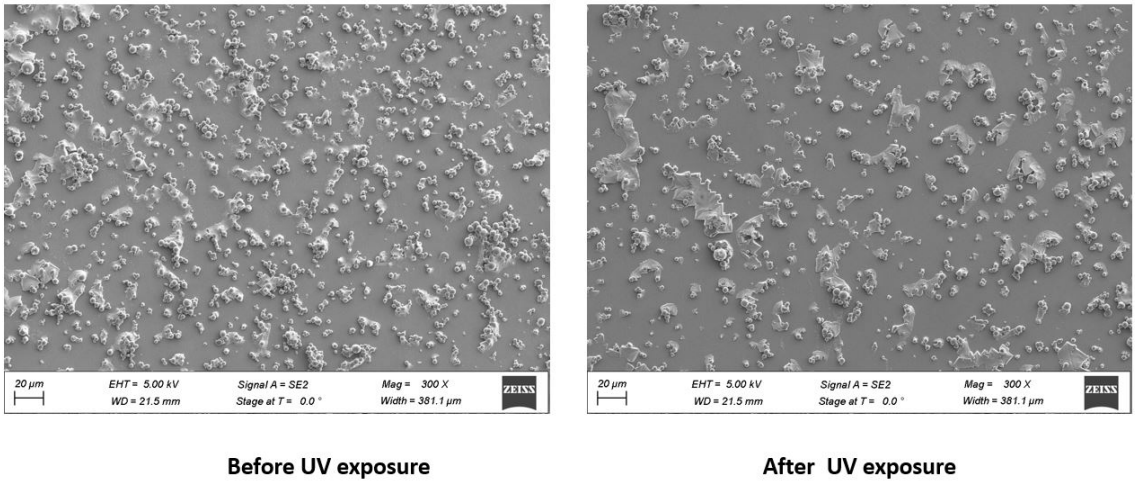

Figure 3.26. 10%Ab2:90% PLA SEM images showing melting before and after UV exposure

30%Ab2:70% PLA microbubbles

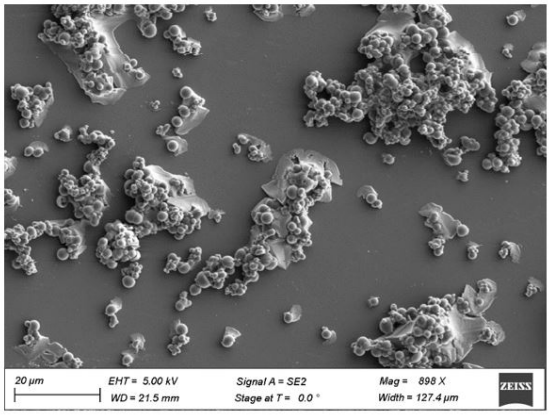

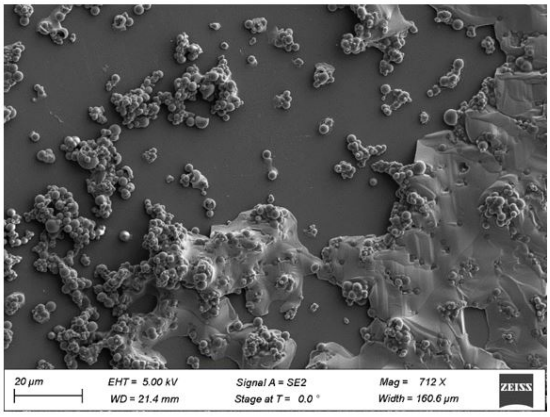

Before UV exposure **After UV exposure**

Figure 3.27. 30%Ab2:70% PLA SEM images showing melting before and after UV exposure

50%Ab2:50% PLA microbubbles

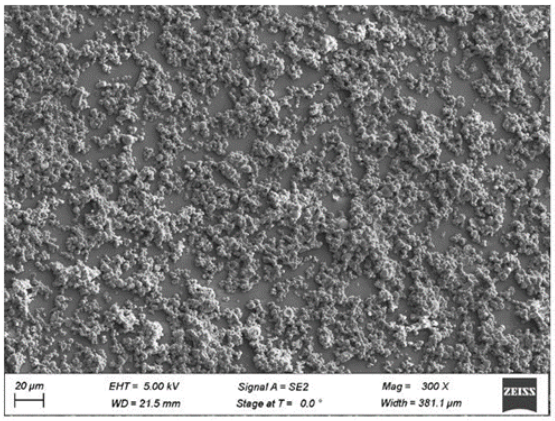

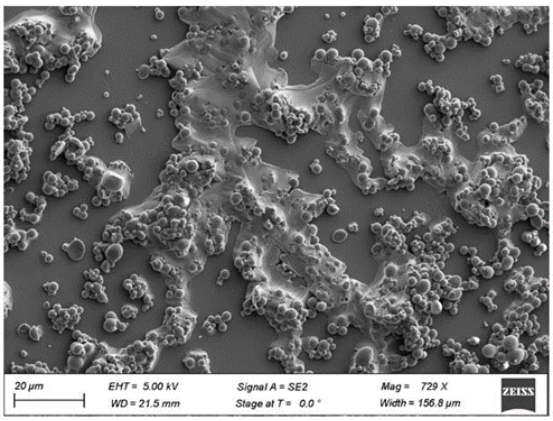

Before UV exposure **After UV exposure**

Figure 3.28. 50%Ab2:50% PLA SEM images showing melting before and after UV exposure

10%Ab1:90% PLA microbubbles

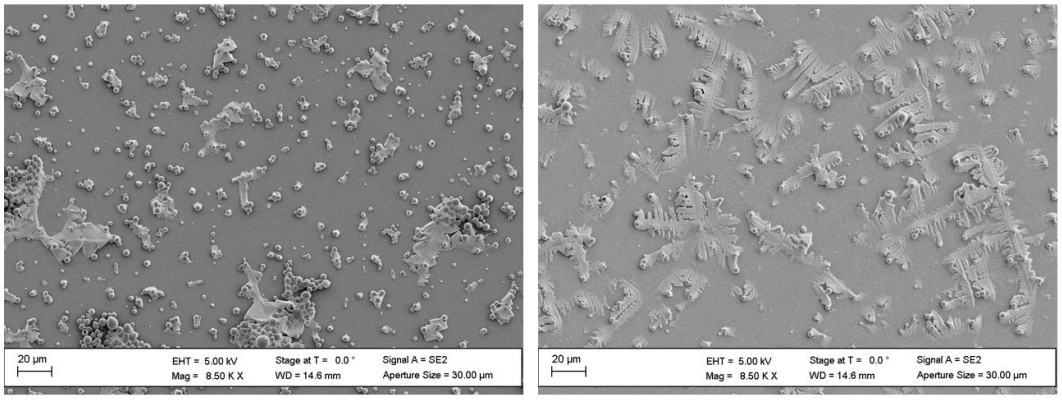

Before UV exposure **After UV exposure**

Figure 3.29. 10%Ab1:90% PLA SEM images showing melting before and after UV exposure

3.8 Conclusion:

Based on the data shown and analyzed, we can conclude that the presence of Azobenzene with PLA inside the microbubble shell was causing pores, cracks, and G-structures after UV exposure. More number of pores, cracks, and g-structures observed at 10% Ab2:90% PLA. The data was supported by quantitative analysis with pie chart representation were before and after data were compared and presented from Figure 3.19 to Figure 3.23 and Table 3.1 to Table 3.5. Increasing the amount/concentration was resulting in the melting and disruption of microbubbles as it was seen in Figure 3.28 and 50% Ab2:50% PLA and Figure 3.29 10% Ab1:90% PLA. One of the reasons in 50%Ab2:50%PLA was less amount of PLA present, and hence maximum microbubbles show cracks, pores, and g-structures even before UV exposure.

3.9 Optimization Studies

This section describes the optimization techniques done for various factors that determine the characterization of microbubbles. These factors included centrifugation speed for the collection of microbubbles, UV light exposure time on the sample, the stability of samples. The task divided into three parts:

3.9.1 Centrifugation Speed Statistical Analysis:

Centrifugation speed was a crucial step in the collection of microbubbles. As mentioned in Chapter 3, polymer microbubbles were washed and then collected using centrifugation at a certain speed. We tested three different speeds with multisizer and compared their data to obtain an average concentration of microbubbles, average mean diameter, average median diameter, and standard deviation. Three different trials performed and the results tabulated from Table 3.6-Table 3.8 for RCF 300,600 and 900

Multisizer results for RCF=300*

Table 3.6. Average concentration of microbubbles/ml, the average mean diameter, and the average median diameter of microbubbles-RCF 300

RCF:300	**Trial 1**	**Trial 2**	**Trial 3**
Average Concentration(microbubbles/ml)	2.93E+09	8.5E+08	3.37E+09
Average Mean Diameter	3.488 μm	3.609 μm	3.853 μm
Average Median Diameter	3.551 μm	3.611 μm	3.911 μm

Multisizer results for RCF=600

Table 3.7. Average concentration of microbubbles/ml, the average mean diameter, and the average median diameter of microbubbles -RCF 600

RCF:600	**Trial 1**	**Trial 2**	**Trial 3**
Average Concentration(microbubbles/ml)	2.46E+09	5.38E+09	2.86E+09
Average Mean Diameter	3.001 μm	3.026 μm	3.585 μm
Average Median Diameter	3.931 μm	2.991 μm	3.716 μm

Multisizer Data for RCF=900

Table 3.8. Average concentration of microbubbles/ml, the average mean diameter, and the average median diameter of microbubbles -RCF 900

RCF:900	**Trial 1**	**Trial 2**	**Trial 3**
Average Concentration(microbubbles/ml)	3.98E+09	4.43E+09	3.61E+09
Average Mean Diameter	3.268 μm	3.142 μm	3.221 μm
Average Median Diameter	3.224 μm	3.049 μm	3.139 μm

An ANOVA test first used to determine if the three speeds (300, 600, and 900 RCF) were significantly different. The ANOVA test returned an F value of 3.843, which was more significant than the critical value 3.403 and proved that there was a significant difference between the speeds. This statistical test was followed by a t-test to determine if the 300 RCF was significantly different from 600 RCF and 900 RCF, respectively. The first t-test showed that 300 RCF and 600 RCF were not significantly different ($p > 0.05$), and the second t-test showed that 300 RCF and 900 RCF were significantly different ($p < 0.05$).

3.11.1.1Microscopic Images:

Bright-field optical and fluorescent microscopy were both done to see the microbubble structures. Nile Red, a fluorescent dye, was incorporated inside the microbubbles shell before the first emulsion with the polymers. Figure 3.30- Figure 3.33 represents microscopy images of bright field and fluorescent microscopy

Microscopy Images for RCF=300

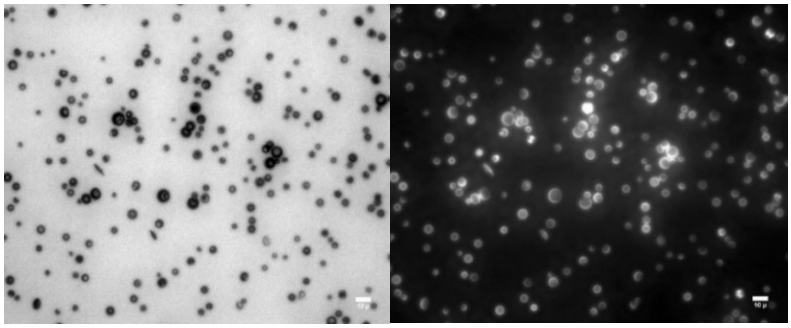

Figure 3.30. RCF 300(A) Bright Field Microscopy Images (B) Fluorescent Microscopy Images

Microscopy Images for RCF=600

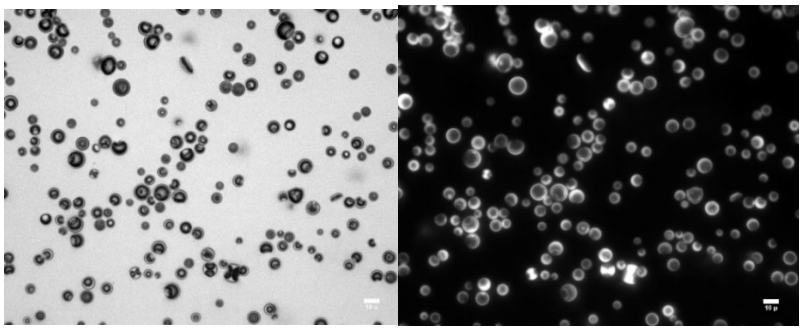

Figure 3.31. RCF 600(A) Bright Field Microscopy Images(B)Fluorescent Microscopy Images

Microscopy Images for RCF=900

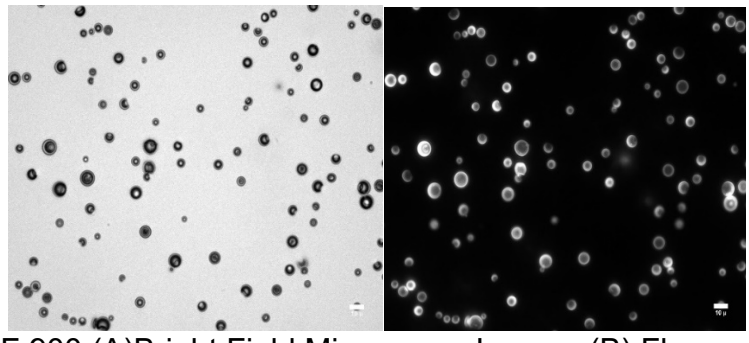

Figure 3.32. RCF 900 (A)Bright Field Microscopy Images (B) Fluorescent Microscopy Images

3.9.2 UV /Vis Spectroscopy of polymer microbubbles at different time intervals of UV exposure

Characterization performed using UV-Vis Spectroscopy to see the effect of UV exposure at different time intervals. The sample exposed at different time intervals starting from 0 minutes to a maximum of 45 minutes. The results were 15 minutes UV exposure time was sufficient to activate the Azobenzene inside the shell of microbubbles, as shown in Figure 3.33 and Figure 3.34.

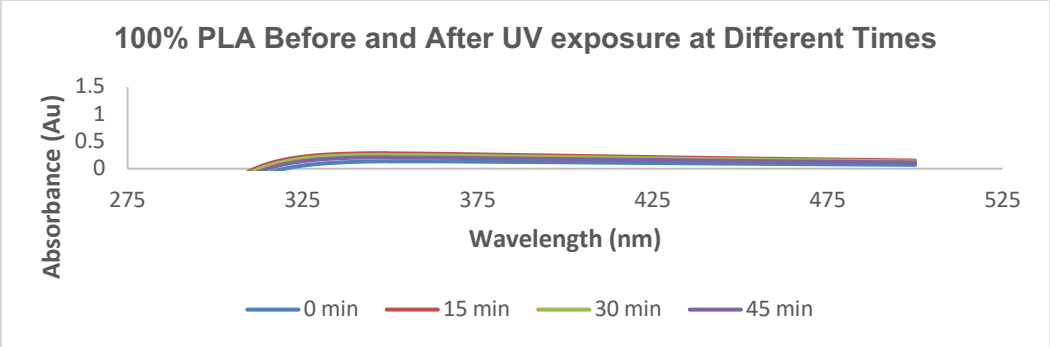

Figure 3.33. UV-Vis Spectroscopy results for 100% PLA Before and After UV exposure at different time interval -Washed sample

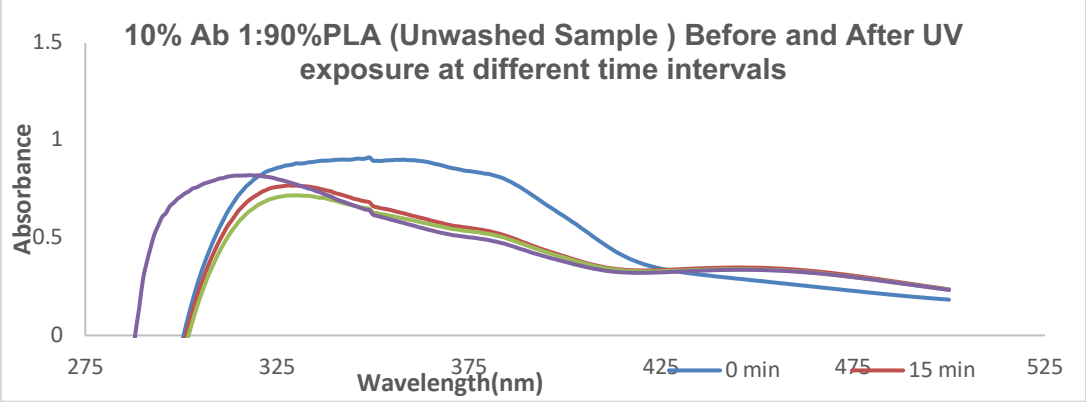

Figure 3.34. UV-Vis Spectroscopy results for 10%Ab 1: 90% PLA Before and After UV exposure at different times-unwashed sample

3.9.3 Quantitative Analysis of Pores, Cracks, Golf ball-like structures after seven days on UV exposed sample

This analysis performed to check the difference in the structure of microbubbles after keeping it in the refrigerator for seven days. As we know that azobenzene photoisomerization is a reversible process. It can go from cis to trans state after milliseconds to few days. The reversible nature of azobenzene inside the microbubbles shell checked. The effect on the microbubbles structures even after formulation was analyzed.SEM images obtained for a few samples of different concentrations of polymer microbubbles and the differences compared with Day-1 of the UV exposed sample. This section represented the SEM images from Figure 3.35 to Figure 3.42, where the images compared from Day 1 of the UV exposed sample with Day 7 of the UV exposed sample. Quantitative analysis was also performed where before UV exposure, after 15 minutes of UV exposure, Day 1, and Day 7 UV exposed samples compared using a pie chart. The results represented in figure 3.43-figure 3.47.

3.11.3.1 Results- Scanning Electron Microscopy Images

- **100% PLA**

Day 1 - After 15 minutes UV exposed

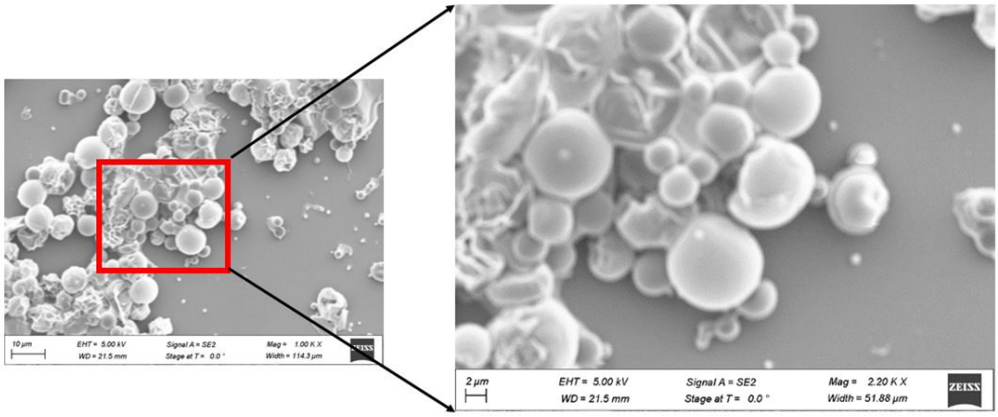

Figure 3.35. SEM Images Day-1 100%PLA

Day 7 - UV exposed sample

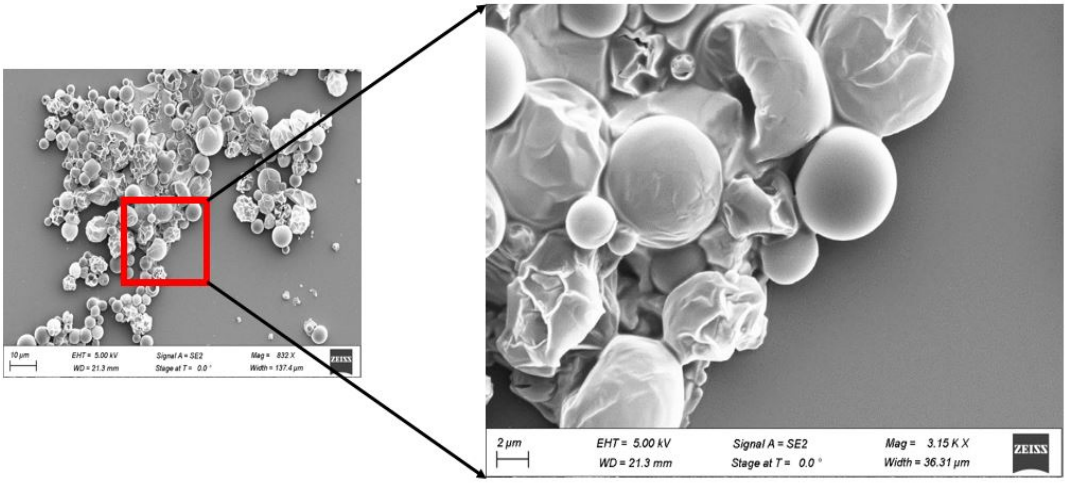

Figure 3.36. SEM Images Day-7 100%PLA

- **10 Ab 2: 90% PLA**

Day 1 - After 15 minutes of UV exposed:

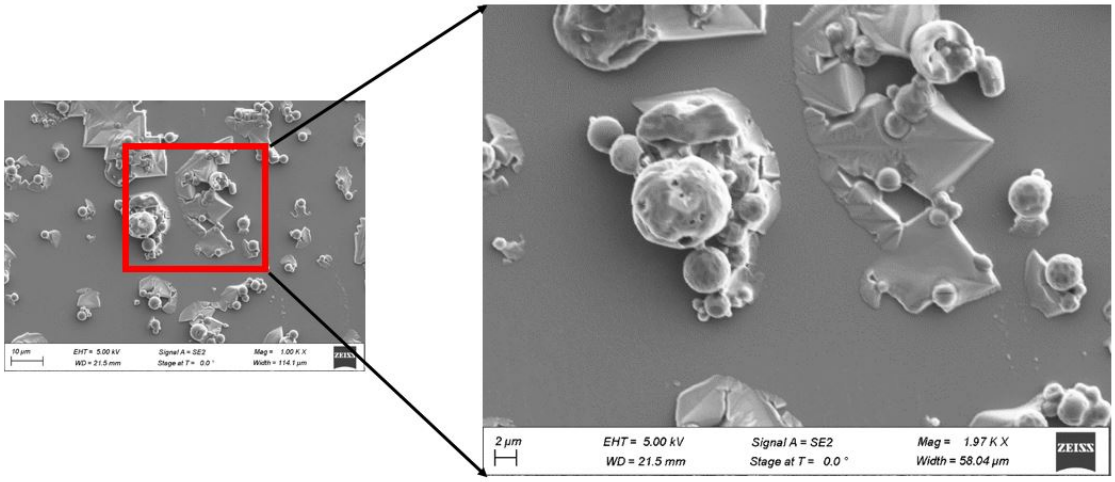

Figure 3.37. SEM Images Day-1 10%Ab2:90%PLA

Day 7 - UV exposed sample:

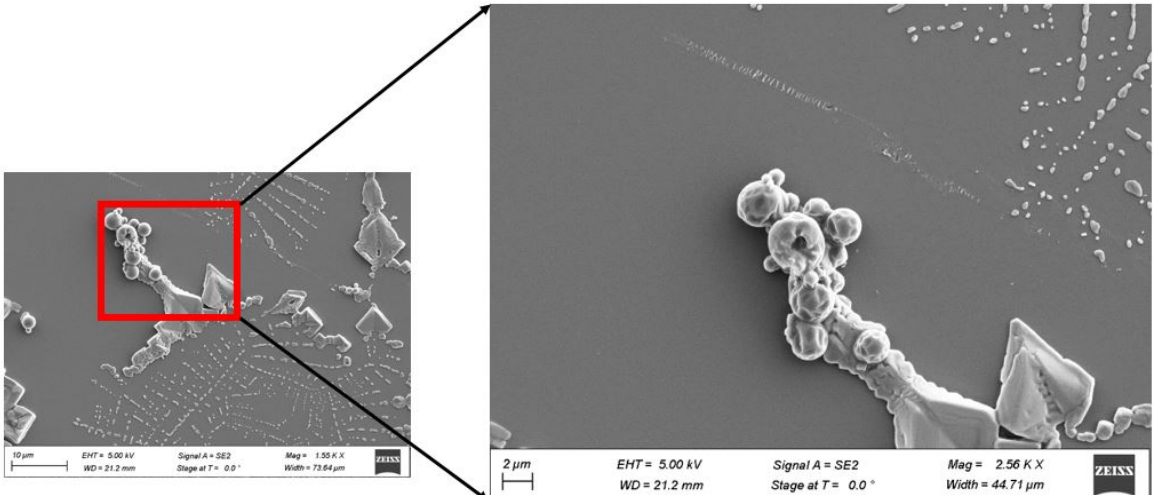

Figure 3.38. SEM Images Day-7 10%Ab2:90%PLA

- **30 %Ab 2: 70% PLA**

Day 1 - After 15 minutes of UV exposed:

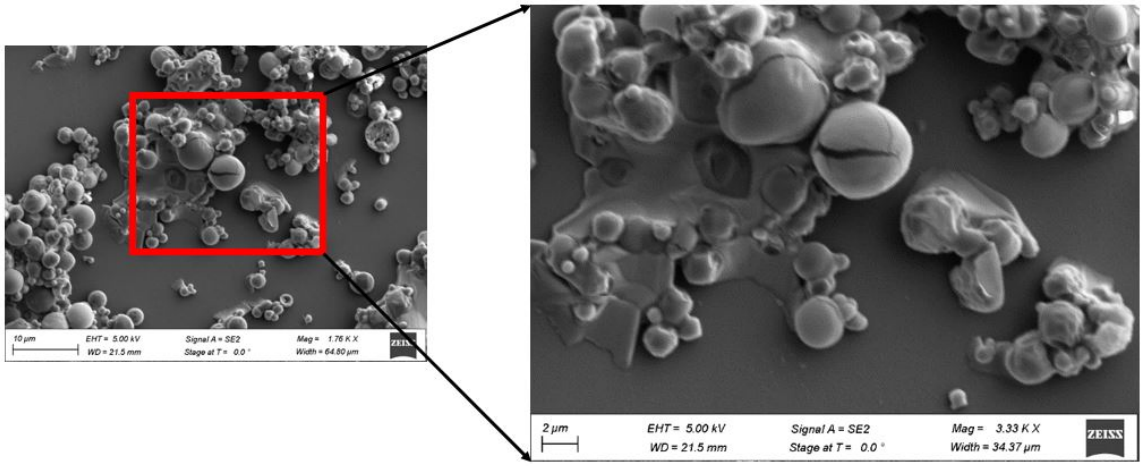

Figure 3.39. SEM Images Day-1 30%Ab2:70%PLA

Day 7 - UV exposed sample:

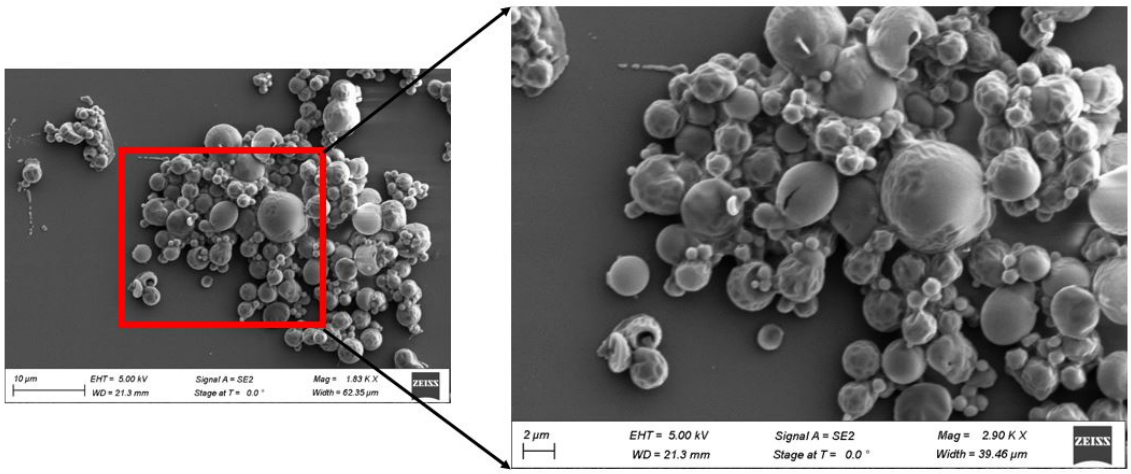

Figure 3.40. SEM Images Day-7 30%Ab2:70%PLA

- **50 Ab 2: 50% PLA**

Day 1 - After 15 minutes of UV exposed:

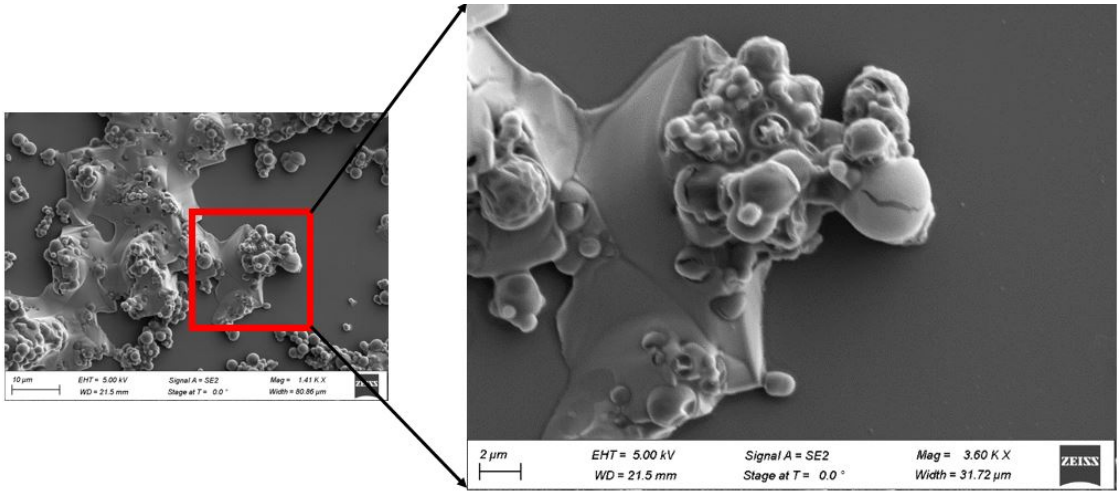

Figure 3.41. SEM Images Day-1 50%Ab2:50%PLA

Day 7 - UV exposed sample:

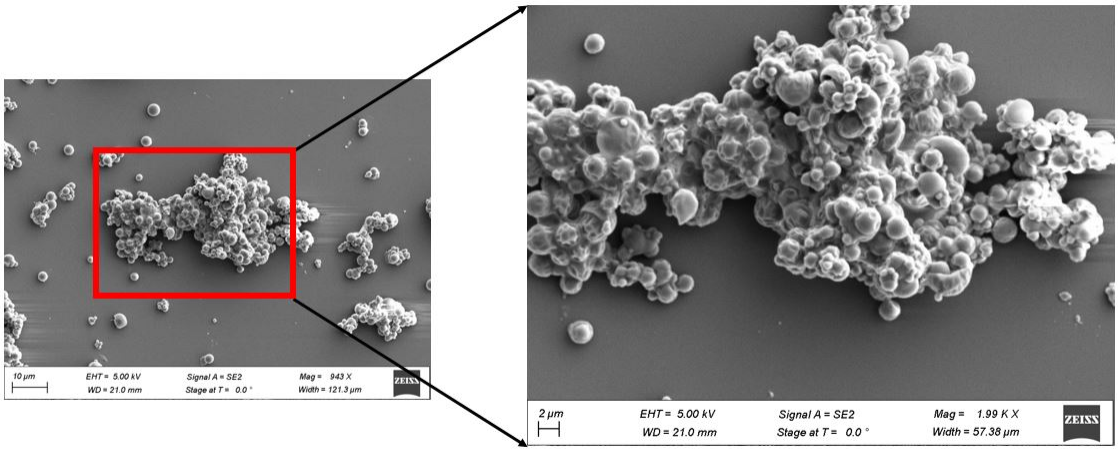

Figure 3.42. SEM Images Day-7 50%Ab2:50%PLA

Quantitative data for UV exposed sample after seven days:

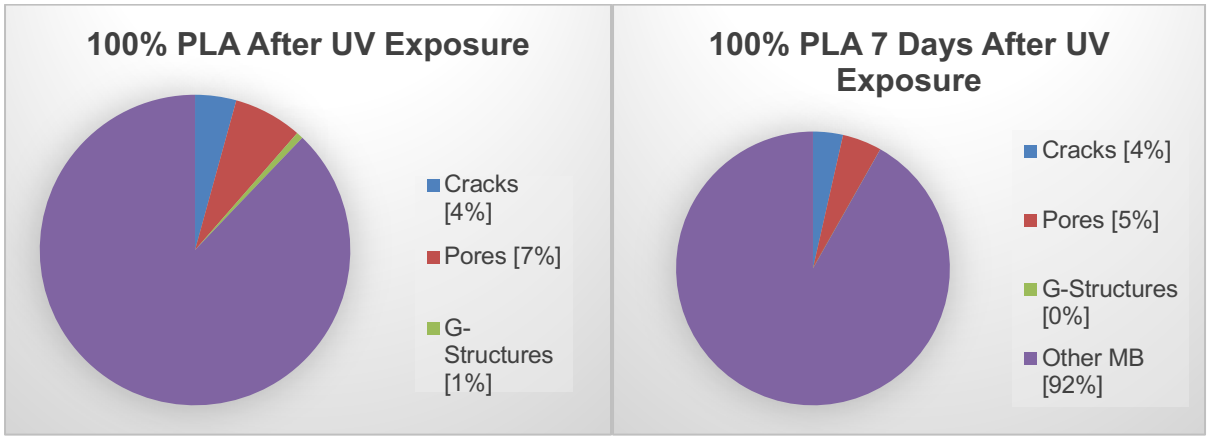

Figure 3.43. 100% PLA UV exposed sample at Day 1 and Day 7

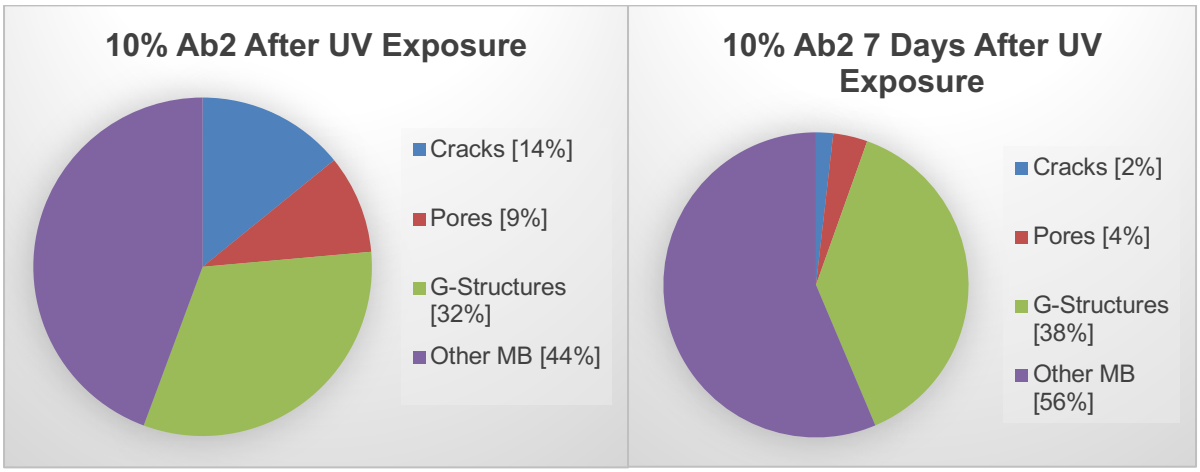

Figure 3.44.10%Ab2:90% PLA UV exposed sample at Day 1 and Day 7

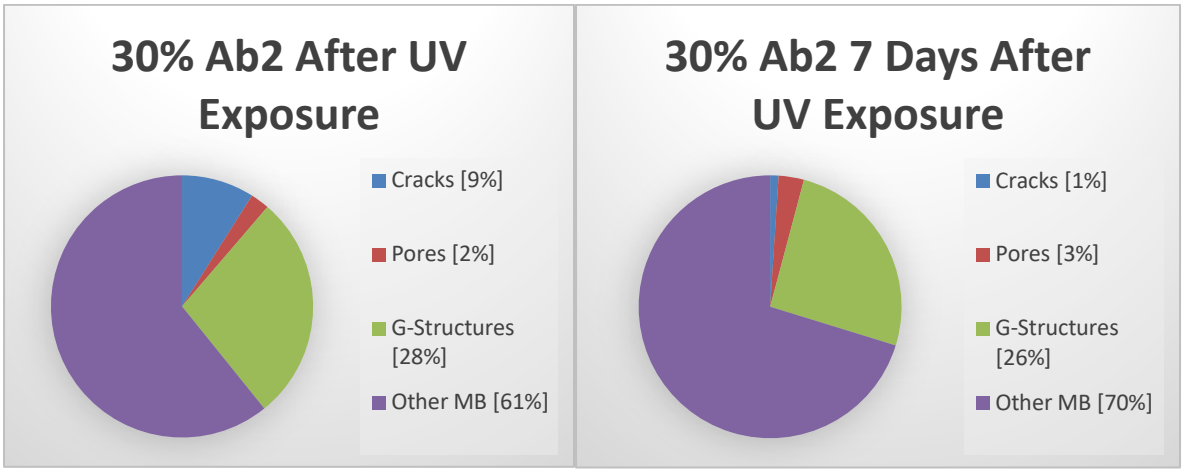

Figure 3.45. 30%Ab2:70% PLA UV exposed sample at Day 1 and Day 7

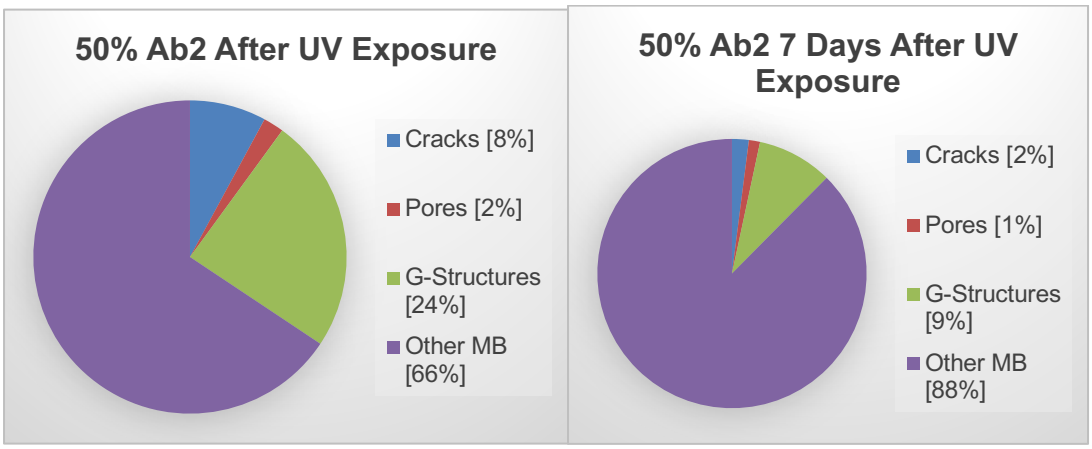

Figure 3.46. 50%Ab2:50% PLA UV exposed sample at Day 1 and Day 7

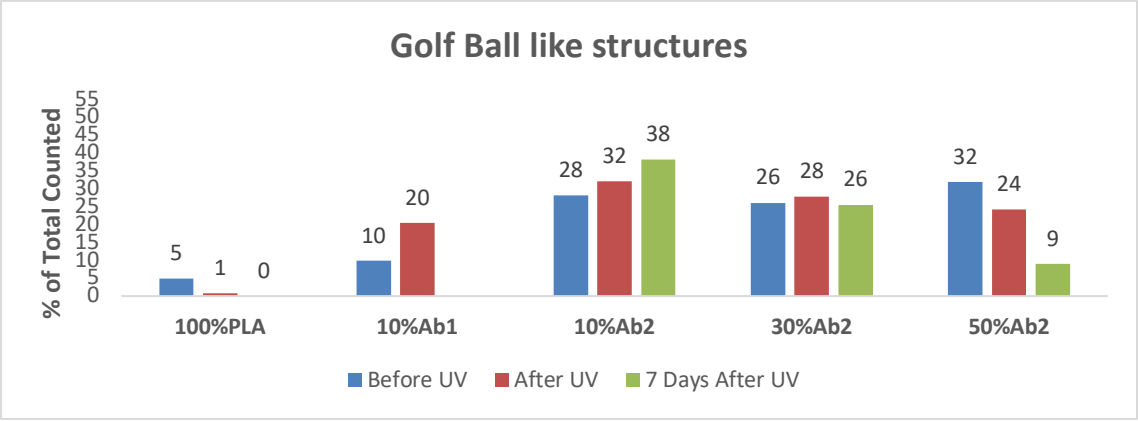

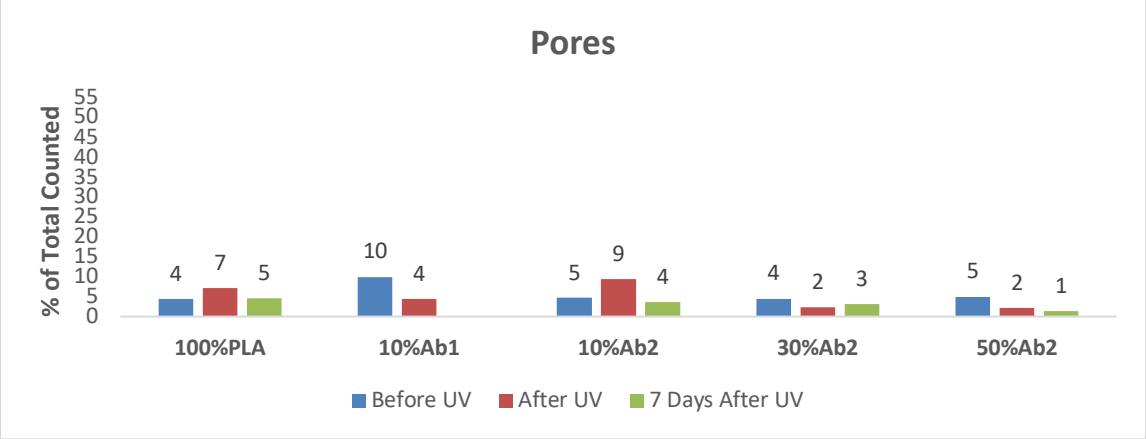

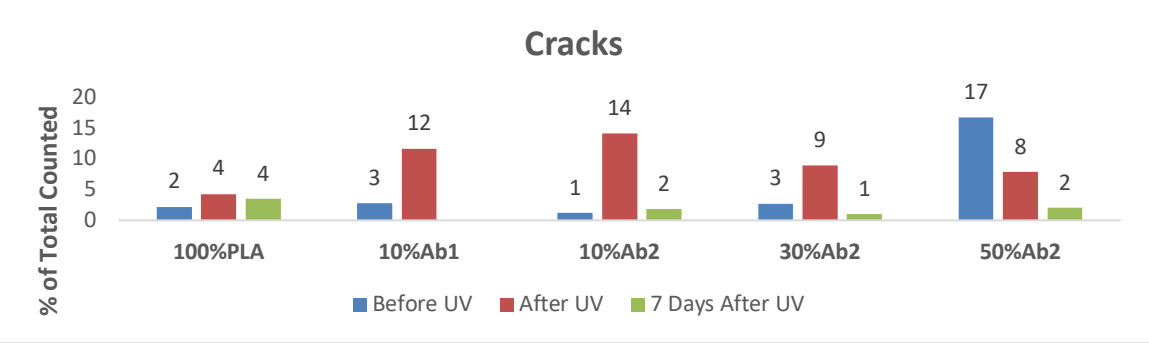

Figure 3.47. Summary of UV exposed sample: Before UV exposure; After 15 minutes UV exposure and UV exposed sample after Day 7 on different blend ratios of Azobenzene/PLA microbubbles. (A)G-structures (B) Pores(C)Cracks

Conclusion:

The structural changes observed after UV exposure. Pores, cracks,g-structures were indicative of these structural differences. Figure 3.47 represents that increasing the amount of Azobenzene or the concentration of Azobenzene in Azobenzene/PLA microbubbles can destroy microbubbles on the application of UV light. The highest amount of melting observed at the highest concentration of Azobenzene incorporation on the application of UV light. It has concluded that 10% Azobenzene (Ab2) and 90% PLA polymer microbubbles gives the desired porous structures with minimum use of Azobenzene.

CHAPTER 4

BIOMEDICAL APPLICATIONS

4.1 Polymer Microbubbles as Biocompatible Porogens for Hydrogel Scaffolds-Tissue Engineering Applications

Tissue engineering is a rapidly growing field that involves the science of improving or replacing biological tissue or organs using the number of approaches. The critical components of tissue engineering are cell material, biomaterial scaffolds, signaling molecules, and bioreactors for the formation of viable tissues. Cell material involves selected or isolated cells, such as stem cells from which show the potential to develop into different cell types. Biomaterial scaffolds provide a platform for cell growth and can classify into natural and synthetic. Signaling molecules such as proteins, growth factors, and bioreactors are required to support the biological environment for cell expansion and differentiation. Over the past few years, research has done on the development of hydrogels as a potential scaffold material for tissue engineering. (Yang et al., 2001)(Salgado et al., n.d.)Hydrogels exhibit excellent biocompatibility and have inherent similarity to the extracellular matrix, and hence cells would be exposed to negligible toxicity. Scaffolds can deliver the seeded cells to the target site in the patient's body, and cell-biomaterial interactions occur followed by cell adhesion. Additionally, they are responsible for providing an adequate amount of transport of gases, nutrients, and growth factors to ensure cell survival, proliferation, and differentiation and control structures and function of engineered tissue. (Spicer, 2020)

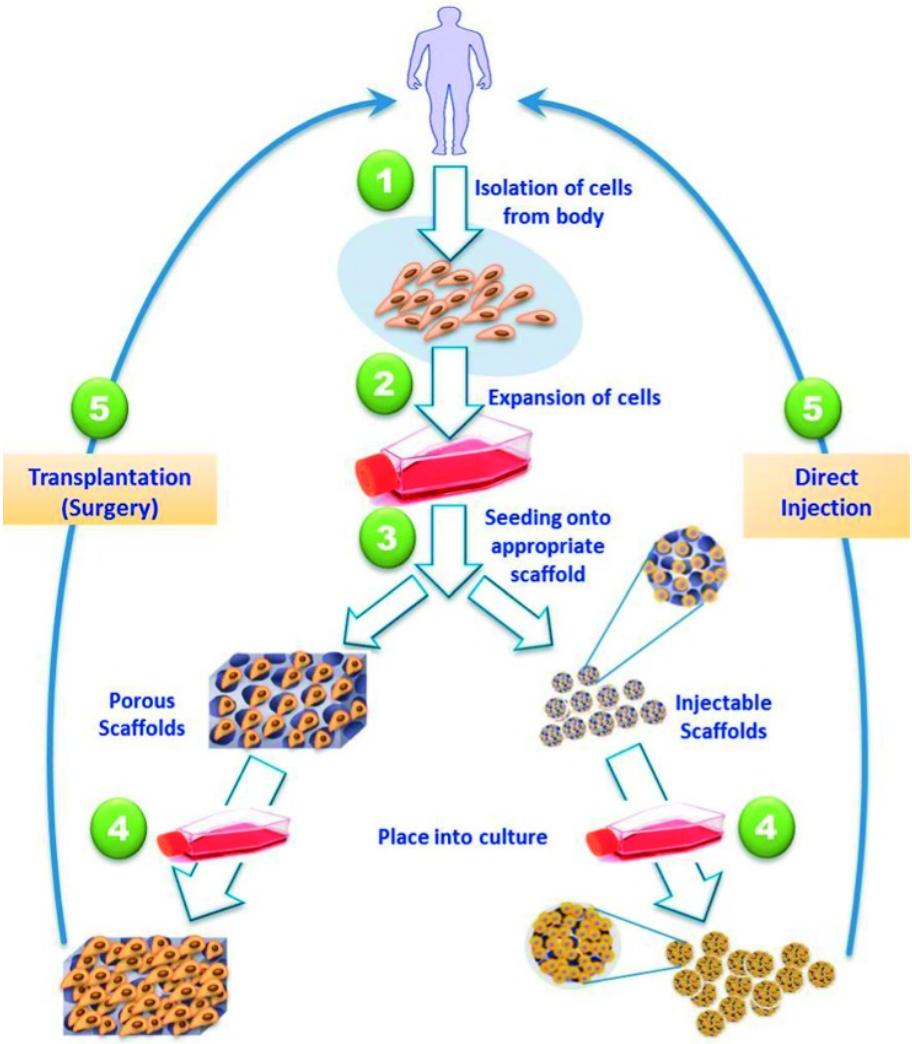

Figure 4.1. Schematic illustration of the most common tissue engineering approaches. Tissue-specific cells are isolated from a small biopsy from the patient, expanded in vitro, seeded into a well-designed scaffold, and transplanted into the patient either through injection or via implantation at the desired site using surgery. (Spicer, 2020)

Aside from being used as a scaffold, hydrogels have also been extensively used in drug delivery applications. They provide localized drug delivery to the target site in a quick manner upon interaction with biomolecular stimuli. Stimuli triggered materials such as photo-polymerizable hydrogels are especially attractive for localized drug delivery due to their ability to adhere and conform to targeted tissue when formed in situ.

4.2 On-demand drug release at tissue scaffold using polymer microbubbles embedded in agarose gel using sonoporation.

While the development of polymer bubbles has predominantly focused on systemic drug delivery to malignant tissue, such as metastatic tumors, there are other potential applications UV-sensitive PLA microbubbles in medical applications. It has previously reported that microbubbles-infused in hydrogels can potentially improve the development of tissue scaffolds in cartilage tissue engineering. (Zhang et al., 2009)

Microbubbles embedded in hydrogels have many advantages, including preserving the nanoporosity of the hydrogel as well as the inherent ease of achieving uniform cell seeding associated with hydrogel scaffolds. The controlled delivery with microbubbles embedded hydrogels can provide great potential in creating space for tissue formation later in a culture, which later results in providing improved mechanical properties. Microbubbles can potentially provide nutrients transfer in cell-seeded hydrogels through mild pressurization with the application of ultrasounds as external stimuli and with spatial-temporal control. (Spicer, 2020)

Agarose gels have extensively used in clinical trials as a scaffold component in chondrocyte tissue scaffolds. (Benya & Shaffer, 1982)(Aydelotte & Kuettner, 1988)(Benya & Shaffer, 1982)(Lee & Bader, 1995). Lipid shelled gas-filled microbubbles were used to achieve the on-demand formation of microporous structure in hydrogels. The functionality of lipid microbubbles first investigated using low-intensity pulsed ultrasound on chondrogenic differentiation of human Mesenchymal stem cells (hMSCs) in 3D printed scaffolds. (Zhang et al., 2009)(Kassem, 2004)(Lijie et al., 2016)

The paper broadly discusses the use of microbubbles as porogens whose functionality can modify in such a way that nutrient release along with entrapment of cell-matrix products. Studies show that the microporosity of agarose hydrogels can be altered by using a controlled dissolution of microbubbles, which allow more effective nutrient transport to embedded cells. (Lima et al., 2012)

A feasibility study has performed to assess the physical properties of microbubble with culture time wherein diffusivity of lipid microbubbles tested. Lipid microbubbles with PFB gas core mixed with agarose gel, as shown in Figure 4.3 The embedded microbubbles were then kept at 37ºC in an incubator for 28 days and examined for changes in mechanical properties. The results indicated on day 7, the bubbles were no longer visible under the microscope. The gas core diffuses away, leaving behind fluid-filled pores. This led to the conclusion that lipid bubbles remain stable at 37ºC for only 1 week. (Calliada et al., 1998)

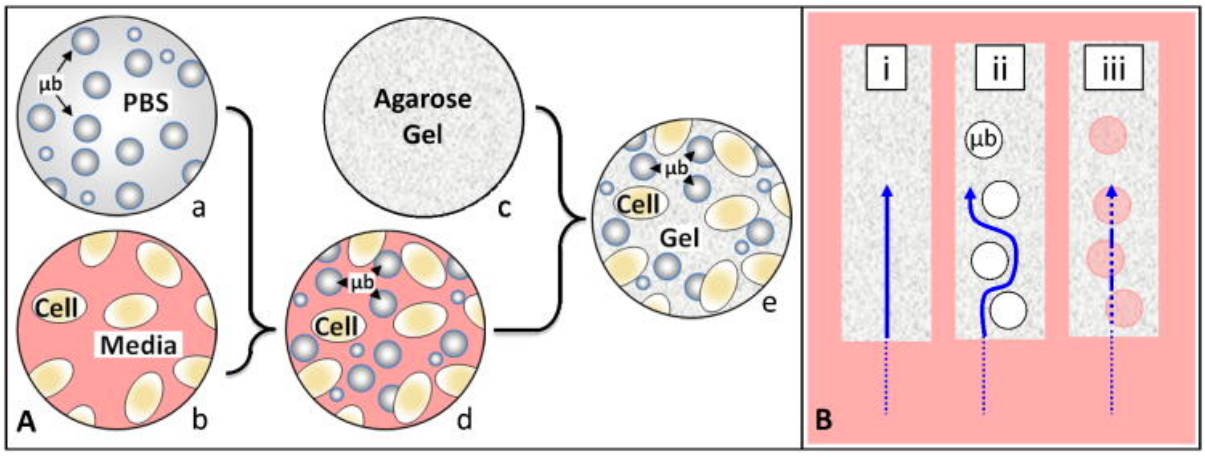

Figure 4.2. Illustration of steps involved in assembling microbubble-infused agarose hydrogel showing Improvement of Nutrient Flow to the cell. (Lima et al., 2012)

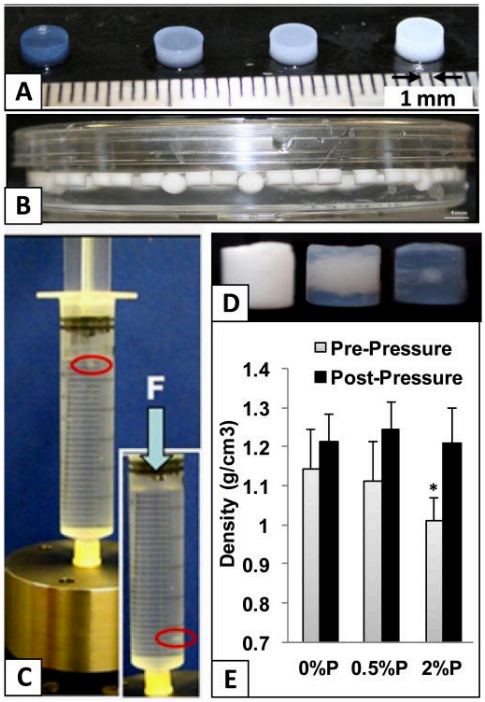

Figure 4.3. Loading of Lipid Microbubbles in Hydrogels. (Lima et al., 2012)

Polymer bubbles, on the other hand, are much more stable and can be used to deliver drugs or growth factors in tissue scaffolds as well as improving porosity of scaffolds, but the on-demand release of drugs is difficult to control. Preliminary work was required to carry out to test for stability. PLGA polymer bubbles were seeded into tissue scaffolds to determine their stability at 37ºC and their resistance to cyclic pressure and focused ultrasound application. Compared to lipid microbubbles, the polymer microbubbles last for much more extended periods with no noticeable degradation over two weeks. The paper's unpublished data indicated that these polymer bubbles at 2% volume loading increased the buoyancy of the agarose scaffolds without disrupting their structural integrity. Furthermore, the agarose plugs remained buoyant for months, indicating polymer bubbles were remaining stable.

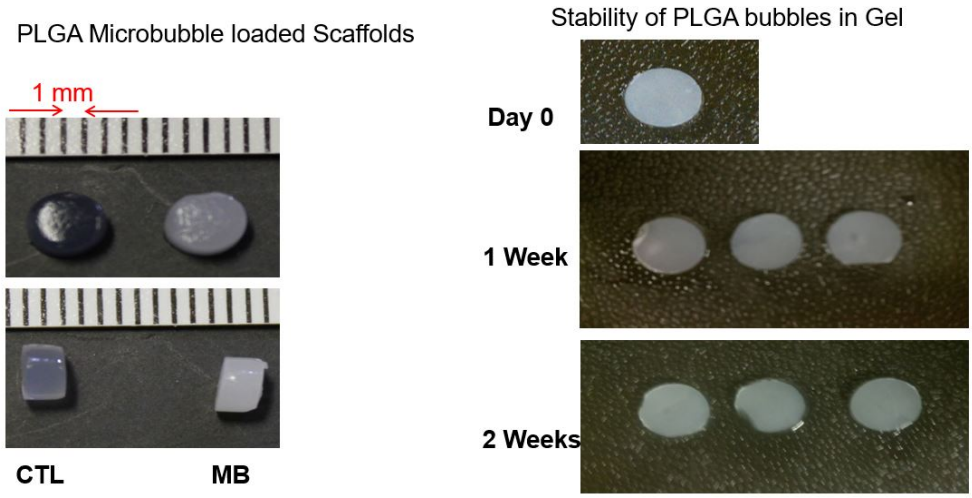

Figure 4.4. PLGA Microbubble loaded Scaffolds (Left) & Stability of PLGA bubbles in Gel(Right)
Dr. Shashank Sirsi took images in the lab of Dr. Mark Borden

It was interesting to note that when subjected to the same cyclic pressure as lipid bubbles used by Lima et al., the PLGA bubbles showed little change in opacity, thus demonstrating improved stability. Cyclic pressures as high as 150 PSI were needed to destroy bubbles within the scaffold.

Microbubbles have shown the ability to deliver nutrients effectively to cells that are deep in the scaffolds. PLGA microbubbles were embedded in the agarose gel to grow chondrocytes from cartilage tissue. Some optical study experiments performed first to test the stability of microbubbles inside agarose gel as it is crucial to support cell culture. Hydrostatic pressure was applied to perform stability tests by using Focused Ultrasound (1MHz) with 0.5% GAS Volume, and a change in opacity with the application of pressure observed. The results obtained are that Agarose becomes less opaque in Ultrasound focus on increasing power.

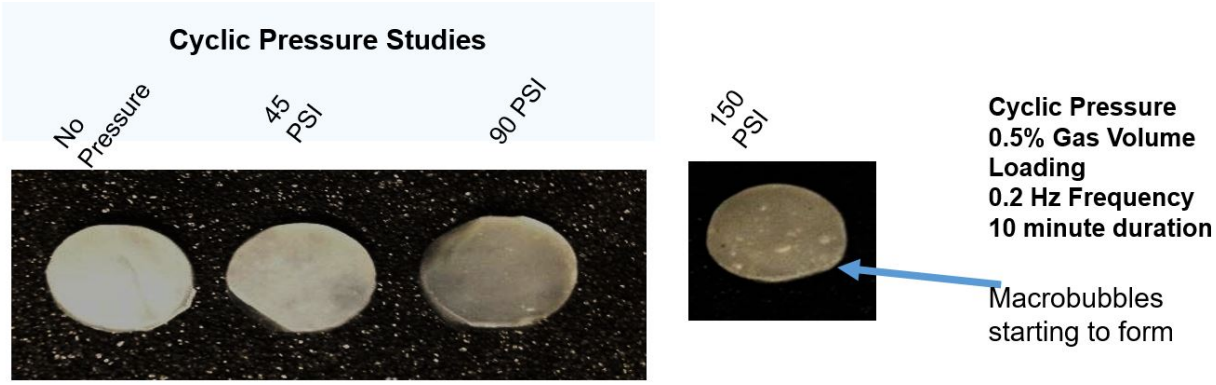

Figure 4.5. Effect of Cyclic Pressure on Polymer Microbubble Stability

Dr. Shashank Sirsi took images in the Lab of Dr. Mark Borden

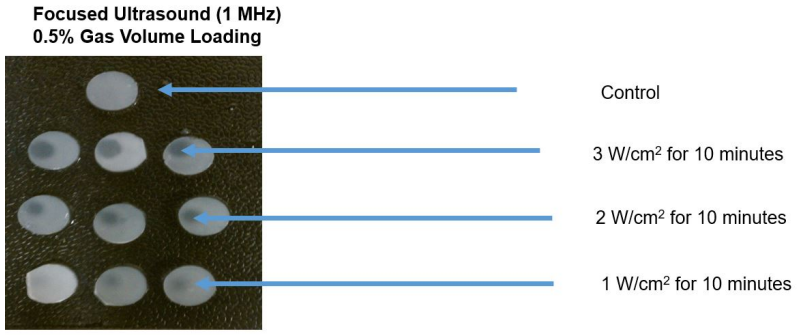

Figure 4.6. Spatial control over Microbubble Destruction in Gel Scaffolds

Dr. Shashank Sirsi took images in the Lab of Dr. Mark Borden

Based on the results obtained with embedded PLGA microbubbles in Figures 4.4 to 4.6, the study can potentially extend to use Azobenzene/PLA microbubbles embedded into an agarose gel for tissue scaffold application. Our ultimate goal is to apply UV sensitive polymer microbubbles towards generating controllable porogens with on-demand drug release capabilities using UV light as a sensitizer. UV sensitive polymer microbubbles embedded in hydrogels have the potential to increase the porosity. Previous studies have

shown that increasing porosity can encourage cell ingrowth, uniform cell distribution, and assist the vascularization of the matrix. With increasing porosity, the size of pores, pores size distribution, pore shape, pore wall roughness, and the pore interconnectivity play a crucial role in designing hydrogel scaffolds. ((PDF) New perspectives in mercury porosimetry | Carlos Leòn - Academia.edu, 2002)Pores interconnectivity can ensure the control transfer of nutrients and oxygen. Pore size can impact cellular penetration and ECM production. All these properties can be achieved by introducing Azobenzene/PLA microbubbles, as in this research, we have successfully achieved porous structures with the application of UV light.

Future experiments on this project could include the use of Azobenzene/PLA microbubbles loaded with growth factors to determine the effects of increased porosity on shell stability and agarose gel porosity. Possible challenges with Azobenzene/PLA microbubbles are to evaluate the biocompatibility of the microbubbles, cytotoxic effect on nutrients due to the presence of Azobenzene, nutrients survival on exposure to UV light while activation of the polymer, effects of thermal response on agarose gels. The observation of possible toxicity due to the chemicals used in the polymerization of these microbubbles embedded in hydrogels, especially when the reaction conversion is incomplete, can happen. Therefore to improve the biocompatibility purification of unreacted chemicals is highly suggested. Purification of these microbubbles embedded hydrogels can be done using dialysis or extensive solvent washing.

CHAPTER 5

CONCLUSIONS

This thesis introduced a novel UV sensitive shape changeable polymer microbubble. Azobenzene is an organic molecule that possesses photochromatic properties. In response to UV light, Azobenzene undergoes isomerization and changes its structure by going from trans to cis state. An unsubstituted form of azobenzene can undergo a reversible process. Since azobenzene is not as biocompatible in comparison to PLA, there is a need to reduce the amount of Azobenzene by achieving significant differences in the structure of microbubbles. There are many fabrication processes used for the formulation of microbubbles, such as single/double emulsions, coacervation, and spray drying. In this thesis, the double emulsification technique used for the development of PLA/Azobenzene microbubbles since PLA/PLGA microbubbles conventionally fabricated by the same method. This method was optimized to achieve the best results using previous optimization studies that focused on centrifugation speed for the collection of microbubbles. ANOVA test first performed to determine the statistical difference between three speeds (300 xg, 600 xg, 900 xg), which results in an F value of 3.843 (which was more significant than critical value 3.403), conveying that all the three speeds are statistically different. Then the test was followed by a t-test to show if these speeds are significantly different. The data was verified and supported by t-test and microscopy images.

A UV-sensitive polymer Azobenzene was mixed with PLA at varying ratios to make polymeric shells of microbubbles. Hence, the formulation of polymeric shell microbubble

achieved. Multisizing with the Coulter counter method gives us the average number concentration of microbubbles and the average size of the microbubbles, which was between 2-4 μm. After the formulation, activation of Azobenzene with exposure to UV light observed with UV-Vis Spectroscopy results. The absolute absorption peak at 375 nm before UV exposure and 450 nm after UV exposure of 15 minutes observed. The results then compared before and after UV exposure. The change in structures observed by Scanning Electron Microscopy and quantitatively analyzed by counting the number of pores, cracks, G-structures which are indicative of structural changes post UV exposure. The stability of these polymer microbubbles confirmed by SEM imaging after seven days of UV exposed sample. It was observed that there was no prominent difference, concluding that microbubbles remain stable even after 7 days.

In Chapter 3, it was concluded that increasing the amount of Azobenzene results in the destruction of microbubbles. As the microbubbles are exposed to UV light for 15 minutes at the intensity of 6.2 mW/cm2, melting was observed with increasing azobenzene content in the shell. Also, it was concluded that the amount of PLA polymer was significantly crucial as PLA polymer contributes towards microbubble formulation rather than azobenzene as per observation. After comparing the optical properties and quantitative analysis from SEM images before and after UV exposure, it can be concluded that 10% Azobenzene (Ab2) and 90% PLA polymer microbubbles gives the desired porous structure with minimum use of the azo compound in Azobenzene.

Future Scope:

Future considerations and experimentations can explore Azobenzene/PLA microbubbles that have been formulated in this thesis. The long term goal of this research project is to increase the elasticity of polymer microbubbles with the application of UV light. Increasing porosity can enlarge the specific surface area, which means an increase in the acoustic reflection area that can eventually result in the improvement of the compressibility of microbubbles. Compressibility can improve the mechanical properties of microbubbles, which in turn can activate with ultrasound to achieve targeted drug delivery. Acoustic studies to determine shell elasticity and compressibility will determine the echogenicity in vitro dose responses, and time response studies. After the acoustic testing, drug encapsulation, and drug release profile for controlled delivery in vivo will be studied. Future studies involve the development of a stable yet elastic drug vehicle that might well suit for both diagnosing as well as for treatment by encapsulating drugs in it.

As discussed in Chapter 4, one of the promising applications of Azobenzene/PLA microbubbles is in tissue engineering as porogens embedded in hydrogel scaffolds to improve on-demand nutrient release upon application of focused ultrasound as an external stimulus. The biocompatibility of UV activated hydrogel can be further improved by purification with dialysis and extensive solvent wash.

APPENDIX A

LIST OF MATERIALS

☐Polylactic acid (PLA):

Supplier: Polysciences, Inc.

Formula: $(C_3H_4O_2)_n$

Molecular weight: ~72g/mol (monomer)

☐Hexane

Supplier: Sigma-Aldrich, Inc.

Formula: C_6H_{14}

Molecular weight: 86.18g/mol

☐Polyvinyl alcohol (PVA):

Supplier: Polysciences, Inc.

Formula: $(C_2H_4O)_n$

Molecular weight: 44.05g/mol (88% Hydrolized)

☐Deionized Water

Supplier: UTD

Formula: H_2O

Molecular weight: 18.02g/mol

☐Camphor (96%)

Supplier: Sigma-Aldrich, Inc.

Formula: $C_{10}H_{16}O$

Molecular weight: 152.23g/mol

☐Isopropanol (70%)

Supplier: Sigma-Aldrich, Inc.

Formula: C_3H_8O

Molecular weight: 60.1g/mol

☐Methylene Chloride

Supplier: Sigma-Aldrich, Inc.

Formula: CH_2Cl_2

Molecular weight: 84.93g/mol

☐ Liquid Nitrogen

Supplier: UTD

Formula: N_2

Molecular weight: ~28g/mol

☐ Azobenzene

Supplier: Ware lab,UTD

Formula: $C_{12}H_{10}N_2$

Molecular weight: 182.23g/mol

☐ Chloroform

Supplier: Sigma-Aldrich, Inc.

Formula: $CHCl_3$

Molecular weight: 119.38g/mol

☐Ammonium Carbonate

Formula: $(NH_4)_2CO_3$

Molecular weight: 96.09g/mol

☐Nile Red

Supplier: Sigma-Aldrich, Inc.

Formula: $C_{20}H_{18}N_2O_2$

Molecular weight: 318.37g/mol

Supplier: Sigma-Aldrich, Inc.

APPENDIX B

TOOLS AND EQUIPMENT'S

1. 0.45 um bottle top filter
2. Stir bar and Stir bar Magnets
3. Weighing machine and Weigh Dish
4. Metal Spatulas
5. Beakers
6. Graduated Cylinders
7. Parafilm
8. Glass Vials, Scintillation Vials(10 ml) with Teflon Caps,Derm Vials with Teflon Caps
9. Disposable Glass Pipette
10. Centrifuge Tubes(50 ml)
11. 1ml Syringes with needle

Fabrication Techniques & Equipment:

1. Sonication

   Instrument: Digital Sonifier

   Model No: Branson Digital Sonifier 450

2. Homogenization

   Instrument: Polytron Homogenizer

   Model No: PT-MR 3100 D

3. Centrifugation

   Instrument: Thermo Scientific Lab High-Speed Centrifuge

   Model No: Lynx4000

   Instrument: Eppendorf Centrifuge

   Model No: 5804 R

4. Lyophilization

Instrument: Harvest Right Pharmaceutical Freeze Dryer

Model No: HR8000-SS

Vacuum Pump Technical Specifications: CFM: 7.2 Motor: 3/4 HP, 1725 RPM

Voltage: Standard 115V 60Hz Plug: US 110V Intake Port: 3/4 JIC flare Intake

Port: 21 oz. (680 cc) Dimensions: 10 1/2″ H x 16″ D x 5 3/4″ W Weight: 35 lbs

Characterization Techniques & Equipments:

5. Microscopy and Fluorescent Microscopy

Instrument: Olympus optical upright microscope + Teledyne Q Imaging camera mount

Model No: BX50F4 & U-LH100HG + 01-ROL-BOLT-M-12

6. Polarized Optical Microscopy

7. Multisizer

Instrument: Beckman Coulter Multisizer

Model No: Multisizer 4 Coulter counter

8. UV-vis Spectroscopy

Instrument: Agilent Technologies Spectrophotometer

Model No: Cary series 7000 UV-Vis-NIR

REFERENCES

(PDF) New perspectives in mercury porosimetry | Carlos Leòn - Academia.edu. (n.d.). Retrieved April 16, 2020, from https://www.academia.edu/6644372/New_perspectives_in_mercury_porosimetry

Aydelotte, M. B., & Kuettner, K. E. (1988). Differences between sub-populations of cultured bovine articular chondrocytes. I. Morphology and cartilage matrix production. Connective Tissue Research, 18(3), 205–222. https://doi.org/10.3109/03008208809016808

Benya, P. D., & Shaffer, J. D. (1982). Dedifferentiated chondrocytes reexpress the differentiated collagen phenotype when cultured in agarose gels. Cell, 30(1), 215–224. https://doi.org/10.1016/0092-8674(82)90027-7

Bertier, G., Carrot-Zhang, J., Ragoussis, V., & Joly, Y. (2016). Integrating precision cancer medicine into healthcare-policy, practice, and research challenges. Genome Medicine, 8(1), 108. https://doi.org/10.1186/s13073-016-0362-4

Bloch, S. H., Wan, M., Dayton, P. A., & Ferrara, K. W. (2004). Optical observation of lipid- and polymer-shelled ultrasound microbubble contrast agents. Applied Physics Letters, 84(4), 631–633. https://doi.org/10.1063/1.1643544

Bunnett, J. F. (1962). Azo and Diazo Chemistry. Aliphatic and Aromatic Compounds. Journal of the American Chemical Society, 84(3), 502–502. https://doi.org/10.1021/ja00862a044

Calliada, F., Campani, R., Bottinelli, O., Bozzini, A., & Sommaruga, M. G. (1998). Ultrasound contrast agents. European Journal of Radiology, 27(SUPPL. 2), S157–S160. https://doi.org/10.1016/S0720-048X(98)00057-6

Cavalieri, F., El Hamassi, A., Chiessi, E., & Paradossi, G. (2005). Stable polymeric microballoons as multifunctional device for biomedical uses: Synthesis and characterization. Langmuir, 21(19), 8758–8764. https://doi.org/10.1021/la050287j

Chomas, J. E., Dayton, P., May, D., & Ferrara, K. (2001). Threshold of fragmentation for ultrasonic contrast agents. Journal of Biomedical Optics, 6(2), 141. https://doi.org/10.1117/1.1352752

Cui, W., Bei, J., Wang, S., Zhi, G., Zhao, Y., Zhou, X., Zhang, H., & Xu, Y. (2005). Preparation and evaluation of poly(L-lactide-co-glycolide) (PLGA) microbubbles as a contrast agent for myocardial contrast echocardiography. Journal of Biomedical Materials Research Part B: Applied Biomaterials, 73B(1), 171–178. https://doi.org/10.1002/jbm.b.30189

de Jong, N., Frinking, P. J., Bouakaz, A., Goorden, M., Schourmans, T., Jingping, X., & Mastik, F. (2000). Optical imaging of contrast agent microbubbles in an ultrasound field with a 100-MHz camera. Ultrasound in Medicine & Biology, 26(3), 487–492. https://doi.org/10.1016/s0301-5629(99)00159-3

de Jong, N., Hoff, L., Skotland, T., & Bom, N. (1992). Absorption and scatter of encapsulated gas filled microspheres: Theoretical considerations and some measurements. Ultrasonics, 30(2), 95–103. https://doi.org/10.1016/0041-624X(92)90041-J

DIJKMANS, P., JUFFERMANS, L., MUSTERS, R., VANWAMEL, A., TENCATE, F., VANGILST, W., VISSER, C., DEJONG, N., & KAMP, O. (2004). Microbubbles and ultrasound: from diagnosis to therapy. European Journal of Echocardiography, 5(4), 245–256. https://doi.org/10.1016/j.euje.2004.02.001

El-Sherif, D. M., & Wheatley, M. A. (2003). Development of a novel method for synthesis of a polymeric ultrasound contrast agent. Journal of Biomedical Materials Research - Part A, 66(2), 347–355. https://doi.org/10.1002/jbm.a.10586

Frangioni, J. V. (2008). New technologies for human cancer imaging. Journal of Clinical Oncology, 26(24), 4012–4021. https://doi.org/10.1200/JCO.2007.14.3065

Fu, J.-W., Lin, Y.-S., Gan, S.-L., Li, Y.-R., Wang, Y., Feng, S.-T., Li, H., & Zhou, G.-F. (2019). Review Article Multifunctionalized Microscale Ultrasound Contrast Agents for Precise Theranostics of Malignant Tumors. https://doi.org/10.1155/2019/3145647

Hartley, G. S. (1937). The cis-form of azobenzene [11]. In Nature (Vol. 140, Issue 3537, p. 281). https://doi.org/10.1038/140281a0

Iqbal, M., Zafar, N., Fessi, H., & Elaissari, A. (2015). Double emulsion solvent evaporation techniques used for drug encapsulation. In International Journal of Pharmaceutics (Vol. 496, Issue 2, pp. 173–190). Elsevier. https://doi.org/10.1016/j.ijpharm.2015.10.057

Kassem, M. (2004). Mesenchymal stem cells: Biological characteristics and potential clinical applications. Cloning and Stem Cells, 6(4), 369–374. https://doi.org/10.1089/clo.2004.6.369

Klibanov, A. L. (2006). Microbubble contrast agents: Targeted ultrasound imaging and ultrasound-assisted drug-delivery applications. In Investigative Radiology (Vol. 41, Issue 3, pp. 354–362). https://doi.org/10.1097/01.rli.0000199292.88189.0f

Lee, D. A., & Bader, D. L. (1995). The development and characterization of an in vitro system to study strain-induced cell deformation in isolated chondrocytes. In Vitro Cellular & Developmental Biology - Animal: Journal of the Society for In Vitro Biology, 31(11), 828–835. https://doi.org/10.1007/BF02634565

Lentacker, I., De Smedt, S. C., & Sanders, N. N. (2009). Drug loaded microbubble design for ultrasound triggered delivery. Soft Matter, 5(11), 2161–2170. https://doi.org/10.1039/b823051j

Lijie, M. A., Zhang, G., & Sarkar, K. (2016). Lipid Coated Microbubbles and Low Intensity Pulsed Ultrasound Enhance Chondrogenesis of Human Mesenchymal Stem Cells in 3D Printed Scaffolds. https://doi.org/10.1038/srep37728

Lima, E. G., Durney, K. M., Sirsi, S. R., Nover, A. B., Ateshian, G. A., Borden, M. A., & Hung, C. T. (2012). Microbubbles as biocompatible porogens for hydrogel scaffolds. Acta Biomaterialia, 8(12), 4334–4341. https://doi.org/10.1016/j.actbio.2012.07.007

Linsley, C. S., & Wu, B. M. (2017). Recent advances in light-responsive on-demand drug-delivery systems. In Therapeutic Delivery (Vol. 8, Issue 2, pp. 89–107). Future Medicine Ltd. https://doi.org/10.4155/tde-2016-0060

Makadia, H. K., & Siegel, S. J. (2011). Poly Lactic-co-Glycolic Acid (PLGA) as biodegradable controlled drug delivery carrier. Polymers, 3(3), 1377–1397. https://doi.org/10.3390/polym3031377

Merino, E., & Ribagorda, M. (2012). Control over molecular motion using the cis-trans photoisomerization of the azo group. In Beilstein Journal of Organic Chemistry (Vol. 8, pp. 1071–1090). Beilstein-Institut. https://doi.org/10.3762/bjoc.8.119

Narayan, P., & Wheatley, M. A. (1999). Preparation and characterization of hollow microcapsules for use as ultrasound contrast agents. Polymer Engineering & Science, 39(11), 2242–2255. https://doi.org/10.1002/pen.11612

Qin, S., Caskey, C. F., & Ferrara, K. W. (n.d.). Ultrasound contrast microbubbles in imaging and therapy: physical principles and engineering. https://doi.org/10.1088/0031-9155/54/6/R01

Romero, J. R., Frey, J. L., Schwamm, L. H., Demaerschalk, B. M., Chaliki, H. P., Parikh, G., Burke, R. F., & Babikian, V. L. (2009). Cerebral ischemic events associated with “bubble study” for identification of right to left shunts. Stroke, 40(7), 2343–2348. https://doi.org/10.1161/STROKEAHA.109.549683

Rustler, K., Maleeva, G., Bregestovski, P., & König, B. (2019). Azologization of serotonin 5-HT $_3$ receptor antagonists. Beilstein Journal of Organic Chemistry, 15(1), 780–788. https://doi.org/10.3762/bjoc.15.74

Salgado, A. J., Coutinho, O. P., & Reis, R. L. (n.d.). Bone Tissue Engineering: State of the Art and Future Trends. https://doi.org/10.1002/mabi.200400026

Sirsi, S. R., & Borden, M. A. (2009). Microbubble compositions, properties and biomedical applications. In Bubble Science, Engineering and Technology (Vol. 1, Issues 1–2, pp. 3–17). NIH Public Access. https://doi.org/10.1179/175889709X446507

Sirsi, Shashank R., & Borden, M. A. (2014). State-of-the-art materials for ultrasound-triggered drug delivery. In Advanced Drug Delivery Reviews (Vol. 72, pp. 3–14). Elsevier. https://doi.org/10.1016/j.addr.2013.12.010

Spicer, C. D. (2020). Hydrogel scaffolds for tissue engineering: The importance of polymer choice. In Polymer Chemistry (Vol. 11, Issue 2, pp. 184–219). Royal Society of Chemistry. https://doi.org/10.1039/c9py01021a

Stewart, M. J. (2003). CONTRAST ECHOCARDIOGRAPHY. Heart, 89(3), 342–348. https://doi.org/10.1136/heart.89.3.342

Szabo, T. L. (2004). Diagnostic Ultrasound Imaging: Inside Out: Second Edition. In Diagnostic Ultrasound Imaging: Inside Out: Second Edition. Elsevier Inc. https://doi.org/10.1016/C2011-0-07261-7

Upadhyay, A., & Dalvi, S. V. (2019). Microbubble Formulations: Synthesis, Stability, Modeling and Biomedical Applications. In Ultrasound in Medicine and Biology (Vol. 45, Issue 2, pp. 301–343). Elsevier USA. https://doi.org/10.1016/j.ultrasmedbio.2018.09.022

UV-Visible Spectroscopy. (n.d.). Retrieved April 2, 2020, from https://www2.chemistry.msu.edu/faculty/reusch/VirtTxtJml/Spectrpy/UV-Vis/uvspec.html

Wheatley, M. A., Forsberg, F., Oum, K., Ro, R., & El-Sherif, D. (2006). Comparison of in vitro and in vivo acoustic response of a novel 50:50 PLGA contrast agent. Ultrasonics, 44(4), 360–367. https://doi.org/10.1016/j.ultras.2006.04.003

Wilson, S. R., & Burns, P. N. (2010). Microbubble-enhanced US in body imaging: What role? In Radiology (Vol. 257, Issue 1, pp. 24–39). Radiological Society of North America, Inc. https://doi.org/10.1148/radiol.10091210

Wu, M., & Shu, J. (2018). Multimodal Molecular Imaging: Current Status and Future Directions. Contrast Media & Molecular Imaging, 2018, 1382183. https://doi.org/10.1155/2018/1382183

Yang, S., Leong, K. F., Du, Z., & Chua, C. K. (2001). The design of scaffolds for use in tissue engineering. Part I. Traditional factors. In Tissue Engineering (Vol. 7, Issue 6, pp. 679–689). https://doi.org/10.1089/107632701753337645

Yu, Y., Nakano, M., & Ikeda, T. (2003). Directed bending of a polymer film by light. *Nature*, *425*(6954), 145. https://doi.org/10.1038/425145a

Zhang, L., Hu, J., & Athanasiou, K. A. (2009). The role of tissue engineering in articular cartilage repair and regeneration. In Critical Reviews in Biomedical Engineering (Vol. 37, Issues 1–2, pp. 1–57). Begell House Inc. https://doi.org/10.1615/CritRevBiomedEng.v37.i1-2.10

Zollinger, H., & Nwslen, E. (n.d.). Azo and Diazo Chemistry. Retrieved April 2, 2020, from https://pubs.acs.org/sharingguidelines

BIOGRAPHICAL SKETCH

Muskan Pawar was born and raised in Haryana, India. In 2017, she was awarded a Bachelor of Technology in Biomedical Engineering from Deenbandhu Chhotu Ram University of Science and Technology. In August 2018, she joined the Biomedical Engineering graduate program at The University of Texas at Dallas. Muskan joined Sirsi Lab at UT Dallas, where she completed her thesis under the guidance of Dr. Shashank R. Sirsi. She will be working towards her career in research and development in the medical device industry.

CURRICULUM VITAE

Muskan Pawar
Email:mxp170025@utdallas.edu

EDUCATION

MASTER OF SCIENCE | August 2018-May 2020 |The University of Texas at Dallas, USA | Biomedical Engineering
BACHELOR OF TECHNOLOGY | August 2013-May 2017 | Deenbandhu Chhotu Ram University of Science and Technology, India |Biomedical Engineering

TECHNICAL SKILLS

- **Medical Modalities:** Microscopy, Scanning Electron Microscopy, UV-Vis Spectroscopy, Polarized Optical Microscopy, Sonicator, Homogenizer, Centrifuge, and Freeze dryer
- **Tools**: MS Office, Image J, Multisizer, Solidworks, MATLAB
- **Quality:** FMEA, Hazard Analysis, Trace Matrix, Inventory Tracking, CAPA, Lean Six Sigma, Validation (IQ, OQ, PQ)

RESEARCH EXPERIENCE

Graduate Researcher (Sirsi Lab), UTD **September 19 – Present**

- Extensive bench experience within a lab environment including protocols modification, data-acquisition, statistical analysis, interpretation, biomaterial surface visualization, and characterization
- Highly skilled at formulating polymer microbubbles as ultrasound contrast agents

Regulatory Student Intern (Texas Biomedical Device Center), UTD March 19-December 19

- Performed Inspection & Validation testing of Class III Medical Devices for quality assurance, damage assessment using work procedures and test protocols
- Created test reports for Incoming Inspection & Validation testing and First Article Inspection
- Gained working knowledge on designing components using Solidworks, Hazard Analysis, Trace Matrix, CAPA, Inventory Tracking, Device Classification and Listing, Quality System Regulations, FMEA

PROFESSIONAL EXPERIENCE

Graduate Teaching Assistant, UTD **January 20-Present**

- Coordinating and monitoring the academic progress of undergraduate students
- Assisting students in MATLAB programming, Arduino UNO, and Solidworks

Alumni Coordinator- BMEN GSA, UTD **September 19 – Present**

- Organizing career discussion panels, networking with alumni
- Understanding industry insights

Intern Philips India Limited, India **May 16-August 16**

- Worked with Clinical Application Specialist on various imaging modalities including Ultrasound, X-Ray, MRI
- Visited hospitals with Field Service Engineers

Biomedical Engineer Trainee - Sir Ganga Ram Hospital, India **May 15 – July 16**

- Gained working exposure of the medical equipment including Ventilators, Patient Monitors, and Syringe Pump
- Acquired working knowledge about Telemetry and Hospital Information System

RESEARCH & PROJECTS

Thesis Research: Formulation and Development of UV Activated Polymer Microbubbles as Ultrasound Contrast Agents for Imaging and Drug Delivery

- Formulated and characterized polymer microbubbles as contrast agents using double emulsification and freeze-drying synthesis techniques

Piezoelectric Energy Harvester for Pacemaker as Secondary Storage

- Simulated working of a polymer-based piezoelectric sensor to harvest electrical energy through the heart's mechanical movements

Self-assembly behavior observed at Interface

- Studied the effects of liquids with different viscosity on a hydrophobic and hydrophilic surfaces

Wearable glove for disabled hand - Awarded the best project of the year

- Designed lost cost wearable hand glove for a disabled person to grasp objects.

COMPETITIONS, LEADERSHIP EXPERIENCE & ORGANIZATIONS

- Attended the prestigious conferences of Biomedical Engineering Society, Philadelphia, USA, as a Student Volunteer and FDA Medical Device Industry Coalition-Medical Device 101, Austin, USA
- Attended discussion group “Focusing the Design FMEA,” held by DFW ASQ Biomedical, Abbott, Texas, USA
- Top 3 Rank Holder at The Department of Biomedical Engineering, DCRUST, India